JAEA-Data/Code
2024-014
DOI:10.11484/jaea-data-code-2024-014

Data Report of ROSA/LSTF Experiment SB-PV-03

-0.2% Pressure Vessel Bottom Break LOCA with
SG Depressurization and Gas Inflow-

Takeshi TAKEDA

Reactor Safety Research Division
Nuclear Safety Research Center
Sector of Nuclear Safety Research and Emergency Preparedness

December 2024

Japan Atomic Energy Agency

日本原子力研究開発機構

JAEA-Data/Code

国立研究開発法人日本原子力研究開発機構　研究開発推進部　科学技術情報課
〒 319-1112　茨城県那珂郡東海村大字村松 4 番地 49
E-mail: ird-support@jaea.go.jp

JAEA-Data/Code 2024-014

Data Report of ROSA/LSTF Experiment SB-PV-03
－0.2% Pressure Vessel Bottom Break LOCA with SG Depressurization and Gas Inflow－

Takeshi TAKEDA

Reactor Safety Research Division
Nuclear Safety Research Center
Sector of Nuclear Safety Research and Emergency Preparedness
Japan Atomic Energy Agency
Tokai-mura, Naka-gun, Ibaraki-ken

(Received October 9, 2024)

An experiment denoted as SB-PV-03 was conducted on November 19, 2002 using the Large Scale Test Facility (LSTF) in the Rig of Safety Assessment-V (ROSA-V) Program. The ROSA/LSTF experiment SB-PV-03 simulated a 0.2% pressure vessel bottom small-break loss-of-coolant accident in a pressurized water reactor (PWR). The test assumptions included total failure of high pressure injection system of emergency core cooling system (ECCS) and non-condensable gas (nitrogen gas) inflow to the primary system from accumulator (ACC) tanks of ECCS. Secondary-side depressurization of both steam generators (SGs) as an accident management (AM) action to achieve the depressurization rate of 55 K/h in the primary system was initiated 10 min after the generation of a safety injection signal, and continued afterwards. Auxiliary feedwater injection into the secondary-side of both SGs was started for 30 min with some delay after the onset of the AM action.

The AM action was effective on the primary depressurization until the ACC tanks began to discharge nitrogen gas into the primary system. The core liquid level recovered in oscillative manner because of intermittent coolant injection from the ACC system into both cold legs. Therefore, the core liquid level remained at a small drop. The pressure difference between the primary and SG secondary sides became larger after nitrogen gas ingress.

Core uncovery occurred by core boil-off during reflux condensation in the SG U-tubes under nitrogen gas influx. When the maximum cladding surface temperature of simulated fuel rods exceeded the pre-determined value of 908 K, the core power was automatically reduced to protect the LSTF core. After the automatic core power reduction, coolant injection from low pressure injection (LPI) system of ECCS into both cold legs led to the whole core quench.

After the continuous core cooling was confirmed through the actuation of the LPI system, the experiment was terminated.

This report summarizes the test procedures, conditions, and major observations in the ROSA/LSTF experiment SB-PV-03.

Keywords: PWR, LSTF, Pressure Vessel Bottom Break, Small Break LOCA, Accident Management, Steam Generator Depressurization, Gas Inflow, Core Boil-off

JAEA-Data/Code 2024-014

ROSA/LSTF 実験 SB-PV-03 データレポート
－ガスが流入する条件での 0.2%圧力容器底部小破断冷却材喪失事故時蒸気発生器減圧－

日本原子力研究開発機構 安全研究・防災支援部門
安全研究センター 原子炉安全研究ディビジョン

竹田 武司

（2024 年 10 月 9 日受理）

ROSA-V 計画において、大型非定常実験装置(LSTF)を用いた実験(実験番号:SB-PV-03)が 2002 年 11 月 19 日に行われた。ROSA/LSTF SB-PV-03 実験では、加圧水型原子炉(PWR)の 0.2%圧力容器底部小破断冷却材喪失事故を模擬した。このとき、非常用炉心冷却系(ECCS)である高圧注入系の全故障とともに、蓄圧注入(ACC)タンクから一次系への非凝縮性ガス(窒素ガス)の流入を仮定した。また、アクシデントマネジメント(AM)策として両蒸気発生器(SG)二次側減圧を安全注入設備信号発信後 10 分に一次系減圧率 55K/h を目標として開始し、その後継続した。さらに、AM 策から少し遅れて両 SG 二次側への 30 分間の補助給水を開始した。

ACC タンクから一次系への窒素ガスの流入開始まで、AM 策は一次系減圧に対して有効であった。ACC 系から両低温側配管への間欠的な冷却材注入により、炉心水位は振動しながら回復した。このため、炉心水位は小さな低下にとどまった。窒素ガスの流入後、一次系と SG 二次側の圧力差が大きくなった。

窒素ガス流入下における SG 伝熱管でのリフラックス凝縮時に、ボイルオフによる炉心露出が生じた。模擬燃料棒の被覆管表面最高温度が LSTF の炉心保護のために予め決定した値(908K)を超えたとき、炉心出力は自動的に低下した。炉心出力の自動低下後、ECCS である低圧注入(LPI)系から両低温側配管への冷却材注入により、全炉心はクエンチした。

LPI 系の作動を通じた継続的な炉心冷却を確認後、実験を終了した。

本報告書は、ROSA/LSTF SB-PV-03 実験の手順、条件および実験で観察された主な結果をまとめたものである。

原子力科学研究所：〒319-1195　茨城県那珂郡東海村大字白方 2-4

Contents

目次

List of Tables

List of Figures

Acronyms and Abbreviations

ACC	Accumulator
AFW	Auxiliary Feedwater
AM	Accident Management
CET	Core Exit Temperature
ECCS	Emergency Core Cooling System
HPI	High Pressure Injection
LPI	Low Pressure Injection
LSTF	Large Scale Test Facility
NEA	Nuclear Energy Agency
OECD	Organisation for Economic Co-operation and Development
PKL	Primärkreisläufe Versuchsanlage
PWR	Pressurized Water Reactor
PZR	Pressurizer
ROSA	Rig-of-Safety Assessment
SBLOCA	Small-Break Loss-of-Coolant Accident
SG	Steam Generator
SI	Safety Injection
UCP	Upper Core Plate

This is a blank page.

1. Introduction

An event occurred at the South Texas Project Unit-1 pressurized water reactor (PWR) in the US in 2003 [1]. Namely, inspections from outside of the pressure vessel revealed that a small amount of residue containing boron was found around the circumference of two instrument-tube penetration nozzles of pressure vessel lower-head. This raised a safety issue concerning structural integrity of pressure vessel. Multiple instrument-tubes may be ejected on account of circumferential cracks at nozzles of pressure vessel lower-head. This would have caused a small-break loss-of-coolant accident (SBLOCA) at the pressure vessel bottom. Liquid-phase break is characterized by fast loss of coolant inventory with slow depressurization of the primary system [2][3]. As for an accident management (AM) measure against SBLOCA, steam generator (SG) secondary-side depressurization being coupled with auxiliary feedwater (AFW) injection into the SG secondary-side is important to depressurize the primary system [4]. This may activate low pressure injection (LPI) system of emergency core cooling system (ECCS), which enables long-term core cooling during SBLOCA especially when high pressure injection (HPI) system of ECCS is in failure. However, experimental data have been scarcely obtained for such a pressure vessel bottom SBLOCA with the AM measure under complete failure of HPI system [5].

An experiment denoted as SB-PV-03 was carried out on November 19, 2002, on a PWR pressure vessel bottom SBLOCA [6]. This test utilized the Large Scale Test Facility (LSTF) [7] in the Rig-of-Safety Assessment-V (ROSA-V) Program. The LSTF simulates a Westinghouse-type four-loop 3423 MW (thermal) PWR by a full-height and 1/48 volumetrically-scaled two-loop system. The break size was equivalent to 0.2% of the volumetrically-scaled (1/48) cross-sectional area of the reference PWR cold leg. Thus, in the LSTF test even for a break at non-cold leg, the break size is based on the scaled cold leg cross-sectional area. Water injection from HPI system of ECCS is expected as a function to mitigate the consequences in such 0.2% break LOCA case. On the contrary, the SB-PV-03 experiment assumed that HPI system of ECCS was unavailable.

In the new regulatory requirements for PWR in Japan, an event of loss of ECCS water injection functions was postulated as one of the accident sequences, which should be evaluated the effectiveness of measures against core damage [8]. A medium-break LOCA or SBLOCA with the assumption of a totally-failed HPI system is the event that represents the loss of ECCS water injection functions [9]. Appropriate measures for this event should be taken such as the primary depressurization through early depressurization of the SG secondary-side because of steam condensation in the SG U-tubes and early actuation of the AFW system to provide feedwater into the SG secondary-side.

In the SB-PV-03 experiment, secondary-side depressurization of both SGs as an AM action

to attain the depressurization rate of 55 K/h in the primary system was taken 10 min after the generation of a safety injection (SI) signal, and continued thereafter. AFW was injected for 30 min into the secondary-side of both SGs with some delay after the initiation of the AM action, which may produce less heat removal from the SG secondary-side system. The SB-PV-03 experiment also supposed non-condensable gas (nitrogen gas) ingress to the primary system from accumulator (ACC) tanks of ECCS due to failure of the ACC system isolation after the coolant injection initiation. The effectiveness of the AM action should thus be confirmed under the influence of nitrogen gas influx from the ACC tanks.

The SB-PV-03 test objectives were as follows; (i) to elucidate thermal-hydraulic phenomena involved, (ii) to clarify the AM action effectiveness for both core cooling and primary depressurization, and (iii) to provide experimental data for the assessment of thermal-hydraulic safety analysis computer codes. The LSTF test data would be useful to define the conditions of counterpart testing by means of other integral test facilities such as PKL (Primärkreisläufe Versuchsanlage) [10]. **Table 1-1** compares major features of the LSTF and PKL. Volumetric scaling is 1/48 in the LSTF, whereas it is 1/145 in the PKL. The LSTF runs at full pressure, whereas the PKL pressure is limited to 5 MPa. The number of loops is two in the LSTF, and four in the PKL. The axial core power profile is a 9-step chopped cosine in the LSTF, whereas it is flat in the PKL. The aim of the counterpart testing is to address scaling problems through thermal-hydraulic phenomena at similar or identical pressure ranges. As summed up in **Table 1-2**, in this regard, the LSTF test data have been provided on SBLOCAs under different conditions of break, AM action and its onset timing, and nitrogen gas inflow to the primary system from the ACC system for the counterpart testing in the PKL-related OECD/NEA Projects [5], [11]-[20].

This report summarizes the test procedures, conditions, and major observations in the ROSA/LSTF experiment SB-PV-03. All the experimental data were processed carefully and qualified to acquire the best possible accuracy.

Table 1-1 Major features of LSTF and PKL

Item	LSTF	PKL
Height	Full	Full
Volumetric scaling	1/48	1/145
Number of loops	2	4
Pressure vessel downcomer	Cylindrical	Double-pipe
Number of U-tubes per SG	141	30
Pressure	Full	Up to 5 MPa
Core power	14%	10%
Axial profile	Chopped cosine	Flat
Radial profile	3-region	3-region

Table 1-2 Major information of LSTF tests for counterpart testing in PKL-related OECD/NEA Projects

Test ID [test year]	Break size, location [orientation]	AM action and onset timing	Nitrogen gas inflow	OECD/NEA Project [references]
SB-HL-18 [2011]	1.5%, hot leg [upward]	[Low pressure phase test] Full open of SG relief valves with AFW injection into SG secondary-side at core exit temperature of 623 K	No-consider	PKL-2 [11][12][13]
SB-CL-32 [1996]	1%, cold leg [horizontal]	SG secondary-side depressurization to achieve depressurization rate of 200 K/h in primary system with AFW injection into SG secondary-side 10 min after break	No-consider	PKL-3 [14][15][16]
SB-HL-12 [1998]	1%, hot leg [downward]	Full open of SG relief valves with AFW injection into SG secondary-side at cladding surface temperature of 600 K	Consider	PKL-3 [16][17][18]
SB-PV-09 [2005]	1.9%, pressure vessel upper head	Full open of SG relief valves with AFW injection into SG secondary-side at core exit temperature of 623 K	Consider	ETHARINUS [5][19][20]

Remarks: (1) The common test assumption was total failure of HPI system. (2) The SB-HL-18 test, broadly divided into the high pressure phase test and low pressure phase test, was conducted in the OECD/NEA ROSA-2 Project. The low pressure phase test corresponded to the counterpart testing. (3) The SB-PV-09 test was performed in the OECD/NEA ROSA Project.

2. Overview of LSTF

Figure 2-1 shows a schematic view of the LSTF that simulates a typical 3423 MW (thermal) four-loop Westinghouse-type PWR with a two-loop system model by full height and 1/48 in volume [7]. **Figure 2-2** gives the schematic diagram of the LSTF. The reference PWR of the LSTF is Tsuruga Unit-2 of Japan Atomic Power Company. The LSTF is composed of a pressure vessel, pressurizer (PZR), and primary loops. Each loop includes an active SG, primary coolant pump, crossover leg, hot leg, and cold leg. The crossover leg is a primary piping that connects the primary coolant pump to the SG. Loops with and without PZR are designated as loop-A and loop-B, respectively. The hot leg and cold leg, 207 mm in inner-diameter each, are sized to conserve the volumetric scale (2/48) and the ratio of length to square root of pipe diameter to better simulate flow regime transitions in the primary loops [21]. Each SG is furnished with 141 full-size U-tubes (inner-diameter of 19.6 mm each), inlet and outlet plena, boiler section, steam separator, steam dome, steam dryer, main steam line, four downcomer pipes, and other internals (see pp.260-273 in Ref. [7]). Each SG is equipped with six instrumentation tubes, which are available to measure differential pressures through differential pressure transducers and fluid temperatures with thermocouples (see pp.53-54 in Ref. [7]). Tubes 1 and 6 are short tubes (Type 1; see p.267 in Ref. [7]), Tubes 2 and 5 are medium tubes (Type 5), and Tubes 3 and 4 are long tubes (Type 9). The LSTF represents the reference PWR bypasses involving eight upper-head spray nozzles (inner-diameter of 3.4 mm each) (see p.202 in Ref. [7]) and the hot leg nozzle (see p.196 in Ref. [7]) leakage. The spray nozzles allow bypass flow that amounts to 0.3% of the total core flow rate during the initial steady state, while bypass area of the hot leg nozzle is set to allow 0.2% bypass flow for each loop. The LSTF core, 3.66 m in active height, mainly consists of 1008 electrically heater rods in 24 rod bundles to simulate the fuel rod assembly and 96 non-heating tie rods to simulate control rod guide thimble (see p.220 in Ref. [7]). The angle of the PZR surge line to the hot leg is 45°. All the types of ECCS fitted to the reference PWR are installed in the LSTF. Nitrogen gas is used for pressurization of ACC tanks of ECCS.

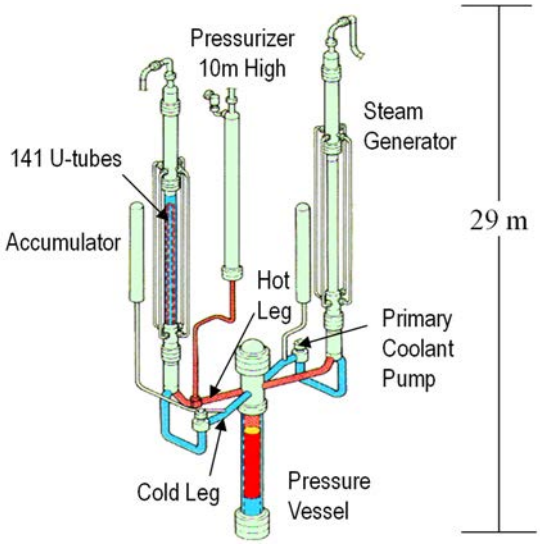

Fig. 2-1 Schematic view of the Large Scale Test Facility (LSTF)

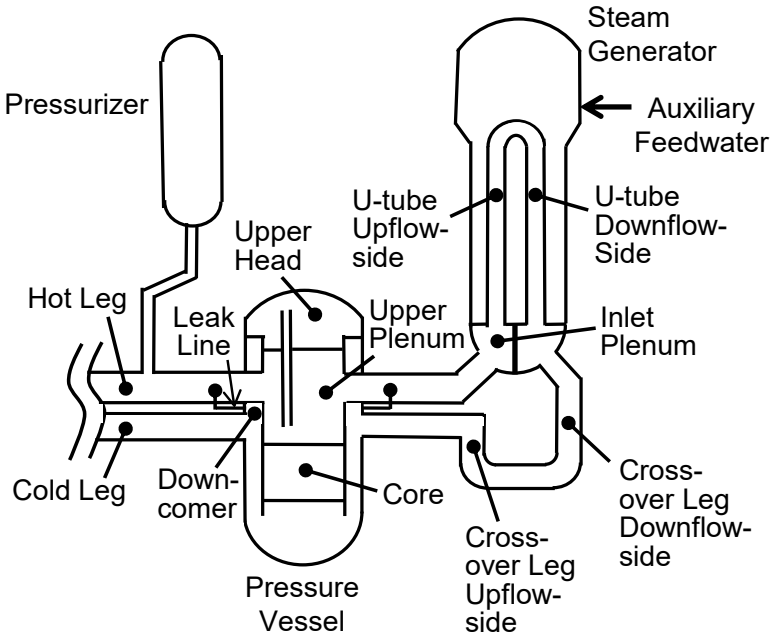

Fig. 2-2 Schematic diagram of the Large Scale Test Facility (LSTF)

3. Test Conditions and Procedures

With respect to the break, ECCS, and control logic, following assumptions were posed to the SB-PV-03 test conditions.

The assumption related to the break is the following;

1) Break size (flow area) corresponds to 0.2% of the volumetrically-scaled (1/48) cross-sectional area of the reference PWR cold leg. This is equal to the size of ten in-core instrumentation tubes (inner-diameter of 10.16 mm each) of pressure vessel lower-head. As presented in **Fig. 3-1**, the break is simulated by using a 4.6 mm inner-diameter sharp-edge orifice fixed at the downstream of a horizontal pipe that is connected to a lower plenum nozzle.

The assumptions concerning the ECCS are as follows;

2) Total failure of HPI system
3) When the primary pressure reduces to 4.51 MPa, ACC system is actuated in both loops. Coolant is provided from the ACC system into both cold legs. The ACC coolant injection flow rate ratio of loop with PZR to loop without PZR is designed to become 1:1. The ACC coolant injection temperature is 320 K.
4) For each loop, non-condensable gas (nitrogen gas) inflow to the primary system from the ACC tank takes place owing to failure of the ACC system isolation after the ACC coolant injection initiation.
5) When the pressure vessel lower plenum pressure declines to 1.24 MPa, LPI system is activated in both loops. Coolant is fed from the LPI system into both cold legs. The LPI coolant injection flow rate ratio of loop with PZR to loop without PZR is intended to become 1:1. The LPI coolant injection temperature is 310 K.

The assumptions regarding the control logic are as below;

6) When the primary pressure drops to 12.97 MPa, a scram signal is generated, causing closure of SG main steam stop valve, coastdown of primary coolant pumps, termination of SG main feedwater, and manual closure of SG main steam isolation valves.
7) Loss of off-site power concurrently with the scram signal generation
8) When the primary pressure lowers to 12.27 MPa, a SI signal is obtained.
9) Secondary-side depressurization of both SGs as an AM action to achieve the depressurization rate of 55 K/h in the primary system is made 10 min after the SI signal generation, and continues thereafter. The primary depressurization rate of 55 K/h is decided with reference to the depressurization rate during procedures of an operator action in PWR accidents where heat removal by SG(s) is possible [6]. The time delay of 10 min is taken account of a grace period to start an operator action [6].
10) AFW is supplied into the secondary-side of both SGs with some delay after the AM action

onset. The AFW injection duration is 30 min, supposing the use of turbine-driven AFW pump due to malfunction of electric AFW pump. The AFW flow rate into the SG secondary-side is planned to be about 0.59 kg/s in loop with PZR and about 0.72 kg/s in loop without PZR. This purpose is to look into an impact of the different AFW flow rate on the SG secondary-side collapsed liquid level. The AFW injection temperature is 310 K.

11) Thresholds of maximum cladding surface temperature for the LSTF core protection system are as follows;
908K=75%, 918K=50%, 919K=25%, 920K=10%, of pre-determined value [22], according to the conditions mentioned in **Table 3-1**.

3.1 Initial Steady State and Boundary Conditions

The specified initial steady state and boundary conditions are listed in **Table 3-1**. Initial steady state conditions such as PZR pressure, fluid temperatures in the hot leg and cold leg were 15.5 MPa, 598 K and 563 K respectively (to be indicated in **Table 4-1**), in accordance with to the reference PWR conditions.

The LSTF initial core power is limited to 10 MW, on account of a limitation in the capacity of power supply. The 10 MW power corresponds to 14% of the volumetrically-scaled (1/48) PWR nominal core power (3423 MW). Radial peaking factors of high-, mean-, and low-power rod bundles are 1.51, 1.00, and 0.66, respectively, in “Case 3” (see p.228 in Ref. [7]) shown in **Table 3-1**. The radial power profile is divided into two high-power heater rod zones (H1 and H2), one mean-power heater rod zone (M), and three low-power heater rod zones (L1, L2, and L3) (see p.228 in Ref. [7]), as mentioned in **Fig. 3-2**. The total number of the heater rods is 360, 180, and 468 for the high-power, mean-power, low-power heater rod zones, respectively. The specified power per heater rod is 9.69 kW in “Case 3”. Axial core power profile is a 9-step chopped cosine with a peaking factor of 1.495 (see p.227 in Ref. [7]). To attain the prototypical initial fluid temperatures with this core power, core flow rate was set to 14% of the 1/48-scaled nominal flow rate. Initial SG secondary-side pressure was raised to 7.3 MPa to limit the primary-to-secondary heat transfer rate to 10 MW, while 6.1 MPa is nominal value in the reference PWR. Initial PZR liquid level was about 7.4 m that is equivalent to about 66% of the PZR vessel height (see p.396 in Ref. [7]). Initial SG secondary-side collapsed liquid level was about 10.2 m that corresponds to the SG medium tube height.

Proportional heaters in the PZR are employed to trim the pressure, while backup heaters mitigate system heat losses. Powers of the PZR proportional and backup heaters were 2.8 kW and 33.7 kW, respectively, as the initial condition. The powers of the PZR proportional and backup heaters turned off when the PZR liquid level became below 2.3 m. Many regions of the LSTF are provided with trace heaters to mitigate environmental heat losses.

The configuration of the break unit is drawn in **Fig. 3-1**. The break was simulated by utilizing a 4.6 mm inner-diameter sharp-edge orifice No.11 (see p.307 in Ref. [7]). The orifice was mounted at the downstream of a horizontal pipe (inner-diameter of 87.3 mm) that was attached to a lower plenum nozzle (N-6b; see p.96 and p.195 in Ref. [7]). The orifice flow area was consistent with 0.2% of the 1/48-scaled cross-sectional area of the reference PWR cold leg. Venturi flow meter (FE-570-BU; see p.303 in Ref. [7]) was installed in the break unit for the purpose of qualitatively monitoring the break flow during the experiment.

For controlling ACC water injection volume (see p.322 in Ref. [7]), the specified initial water level and volume above the standpipe were 1.58 m and 1.12 m^3 respectively for both loops. The specified initial volume of non-condensable gas (nitrogen gas) in the ACC tank was 0.46 m^3 for both loops. The angle of the coolant injection from the ACC tank into the cold leg via the ECCS nozzle (N-14a or N-14b; see p.83 and pp.239-240 in Ref. [7]) is 90° for loop with PZR (loop-A) and 45° for loop without PZR (loop-B) (see pp.397-398 in Ref. [7]).

3.2 Test Procedures

Table 3-2 shows the specified control logic, operation set points, and conditions. The experiment was launched at time zero by opening a break valve located downstream of the break orifice at the pressure vessel bottom. At the same time, rotation speed of primary coolant pumps was increased up to about 1550 rpm in 4 s for better simulation of pressure and temperature transients in the reference PWR.

When the primary pressure dropped to 12.97 MPa, a scram signal was generated. This produced the closure of the SG main steam stop valve, the coastdown of the primary coolant pumps, the termination of the SG main feedwater, and the manual closure of the SG main steam isolation valves. **Table 3-3** shows the specified rotation speed ratio of primary coolant pump after the scram signal. The specified pump rotation speed was reduced to zero 250 s after the scram signal.

Table 3-4 shows the pre-determined core power decay curve after the scram signal, based on calculations by making use of the RELAP5 code considering delayed neutron fission power and stored heat in PWR fuel rod [22]. The core power was held at the initial value of 10 MW for 18 s until the scaled PWR core decay power dropped to 10 MW. The LSTF core power began a decay afterwards according to the specified core power.

The pressure set points for opening and closure of the SG relief valves are 8.03 MPa and 7.82 MPa, respectively, referring to the corresponding values in the reference PWR. The SG relief valve was simulated by employing a 16.2 mm inner-diameter sharp-edge orifice to provide steam flow rate of 2 kg/s when the SG secondary-side pressure is 8 MPa.

The ACC system is actuated in both loops at the primary pressure of 4.51 MPa according to the reference PWR. The ACC coolant injection flow rate ratio of loop with PZR to loop without PZR was designed to become 1:1 (to be plotted in **Figs. 4-13 and 4-14**). The ACC coolant injection temperature is 320 K, which is the same as that in the reference PWR.

The LPI system is activated in both loops at the pressure vessel lower plenum pressure of 1.24 MPa. As seen in **Table 3-5**, the LPI coolant injection flow rate is decided on the basis of Q-H curve for the LPI pump. The LPI coolant injection flow rate ratio of loop with PZR to loop without PZR was intended to become 1:1 (to be indicated in **Fig. 4-15**). The LPI coolant injection temperature is 310 K, which is equal to that in the reference PWR.

When the primary pressure lowered to 12.27 MPa, a SI signal was obtained. **Figure 3-3** shows the schematic view of the SG steam line (see pp.257-258 in Ref. [7]). There are two types of valves (i.e., gate valve and flow control valve) in the turbine bypass line, being parallel to the SG relief valve line. The SG secondary-side depressurization exploiting the flow control valves [Valve No.; FCV (flow control valve) -441 and FCV-442] (see p.106 in Ref. [7]) in both SGs was controlled such that the primary depressurization rate becomes to be 55 K/h. At that time, the gate valves [Valve No.; AOV (air-operated valve) -150 and AOV-180] (see pp.111-112 in Ref. [7]) and the relief valves [Valve No.; AOV-151 and AOV-181] (see pp.111-112 in Ref. [7]) in both SGs were open and closed, respectively. The SG secondary-side pressure drop curve after the initiation of the AM action was pre-determined, as listed in **Table 3-6**. This was based on the primary saturation temperature under an assumption that the primary pressure may closely follow the SG secondary-side pressure.

The AFW was supplied at 310 K into the secondary-side of both SGs with some delay after the start of the AM action (to be presented in **Figs. 4-8 and 4-16**). This avoids a significant drop in the SG secondary-side collapsed liquid level. The operator manually injected the AFW into each SG secondary-side for 30 min by monitoring the narrow-range (0-1 kg/s) feedwater flow rate [Tag Name; FE520B-PAA (for secondary-side of SG in loop with PZR), FE530B-PAB (for secondary-side of SG in loop without PZR)] (see pp.257-258 in Ref. [7]). The AFW flow rate into the SG secondary-side was expected to be about 0.59 kg/s in loop with PZR and about 0.72 kg/s in loop without PZR (to be indicated in **Fig. 4-9**). The AFW flow rate of about 0.72 kg/s in loop without PZR was nearly equivalent to the volumetric-scaled flow rate of the reference PWR.

3.3 Instrumentation

Instruments are equipped in the LSTF to understand and evaluate thermal-hydraulic responses during simulated accidents and transients.

3.3.1 Measured Data

A list of available experimental data is shown in **Table A-1**, which is composed of Sequential No., Function ID., Tag Name, measurement location, range, unit, and uncertainty. The Tag Name is a fixed naming unique to each measurement. The alphabetical prefix in the Function ID. and Tag Name represents the kind of variable or the kind of measurement as follows;

TE, fluid temperature,

DT, differential temperature,

TW, heater rod and structure temperature,

FE, flow rate measured with conventional (differential pressure) flow meters,

PE, pressure,

MI, miscellaneous instrumented-signal (power, pump rotation speed, etc.),

LE, liquid level,

DP, differential pressure,

DE, fluid density measured with gamma-ray densitometer.

After the experiment, data from these measurements are processed to obtain the “secondary” data, such as area-averaged fluid density derived from measurement with three-beam gamma-ray densitometer. These data are stored with Function ID. starting with a prefix of “RC”. The measurement uncertainty is assessed according to the accuracy of the relevant instrument.

3.3.2 Data Conversion, Reduction, and Calibration

The instrumented-signals are recorded in volts by the data logger of DARWIN system (Yokogawa Electric Corporation), and are converted into engineering units utilizing appropriate conversion equations and factors. Differential pressure (DP) cell is a device that measures the differential pressure between two inputs. Some parameters such as flow rate (FE) and liquid level (LE) that employ DP cell data require the calculation of the single-phase coolant density based on local pressure and fluid temperature data using steam table.

DP cell data for both the differential pressures and liquid levels are corrected on the basis of a similar calibration test for static pressure effect, which is performed separately. Three-valve manifold is operated for each of DP cells to obtain zero calibration data for 200 s twice at a little before the break valve opening and at a little after the closure of the break valve.

The applicability of flow rates measured with the conventional flow meters employing venturi, orifice or nozzle and DP cell is limited in principle to either single-phase liquid or vapor flow. In addition, the accuracy is poor when the readings are below about 20% of the measurement range. This is explained by the fact that the flow rate is proportional to the square root of the

measured DP. For example, a zero level drift of 1% in the DP cell output may result in the flow rate reading of 10% of the measurement range especially when the actual flow rate is nearly equal to zero. It is thus good to pay attention when the flow rate is below about 20% of the measurement range even though the data are corrected based on a calibration test for static pressure effect.

Two-phase flow instruments, such as gamma-ray densitometers, use certain conversion equations considering attenuation effects of gamma-ray that goes through coolant flow.

After the data acquisition, some experimental data are calibrated. The high-range pressure data in the PZR and the upper plenum, for example, are corrected on the basis of a zero level shift using the low-range pressure data first, and then all the density data are calibrated at two points with different fluid conditions.

3.3.3 Data Qualification

The experimental data are qualified manually. Thermocouple data are reviewed by employing pre-test ambient temperature data for anomalous readings, and are mutually compared with readings of instruments in the same vicinity. Pressure transducers are checked for zero level drift as well as any other suspicious behaviors. The outputs of conductance probe, power meters, pump speed and vibration meters, and valve position indicators are individually reviewed for inconsistent readings.

The flow meters, DP transducers, gamma-ray densitometers, and drag disk transducers require extensive manual qualification efforts. The validity of the flow meters and differential pressure data mostly depends on whether the reading is in the sensitive range of the measurement or not. The data from these instruments are presented with appropriate corrections based on calibration data for each transducer.

Available experimental data are “Good” defined as follows. “Good” means that the type of data has been reviewed manually, and is presumed to lie within the range and uncertainty values of the instruments based on the design specification which are published in the reference [7]. However, certain measurements may be affected by various extraneous factors such as flow velocity, flow regime, and wall effects. **Table A-1** shows the list of available experimental data qualified as “Good” for LSTF SB-PV-03 (Run ID named to be SP3).

Table 3-1 Specified initial steady state and boundary conditions (1/2)

Core	Initial core power	10 MW
	Radial core power profile	Case 3
	Axial core power profile	9-step chopped cosine, peaking factor = 1.495
Primary Loops	Initial hot leg fluid temperatures	598.1 K
	Initial cold leg fluid temperatures	562.4 K
	Initial mass flow rate	24.3 kg/s / loop
	Initial downcomer-to-hot leg bypass	0.049 kg/s / loop
Pressurizer (PZR)	Initial pressure	15.5 MPa
	Initial liquid level	7.2 m
	Inner-diameter of relief valve orifice	6.83 mm
	Relief valve open / closure	Primary pressure = 16.20 / 16.07 MPa
	Inner-diameter of safety valve orifice	14.4 mm
	Safety valve open / closure	Primary pressure = 17.26 / 17.06 MPa
Steam Generators (SGs)	Initial secondary-side pressure	7.3 MPa
	Initial secondary-side liquid level	10.3 m
	Initial main steam flow rate	2.74 kg/s
	Initial main feedwater flow rate	2.74 kg/s
	Main feedwater temperature	495.2 K
	Inner-diameter of relief valve orifice	16.2 mm
	Relief valve open / closure	SG secondary-side pressure = 8.03 / 7.82 MPa
	Inner-diameter of safety valve orifice	26.6 mm
	Safety valve open / closure	SG secondary-side pressure = 8.68 / 7.69 MPa

Table 3-1 Specified initial steady state and boundary conditions (2/2)

Break

Location	Pressure vessel lower plenum (see **Fig. 3-1**)
Type	Sharp-edge orifice
Inner-diameter of orifice	4.6 mm

ECCS

High pressure injection (HPI) system		Not actuated
Accumulator (ACC) system	Initiation of system	Primary pressure = 4.51 MPa
	Water temperature	320 K
	Initial water level above tank bottom in both loops	6.8 m
	Standpipe level above tank bottom in both loops	5.22 m
	Initial water volume above standpipe in both loops	1.12 m^3*
	Initial gas volume in both loops	0.46 m^3
	Cross-sectional flow area above standpipe	0.7085 m^2
	Orifice diameter (d) in loops with / without PZR	38.2 mm / 35.0 mm
	Connecting pipe diameter (D) in both loops	97.1 mm
	Contraction ratio (d/D) in loops with / without PZR	0.393 / 0.360
	Coolant injection flow rate ratio of loop with PZR to loop without PZR	1:1
	Injection location	Cold legs in both loops
Low pressure injection (LPI) system	Initiation of system	Pressure vessel lower plenum pressure = 1.24 MPa
	Q-H pump characteristic	See **Table 3-5**
	Water temperature	310 K
	Coolant injection flow rate ratio of loop with PZR to loop without PZR	1:1
	Injection location	Same with ACC system

* (6.8－5.22 [m])×0.7085 [m^2] ≒ 1.12 [m^3]

LSTF Core Protection System Logic

Control of core power to	Maximum cladding surface temperature reaches
75%	908 K
50%	918 K
25%	919 K
10%	920 K

Table 3-2 Specified control logic, operation set points, and conditions

Event	Condition
Break	Time zero
Generation of scram signal	Primary pressure = 12.97 MPa
PZR proportional heater off	Generation of scram signal or PZR liquid level < 2.3 m
PZR backup heater off	PZR liquid level < 2.3 m
Initiation of core power decay curve simulation	Generation of scram signal
Initiation of primary coolant pump coastdown	Generation of scram signal
Closure of SG main steam stop valve	Generation of scram signal
Manual closure of SG main steam isolation valves	Generation of scram signal
Termination of SG main feedwater	Generation of scram signal
Generation of safety injection (SI) signal	Primary pressure = 12.27 MPa
Initiation of secondary-side depressurization of both SGs as AM action to achieve depressurization rate of 55 K/h in primary system	10 min after SI signal generation
Initiation of auxiliary feedwater injection into secondary-side of both SGs	With some delay after initiation of AM action
Initiation of ACC system in both loops	Primary pressure = 4.51 MPa
Initiation of LPI system in both loops	Pressure vessel lower plenum pressure = 1.24 MPa

Table 3-3 Specified pump rotation speed ratio after scram signal

Time (s)	Rotation Speed Ratio	Time (s)	Rotation Speed Ratio	Time (s)	Rotation Speed Ratio
0	1.000	30	0.280	80	0.125
2	0.850	40	0.220	90	0.110
5	0.730	50	0.185	100	0.100
10	0.540	60	0.160	250	0.000
20	0.370	70	0.140		

Table 3-4 Pre-determined core power decay curve after scram signal

Time (s)	Power (MW)	Time (s)	Power (MW)	Time (s)	Power (MW)
0	10	150	2.589	2000	1.404
18	10	200	2.429	3000	1.262
20	8.316	300	2.246	4000	1.169
30	5.532	400	2.166	5000	1.103
40	4.670	500	2.079	6000	1.052
50	4.072	600	1.998	8000	0.980
60	3.704	800	1.743	10000	0.929
80	3.209	1000	1.653		
100	2.929	1500	1.508		

Table 3-5 Pressure vessel lower plenum pressure versus LPI flow rate

Pressure vessel lower plenum pressure (MPa)	LPI flow rate in loop with PZR (kg/s)	LPI flow rate in loop without PZR (kg/s)
1.24	0.76	0.76
1.20	1.07	1.07
1.15	1.41	1.41
1.10	1.70	1.70
1.05	1.94	1.94
1.0	2.15	2.15
0.9	2.49	2.49
0.8	2.76	2.76

Table 3-6 Pre-determined secondary pressure drop curve after AM action onset

Time (s)	Pressure (MPa)	Time (s)	Pressure (MPa)	Time (s)	Pressure (MPa)
0	7.82	3600	3.24	8100	0.77
60	7.7	4500	2.5	9000	0.54
900	6.35	5400	1.9	10800	0.25
1800	5.11	6030	1.46		
2700	4.06	7200	1.07		

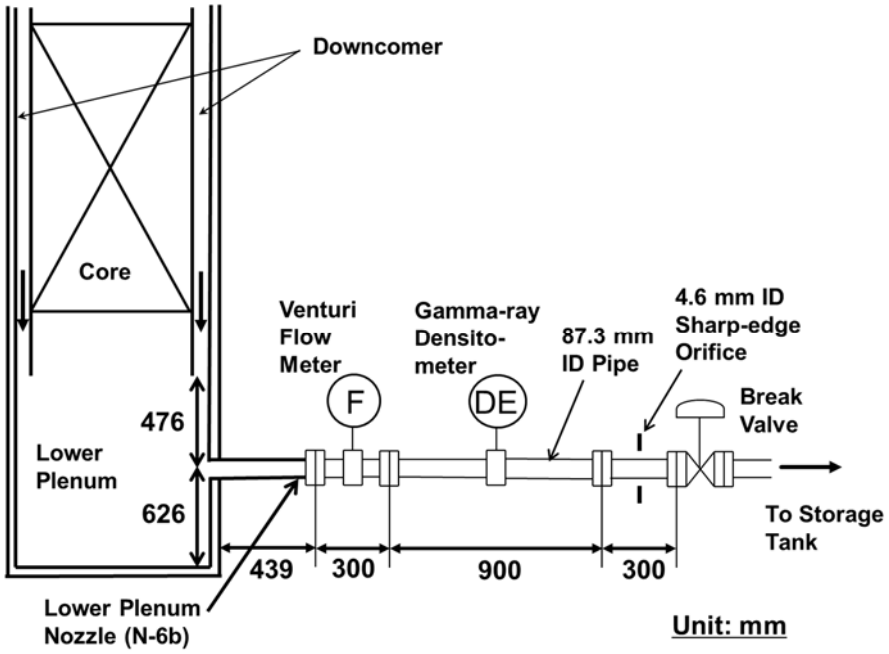

Fig. 3-1 Configuration of break unit

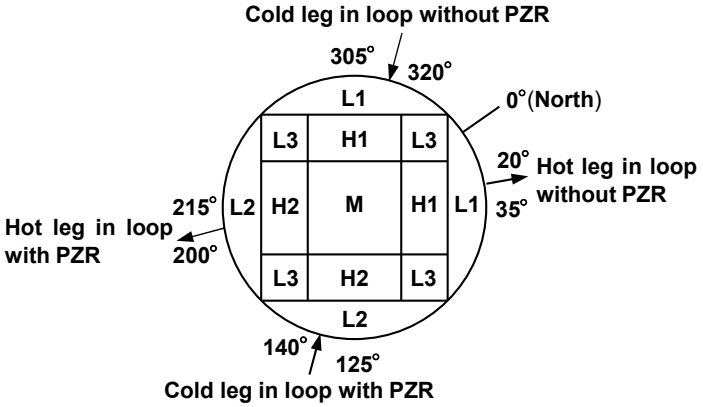

Heater Rod Zone	No. of Heater Rods	Radial Profile = Case 3	
		Peaking Factor	Heater Power
L1 (low-power)	144	0.66	9.69kWx0.66x 144=921kW
L2 (low-power)	144		9.69kWx0.66x 144=921kW
L3 (low-power)	180		9.69kWx0.66x 180=1151kW
H1 (high-power)	180	1.51	9.69kWx1.51x 180=2634kW
H2 (high-power)	180		9.69kWx1.51x 180=2634kW
M (mean-power)	180	1.00	9.69kWx1.00x 180=1744kW

Fig. 3-2 Core heater rod zone and heater power

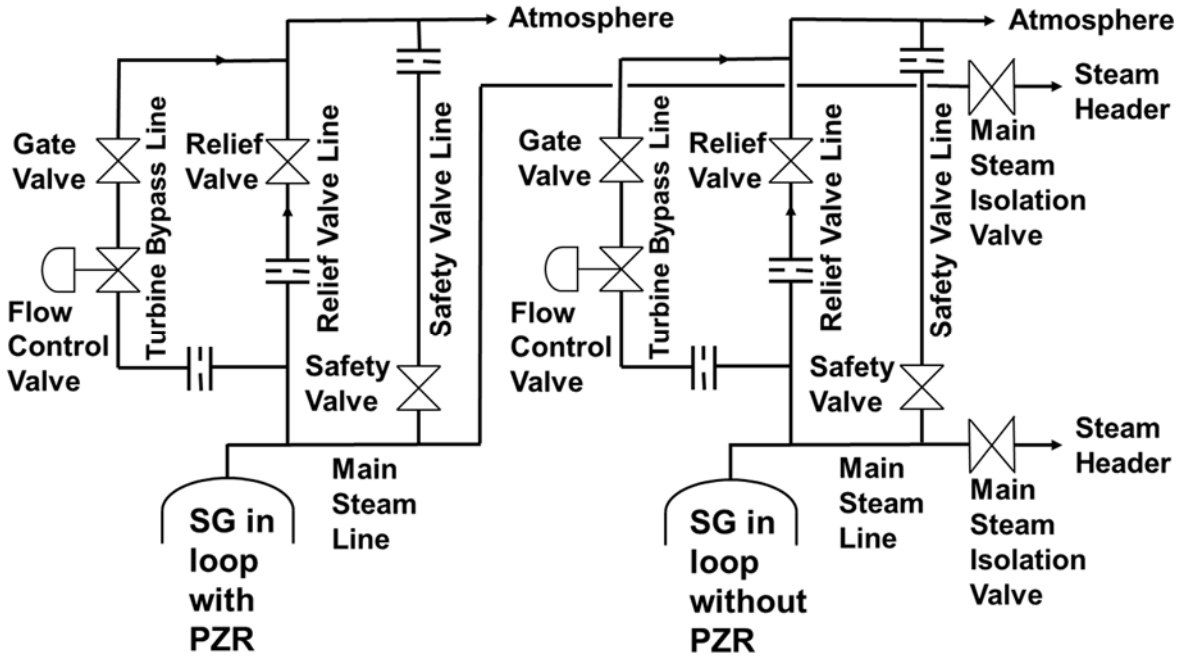

Fig. 3-3 Schematic view of SG steam line

4. Experimental Results

4.1 Initial and Boundary Conditions

Initial steady state conditions achieved in the experiment were in reasonable agreement with the specified values, as mentioned in **Table 4-1**. The measured values indicated are those averaged for the last 60 s prior to the onset of the break. Initial SG re-circulation ratio estimated from the measured flow rates in the downcomer and SG main steam line was 6.5 in loop with PZR (loop-A) and 6.3 in loop without PZR (loop-B). **Table 4-2** shows the chronology of major events until 9935 s when the break valve was closed.

4.2 Thermal-hydraulic Responses Concerning Boundary Conditions

As presented in **Fig. 4-1**, the core power began to decay at 270 s. The core power was automatically reduced by the LSTF core protection system at 9180 s when the maximum cladding surface temperature exceeded 908 K (to be depicted in **Fig. 4-24**). The core power was controlled to 10% of the pre-determined value [22] at 9198 s when the maximum cladding surface temperature reached 920 K. The core power turned off at 9870 s.

As noted in **Fig. 4-2,** the power values of the PZR proportional and backup heaters were initially kept constant at 2.8 kW and 33.7 kW, respectively. After the break, they began to increase up to 8.2 kW and 87.2 kW, respectively. The PZR proportional and backup heater powers turned off by 183 s and 184 s, respectively, because the PZR liquid level became below 2.3 m (as set out in **Fig. 4-3**). The PZR liquid level degraded immediately and monotonously after the break. The PZR became voided by 330 s.

Figures 4-4 and 4-5 show the primary coolant pump rotation speed and the primary loop mass flow rate measured by using a venturi flow meter at each primary coolant pump suction leg, respectively. The pump rotation speed started an increase simultaneously with the break, and attained about 1550 rpm in 4 s. The pump coastdown initiated at 252 s, following the scram signal. The pump rotation speed reduced thereafter, which led to a decrease in the primary loop mass flow rate. The primary loop was in two-phase natural circulation following the primary coolant pumps stop. The primary loop mass flow rate gradually declined after water column drained in instrumented SG U-tubes in non-uniform manner (to be plotted in **Figs. 4-42 through 4-45**). The primary loop mass flow rate oscillated during intermittent ACC coolant injection periods (to be presented in **Fig. 4-13**). After the termination of the ACC coolant injection, the primary loop mass flow rate became close to zero, suggesting that reflux condensation should occur in the SG U-tubes (to be noted in **Figs. 4-42 through 4-45**).

Figures 4-6 and 4-7 show the SG main steam and feedwater flow rates, respectively. The SG main steam was terminated by the closure of the SG main steam stop valve [Valve No.;

AOV-220] (see p.113 in Ref. [7]) at 250 s concurrently with the scram signal. The main feedwater injection into the secondary-side of both SGs was ended by the closure of the SG main feedwater line valve [Valve No.; AOV-260] (see p.113 in Ref. [7]) at 253 s, following the scram signal. The main steam isolation valves of both SGs [Valve No.; AOV-170 and AOV-200] (see pp.111-112 in Ref. [7]) were manually closed at 280 s, following the SG main steam stop valve closure.

Figures 4-8 and 4-9 show the SG secondary-side collapsed liquid level and AFW flow rate, respectively. The SG secondary-side liquid level began to rise after the main steam stop valve closure and the main feedwater termination (**Figs. 4-6 and 4-7**). This seems to be attributed to the decrease in the net upward steam flow through the SG boiling section. The SG secondary-side liquid level gradually dropped with some fluctuation owing to cyclic opening of the SG relief valves (to be indicated in **Fig. 4-17**). During the time period other than the AFW pump operation, flow meter (see pp.257-258 in Ref. [7]) for AFW counts flow rate in the return line from the AFW pump to the refueling water storage tank. The AFW injection into the secondary-side of both SGs was initiated at 950 s following the AM action onset, and terminated at 2750 s. The AFW flow rate into the SG secondary-side was about 0.59-0.60 kg/s in loop with PZR and about 0.72-0.73 kg/s in loop without PZR. The SG secondary-side liquid level steadily increased after the AFW injection start. The reason is that the AFW flow rate was greater than the steam discharge flow rate through the SG flow control valve employed for the AM action. The SG secondary-side liquid level turned to fall after the end of the AFW injection. The liquid level difference in the secondary-side of both SGs was the largest at the AFW injection termination, and then descended little by little. The SG secondary-side was not emptied of liquid throughout the experiment, which produced continuous heat removal from the SG secondary-side system.

The break unit as illustrated in **Fig. 3-1** is located at about 1.7 m below the core bottom (see p.194 in Ref. [7]). **Figure 4-10** shows the time-integrated break flow evaluated from the liquid level increase in the storage tank, and the break flow rate derived as the differential of the time-integrated break flow. **Figure 4-11** depicts the lower plenum fluid temperatures at 0.3 m, 1.5 m, 1.8 m, and 2.1 m below the core bottom. The break flow rate reduced roughly stepwise. The break flow turned from single-phase liquid to two-phase flow at around 1300 s because the lower plenum fluid became saturated. This brought about a decrease in the break flow rate. The break flow returned to single-phase liquid at around 9300 s after the actuation of the LPI system (to be mentioned in **Fig. 4-15**).

Figure 4-12 shows the liquid level in the ACC tank. **Figures 4-13 and 4-14** give the coolant injection flow rate from the ACC tank derived from the liquid level history in the ACC tank. Another name for the ACC tank in loop with PZR is ACC-cold tank, while that for the ACC tank

in loop without PZR is ACC-hot tank. The coolant injection temperature is 320 K in both the ACC-cold tank and ACC-hot tank, but the heater capacity of the ACC-hot tank is designed to be twice that of the ACC-cold tank. When the primary pressure lowered to 4.53 MPa, the ACC system initiated at 3230 s in loop with PZR and 3250 s in loop without PZR. The initial water level above the ACC tank bottom was 6.72 m in loop with PZR and 6.73 m in loop without PZR. The final water level above the ACC tank bottom was 5.28 m in loop with PZR and 5.24 m in loop without PZR. When the primary pressure dropped to about 1.6 MPa, the ACC system ended at 6740 s in loop with PZR and 7100 s in loop without PZR. The coolant injection periods from the ACC-cold tank included around 3230-5800 s, 5850-5910 s, 5960-6030 s, 6060-6150 s, 6200-6450 s, and 6590-6740 s. On the other hand, the coolant injection periods from the ACC-hot tank contained around 3250-5800 s, 5850-5910 s, 5960-6030 s, 6060-6150 s, 6200-6450 s, 6590-6830 s, and 7030-7100 s.

When the pressure vessel lower plenum pressure reduced to 1.23 MPa, coolant was fed from the LPI system into both cold legs at 9280 s in accordance with the discharge pressure of the LPI pump, as set out in **Fig. 4-15**.

4.3 Transient Thermal-hydraulic Responses

Figure 4-16 shows the primary and secondary pressures. The primary pressure initiated a decrease at time zero when the break valve was opened. Small size of break resulted in a slow primary depressurization. When the primary pressure lowered to 12.97 MPa, the scram signal was generated at 250 s. This gave rise to the closure of the SG main steam stop valve, the coastdown of the primary coolant pumps, the termination of the SG main feedwater, and the manual closure of the SG main steam isolation valves. The SG secondary-side pressure rapidly raised up to about 8 MPa after the closure of the SG main steam stop valve. The SG secondary-side pressure fluctuated between 8.03 MPa and 7.82 MPa. This is because the relief valves of both SGs cyclically opened during the time period of around 200-950 s, as presented in **Fig. 4-17**. When the primary pressure dropped to 12.27 MPa, the SI signal was obtained. Secondary-side depressurization of both SGs as the AM action to achieve the primary depressurization rate of 55 K/h was undertaken at 945 s: 10 min after the SI signal generation, and went on afterwards. The primary pressure fell following the SG secondary-side pressure after the AM action onset, which led to the activation of the ACC system (**Figs. 4-13 and 4-14**). When the primary pressure declined to about 1.6 MPa, the ACC system was completed. As plotted in **Fig. 4-16**, the primary depressurization rate decreased and thus the pressure difference increased between the primary and SG secondary sides after around 7200 s. This was induced by the accumulation of nitrogen gas in the SG U-tubes (to be described in **Section 4.3.3**). Nitrogen gas enters cold legs through the ECCS nozzles first, and then migrates to hot legs through downcomer and bypass lines simulating hot leg leakage that

connect the downcomer to the hot legs (as denoted in **Chapter 2**). Nitrogen gas finally flows into the SG U-tubes. The nitrogen gas accumulation implies degradation in the condensation heat transfer in the SG U-tubes. After the initiation of the automatic core power reduction at 9180 s, the LPI system was actuated in both loop at 9280 s (**Fig. 4-15**).

The major components of the LSTF, whose thermal-hydraulic responses are described below, can be seen in **Fig. 2-2**.

4.3.1 Thermal-hydraulic Responses in Pressure Vessel

Liquid level behaviors in upper plenum and core

The upper plenum collapsed liquid level is shown in **Figs. 4-18 and 4-19**, while the core collapsed liquid level is given in **Figs. 4-20 and 4-21**. A small drop began in the core liquid level at 4710 s after the upper plenum became empty of liquid at 4670 s. The cladding surface temperature increase at Position 9 (near the core top) remained at about 8 K at around 5450-5785 s (to be depicted in **Fig. 4-25**). The liquid levels recovered in the upper plenum and core in oscillative way because of the periodic coolant injection from the ACC system into both cold legs (**Figs. 4-13 and 4-14**). The upper plenum became voided again at 8300 s, following the primary coolant inventory depletion after the termination of the ACC system. A significant depression started in the core liquid level at 8340 s. Core uncovery thus took place owing to core boil-off at 8575 s (to be noted in **Figs. 4-24, 4-26, and 4-28**). The core liquid level abruptly increased after the actuation of the LPI system at 9280 s (**Fig. 4-15**). The entire core was quenched by 9682 s (to be presented in **Figs. 4-24 and 4-26**). The liquid level recovered in the upper plenum at around 9730 s.

Responses of core exit temperature (CET) and cladding surface temperature of simulated fuel rods

Figures 4-22 and 4-23 show the typical CETs at the center [Tag Name; TE-EX040-B21-UCP, -B23-UCP], peripheral region [TE-EX040-B11-UCP, -B14-UCP], and outer region [TE-EX040-B01-UCP, -B02-UCP] of upper core plate (UCP). The representative CETs account for the first and second highest CETs at each region of UCP. Thickness of UCP is 76.2 mm. The core exit thermocouples are installed 13 mm above the upper surface of UCP. The vertical and radial measurement positions of the CETs are presented in Ref. [7] (pp.377-378) and Ref. [7] (pp.385-386), respectively. The CETs were maintained saturated until 9180 s even after the core uncovery began partly at 8575 s (to be set out in **Fig. 4-28**). This was ascribed to condensate falling from hot leg nozzles (see p.196 in Ref. [7]). Subsequently, the CETs started to rise. The CET was elevated to 510 K, which was not above the initial value. Therefore, the CET increase remained at about 45 K. The CET, which recorded 510 K, was seen at the center [TE-EX040-B23-UCP] of UCP located above the B23 rod bundle at 9680 s. The CETs were kept saturated again after around 9725 s.

Figures 4-24 through 4-26 show the typical cladding surface temperatures of the simulated fuel rods at Positions 9 through 1. Positions 9, 8, 7, 6, 5, 4, 3, 2, and 1 are placed at 3.610 m, 3.048 m, 2.642 m, 2.236 m, 1.830 m, 1.242 m, 1.108 m, 0.612 m, and 0.050 m, respectively, above the core bottom (see p.222 in Ref. [7]). The representative cladding surface temperatures stand for the cladding surface temperatures of the rod bundles where the highest temperature emerges at each position. The arrangement of high-, mean-, and low-power rod bundles is presented in Ref. [7] (p.228). The cladding surface temperatures were affected by the axial core power profile (i.e., the 9-step chopped cosine) and the core liquid level behavior (**Figs. 4-20 and 4-21**). No cladding surface temperatures at Positions 2 and 1 rose. During the core uncovery period the cladding surface temperatures at Positions 9, 8, 7, 6, 5, 4, and 3 began to increase at 8695 s, 8575 s, 8655 s, 8755 s, 8860 s, 8960 s, and 9110 s, respectively. The core power was controlled to 10% of the pre-determined value at the maximum cladding surface temperature of 920 K (**Fig. 4-1**). Just after that, the peak cladding temperature of 925 K was observed at Position 6. The maximum cladding surface temperatures at Positions 9, 8, 7, 5, 4, and 3 were 629 K, 779 K, 913 K, 862 K, 738 K, and 568 K, respectively. They reached at 9595 s, 9560 s, 9200 s, 9200 s, 9200 s, and 9205 s, respectively. The whole core was quenched by 9682 s due to the core liquid level recovery because of coolant injection from the LPI system into both cold legs.

Figures 4-27, 4-28, 4-29, 4-30, 4-31, 4-32, and 4-33 show the distributions of the cladding surface temperatures of the simulated fuel rods at Positions 9, 8, 7, 6, 5, 4, and 3, respectively. At Position 9 (**Fig. 4-27**), the cladding surface temperatures rose earlier in the order of the B17, B22, and B08 rod bundles. The maximum cladding surface temperature was higher in the order of the B17, B22, and B08 rod bundles. The quenching of the cladding surfaces of the B08, B17, and B22 rod bundles was simultaneous.

At Position 8 (**Fig. 4-28**), the cladding surface temperature increases were earlier in the order of the B13, B10, and B03 rod bundles. The maximum cladding surface temperature was higher in the order of the B13, B10, and B03 rod bundles. The cladding surfaces of B03, B10, and B13 rod bundles were quenched at the same time.

At Position 7 (**Fig. 4-29**), the cladding surface temperature rises of the B13 and B17 were simultaneous, and were earlier than those of other rod bundles. The cladding surface temperatures increased faster in the order of the B10, B08, and B03 rod bundles. The maximum cladding surface temperature was higher in the order of the B13, B17, B22, B10, B08, and B03 rod bundles. The quenching of the cladding surface of the B03 rod bundle was a little earlier than that of other rod bundles.

At Position 6 (**Fig. 4-30**), the cladding surface temperatures increased earlier in the order of the B13, B10, and B03 rod bundles. The maximum cladding surface temperature was higher

in the order of the B13, B10, and B03 rod bundles. The cladding surfaces of B03, B10, and B13 rod bundles were quenched at the same time.

At Position 5 (**Fig. 4-31**), the cladding surface temperatures of the B08, B17, and B22 rod bundles rose at the same time. The maximum cladding surface temperature was higher in the order of the B17, B22, and B08 rod bundles. The quenching of the cladding surfaces of the B08, B17, and B22 rod bundles was simultaneous.

At Position 4 (**Fig. 4-32**), the cladding surface temperatures of the B03, B10, and B13 rod bundles increased simultaneously. The maximum cladding surface temperature was higher in the order of the B13, B10, and B03 rod bundles. The cladding surfaces of the B03, B10, and B13 rod bundles were quenched at the same time.

At Position 3 (**Fig. 4-33**), the cladding surface temperatures of the B08, B17, and B22 rod bundles rose at the same time. The maximum cladding surface temperature was higher in the order of the B17, B22, and B08 rod bundles. The quenching of the cladding surfaces of the B08, B17, and B22 rod bundles was simultaneous.

Coolant behaviors in pressure vessel

Figure 4-34 shows the downcomer collapsed liquid level. The liquid level formed in the downcomer at 560 s. Similar to the core liquid level after the emptying of the upper plenum, a small reduction appeared in the downcomer liquid level (**Figs. 4-20 and 4-21**). The oscillating recovery was seen in the downcomer liquid level resulting from the periodic coolant injection from the ACC system into both cold legs (**Figs. 4-13 and 4-14**). A notable drop initiated in the downcomer liquid level at 7810 s. The downcomer liquid level recovered at 9320 s with the coolant injection from the LPI system into the cold legs (**Fig. 4-15**).

Figure 4-35 shows the upper-head collapsed liquid level. An abrupt depression started in the upper-head liquid level at 430 s. After 940 s the upper-head liquid level was maintained at around 0.07-0.12 m, except for the intermittent ACC coolant injection periods.

4.3.2 Thermal-hydraulic Responses in Primary Loops

Figures 4-36 and 4-37 show the liquid levels and fluid temperatures in the hot legs, respectively. The hot leg liquid level is estimated from the fluid densities measured by use of a three-beam gamma-ray densitometer. The hot leg fluid became saturated at 360 s almost concurrently with the liquid level formation in the hot leg. The liquid level in the hot leg with an inner-diameter of 0.207 m was kept at around 0.12-0.14 m in both loops at around 1390-3650 s. The hot leg liquid level became close to zero at 4000 s after an abrupt decrease initiated in the upper plenum liquid level at 3960 s (**Figs. 4-18 and 4-19**). The liquid level recovery was oscillative in the hot leg with the periodic ACC coolant injection into the cold leg (**Figs. 4-13**

and 4-14). The hot leg fluid temperature indicated superheating after around 8800 s because the hot leg liquid level became close to zero again.

Figure 4-38 and 4-39 show the liquid levels and fluid temperatures in the cold legs, respectively. The cold leg liquid level is evaluated from the fluid densities measured by means of a three-beam gamma-ray densitometer. The cold legs were filled with subcooled water until the primary pressure dropped to around 10 MPa (**Fig. 4-16**). The liquid levels formed in the cold legs at 680 s. When the liquid level in the cold leg with an inner-diameter of 0.207 m depressed to around 0.16 m, the cold leg fluid became saturated. The cold leg liquid level dropped to around 0.02 m thereafter. The oscillating recovery was observed in the cold leg liquid level with the intermittent ACC coolant injection into the cold leg (**Figs. 4-13 and 4-14**). The cold leg fluid temperature showed some superheating after around 7500 s especially in loop with PZR because the cold leg became empty of liquid. After the activation of the LPI system (**Fig. 4-15**), the recovery in the cold leg liquid level brought about the reduction in the cold leg fluid temperature.

Figures 4-40 and 4-41 show the collapsed liquid levels in the downflow-side and upflow-side of the crossover legs, respectively. The crossover leg downflow-side liquid level started to drop at 2380 s in loop with PZR and 2960 s in loop without PZR. A large decline laid in the crossover leg liquid level at 5730 s in the downflow-side and 5780 s in the upflow-side. During the intermittent ACC coolant injection periods (**Figs. 4-13 and 4-14**) the liquid levels in the downflow-side and upflow-side of the crossover legs decreased and increased, respectively.

4.3.3 Thermal-hydraulic Responses of Steam Generators

Figures 4-42 through 4-45 show the collapsed liquid levels in the instrumented SG U-tubes. The instrumented SG U-tubes designated as Tubes 1 and 6 are short tubes (Type 1; see p.267 in Ref. [7]), Tubes 2 and 5 are medium tubes (Type 5), and Tubes 3 and 4 are long tubes (Type 9). The liquid level in the upflow-side balanced that in the downflow-side for each SG U-tube. Non-uniform flow behaviors were seen in the SG U-tubes. The trend of the liquid level change was mostly similar for the two same-length SG U-tubes consisting of short, medium, and long tubes. The liquid level behaviors in the SG U-tubes were asymmetrical between two loops. The liquid level drop in the downflow-side and upflow-side of the SG U-tubes continued down to the crossover leg downflow-side (**Fig. 4-40**) and the SG inlet plenum (to be plotted in **Fig. 4-50**), respectively. The SG U-tubes were emptied of liquid the earliest in Tube 1 or Tube 6 and the latest in Tube 2.

To investigate the accumulating status of nitrogen gas in the SG U-tube, nitrogen gas mole fraction M in the steam-gas mixture is expressed by

$$\mathrm{M} = \frac{P - P_S}{P} \quad (1)$$

where P is the total pressure of the steam-gas mixture that is represented by the PZR pressure (**Fig. 4-16**). P_S is the steam pressure that is equivalent to the steam saturation pressure based on the SG U-tube fluid temperature by assuming 100% relative humidity of saturated steam in the steam-gas mixture. The fluid temperatures in the downflow-side of the SG U-tubes at Position 1 (= at 0.811 m above the SG U-tube bottom) were chosen as the SG U-tube fluid temperatures for evaluating the nitrogen gas mole fraction. This selection considered that the SG U-tubes remained empty of liquid after the termination of the ACC system (**Figs. 4-42 through 4-45**). **Figures 4-46 and 4-47** show the fluid temperatures at Position 1 in the downflow-side of the SG U-tubes in loops with and without PZR, respectively, from 7200 s to 8800 s. Here, the fluid temperatures of Tube 4 (one of two long tubes) in loop with PZR and Tube 5 (one of two medium tubes) in loop without PZR were unavailable on account of the bad trends. The tendency of the fluid temperature variation among the SG U-tubes was similar, except for the long tube around 7550-7750 s. The SG U-tube fluid temperature was lower in loop without PZR than in loop with PZR. **Figures 4-48 and 4-49** show the estimated nitrogen gas mole fractions of the SG U-tubes in loops with and without PZR, respectively. The nitrogen gas mole fractions of the SG U-tubes exceeded zero at around 7200 s. The nitrogen gas mole fraction of the SG U-tube in loop without PZR was generally greater than that in loop with PZR. The reason is that the steam pressure P_S was lower in loop without PZR than in loop with PZR, relying on the SG U-tube fluid temperature. For example, the nitrogen gas mole fractions of the SG U-tubes in loops with and without PZR were evaluated to be approximately 0.35 and 0.38, respectively, at around 8600 s (i.e., at early stage of the cladding surface temperature rise).

Figure 4-50 shows the SG inlet plenum collapsed liquid level. A substantial depression initiated in the SG inlet plenum liquid level at 2400 s in loop with PZR and 2980 s in loop without PZR. The SG inlet plenum became empty of liquid at 3000 s in loop with PZR and 3640 s in loop without PZR. The SG inlet plenum liquid level recovered up to about 0.2 m at 7230-7360 s in loop with PZR and about 0.4 m at 7230-7560 s in loop without PZR. The liquid level behavior of the SG inlet plenum was in response to that of the hot leg (**Figs. 4-36 and 4-37**).

Figures 4-51 and 4-52 show the SG secondary-side fluid temperatures in loops with and without PZR, respectively. Positions 1, 3, 5, 7, and 9 are placed at 0.811 m, 2.101 m, 3.381 m, 5.941 m, and 8.501 m, respectively, above the SG U-tube bottom. The SG secondary-side fluid temperature is dependent on the SG secondary-side liquid level. The SG secondary-side fluid temperature at Position 1 was held saturated. The reason is that the SG secondary-side liquid level remained at around 0.8 m when the LPI system was actuated in both loops (**Figs. 4-8 and 4-15**). The SG secondary-side fluid temperatures at Positions 3, 5, 7, and 9 indicated

superheating after 9280 s, 8580 s, 7000 s, and 5400 s, respectively, in loop with PZR. By contrast, the SG secondary-side fluid temperatures at Positions 3, 5, 7, and 9 showed superheating after 6000 s, 8850 s, 9360 s, and 9340 s, respectively, in loop without PZR.

Table 4-1 Initial steady state conditions

Items	Tag Name (Loops with / without PZR)	Specified (Loops with / without PZR)	Measured *1 (Loops with / without PZR)
Pressure vessel			
Core power (MW)	WE270A-T	10.0±0.07	10.07
Downcomer-to-upper head bypass (%)	None	0.3	Not Measured
Primary loop			
Hot leg fluid temperature (K)	TE020C-HLA /TE160C-HLB	598.1±2.75	598.6 / 598.2
Cold leg fluid temperature (K)	TE070C-CLA /TE210C-CLB	562.4±2.75	563.8 / 563.4
Mass flow rate (kg/s / loop)	FE020A-LSA / FE160A-LSB	24.3±1.25	24.70 / 24.30
Downcomer-to-hot leg bypass (kg/s)	FE010-HLA / FE150-HLB	0.049±0.01	0.049 / 0.044
PZR			
Pressure (MPa)	PE300A-PR	15.5±0.108	15.53
Liquid level (m)	LE280-PR	7.2±0.25	7.27
Steam generator			
Secondary-side pressure (MPa)	PE430-SGA / PE450-SGB	7.3±0.054	7.37 / 7.40
Secondary-side liquid level (m)	LE430-SGA / LE450-SGB	10.3±0.38	10.23 / 10.21
Steam flow rate (kg/s)	FE440-SGA / FE480-SGB	2.74±0.10	2.67 / 2.59
Main feedwater flow rate (kg/s)	FE430-SGA / FE470-SGB	2.74±0.05	2.79 / 2.62
Main feedwater temperature (K)	TE430-SGA / TE470-SGB	495.2±2.63	495.4 / 495.2
Auxiliary feedwater temperature (K)	TE880-RWST	310±2.37	309.4
Accumulator system			
Pressure (MPa)	PE650-ACC / PE660-ACH	4.51±0.054	4.53 / 4.53
Temperature (K)	TE660-ACC / TE700-ACH	320±2.3 / 2.4	321.7 / 322.8
Water level above tank bottom (m) *2	LE650-ACC / LE660-ACH	6.8±0.12/0.15	6.72 / 6.73
Low pressure injection system			
Temperature (K)	TE840-PL	310±2.63	309.9

*1 Averaged for 60 s (-60 to 0 s)

*2 Distance from standpipe top to tank bottom is 5.22 m.

Table 4-2 Chronology of major events until break valve closure

Time (s)	Event
0	Break valve open, start of primary coolant pumps rotation speed increase (to 1550 rpm in 4 s)
250	Scram signal generation, closure of SG main steam stop valve
252	Initiation of coastdown of primary coolant pumps
253	Termination of SG main feedwater
270	Initiation of core power decay
280	Manual closure of SG main steam isolation valves
300-950	Cyclic opening of relief valves in both SGs
340	Safety injection signal generation
500	Stop of primary coolant pumps
945	Initiation of secondary-side of both SGs as AM action to achieve depressurization rate of 55 K/h in primary system
950	Initiation of AFW injection into secondary-side of both SGs
2750	Termination of AFW injection into secondary-side of both SGs
3230	Initiation of ACC system in loop with PZR
3250	Initiation of ACC system in loop without PZR
4670	Upper plenum became empty of liquid.
5450-5785	Cladding surface temperature increase at Position 9 remained at about 8 K.
6740	Termination of ACC system in loop with PZR
7100	Termination of ACC system in loop without PZR
7200	Start of degradation in primary depressurization after nitrogen gas inflow
8300	Upper plenum became empty of liquid again.
8575	Start of increase in cladding surface temperature at Position 8
9180	Initiation of automatic core power reduction at maximum cladding surface temperature of 908 K
9198	Core power was controlled to 10% of pre-determined value at maximum cladding surface temperature of 920 K.
9200	Peak cladding temperature of 925 K was observed at Position 6.
9280	Initiation of LPI system in both loops
9680	Core exit temperature, which recorded 510 K, was seen at center of upper core plate.
9682	Whole core quench
9870	Core power off
9935	Break valve closure

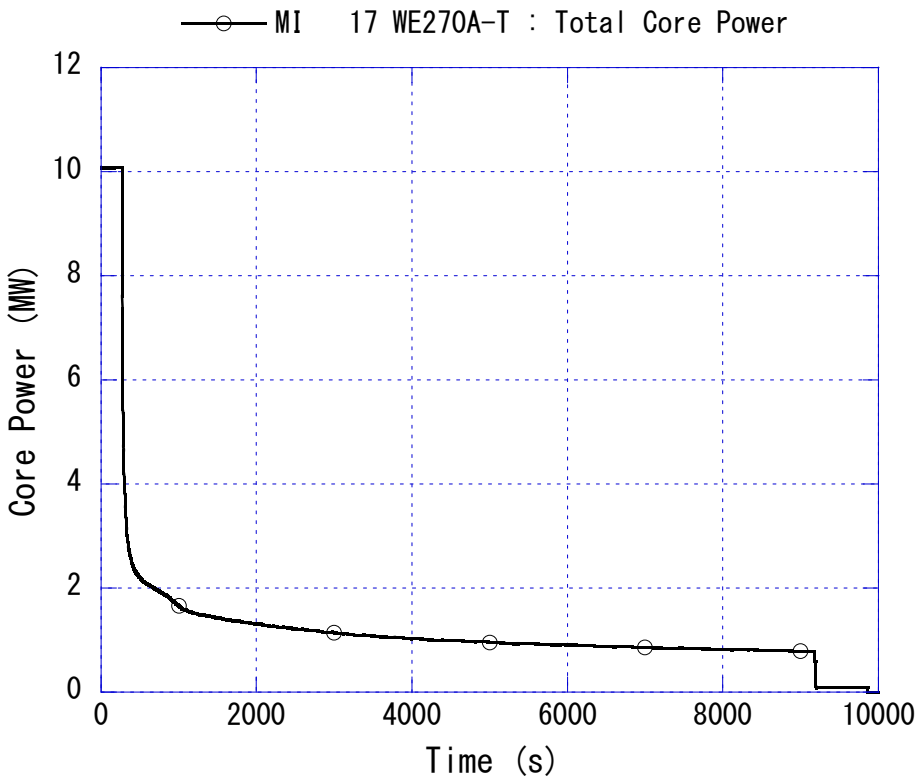

Fig. 4-1 Core power

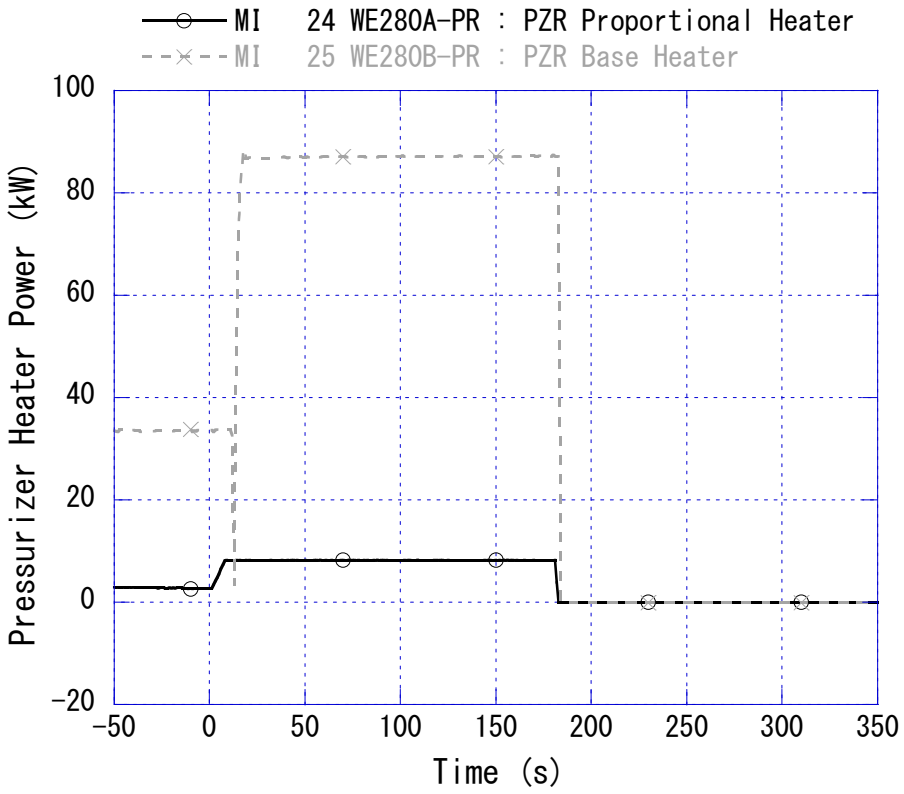

Fig. 4-2 Pressurizer heater power

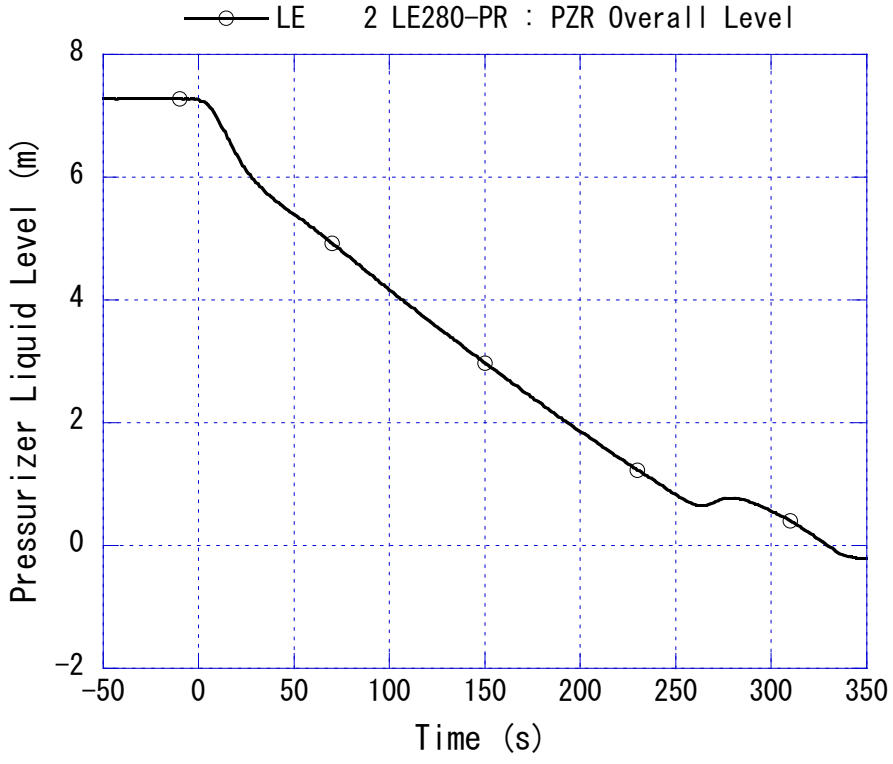

Fig. 4-3 Pressurizer liquid level

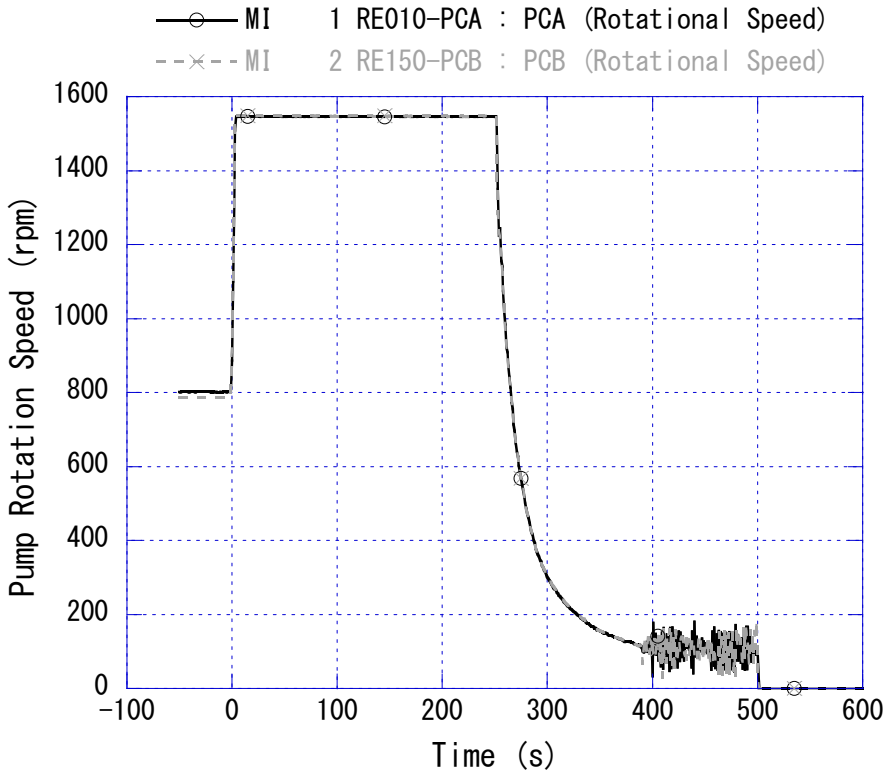

Fig. 4-4 Primary coolant pump rotation speed

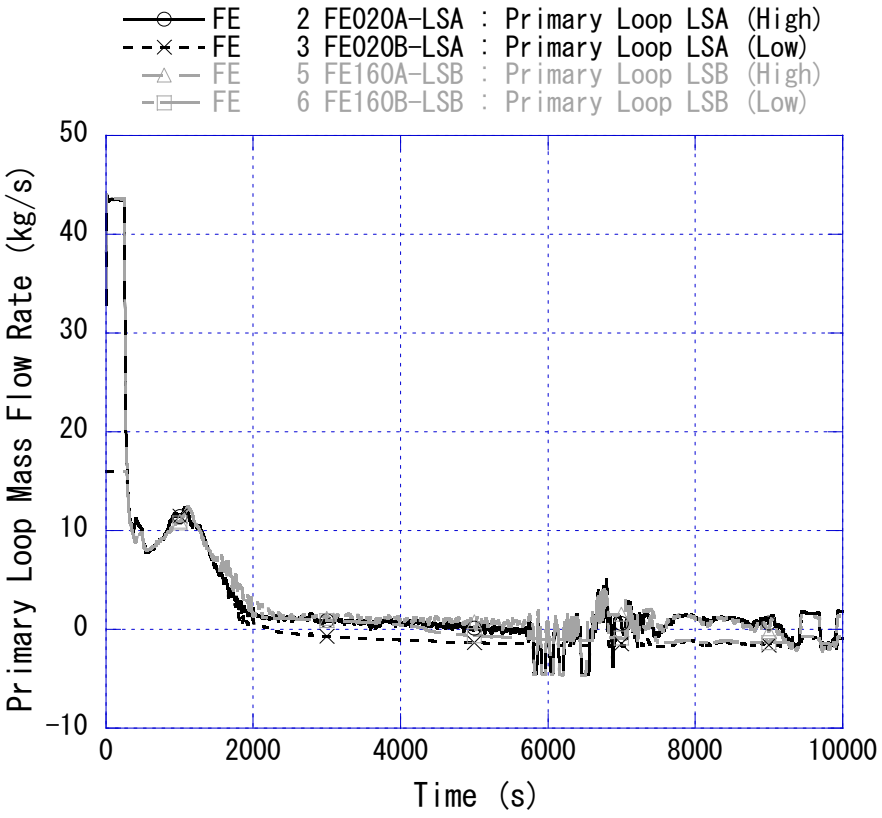

Fig. 4-5 Primary loop mass flow rate

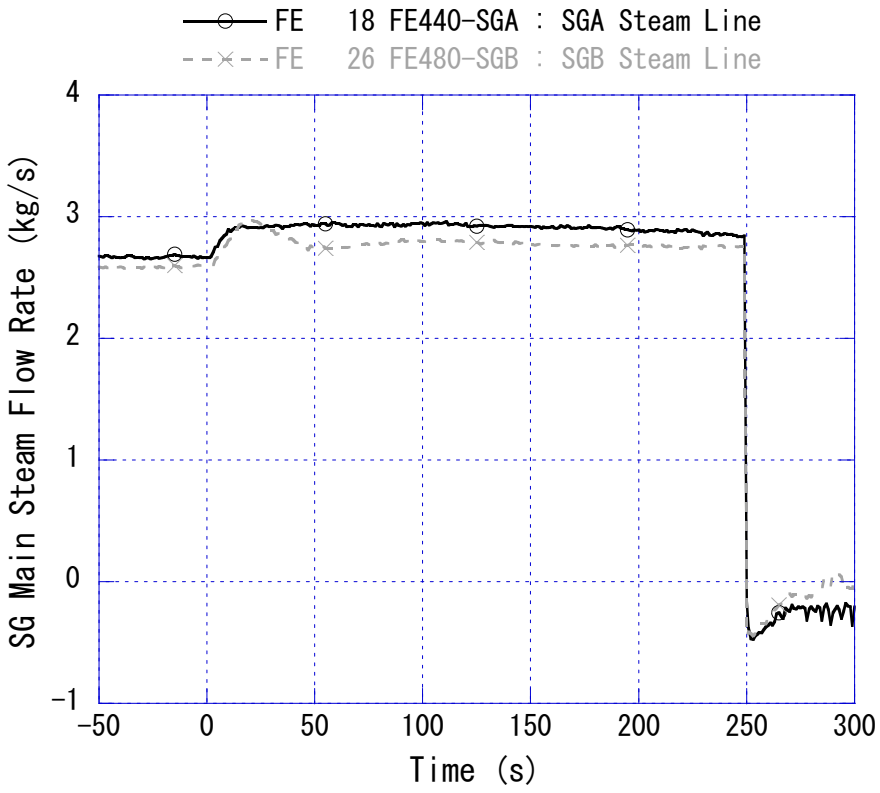

Fig. 4-6 SG main steam flow rate

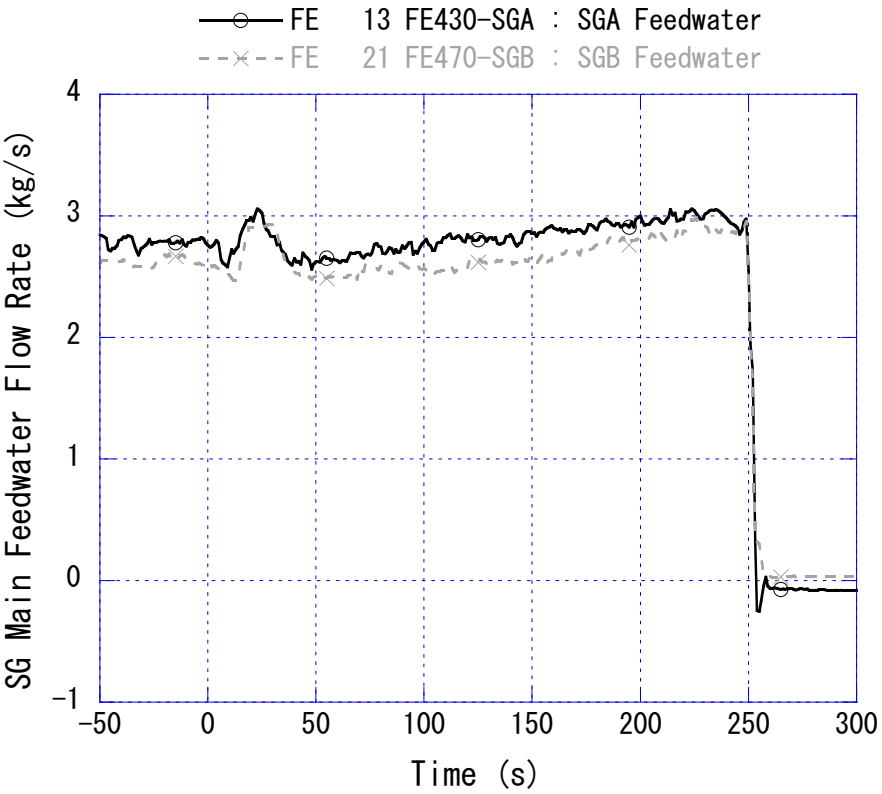

Fig. 4-7 SG main feedwater flow rate

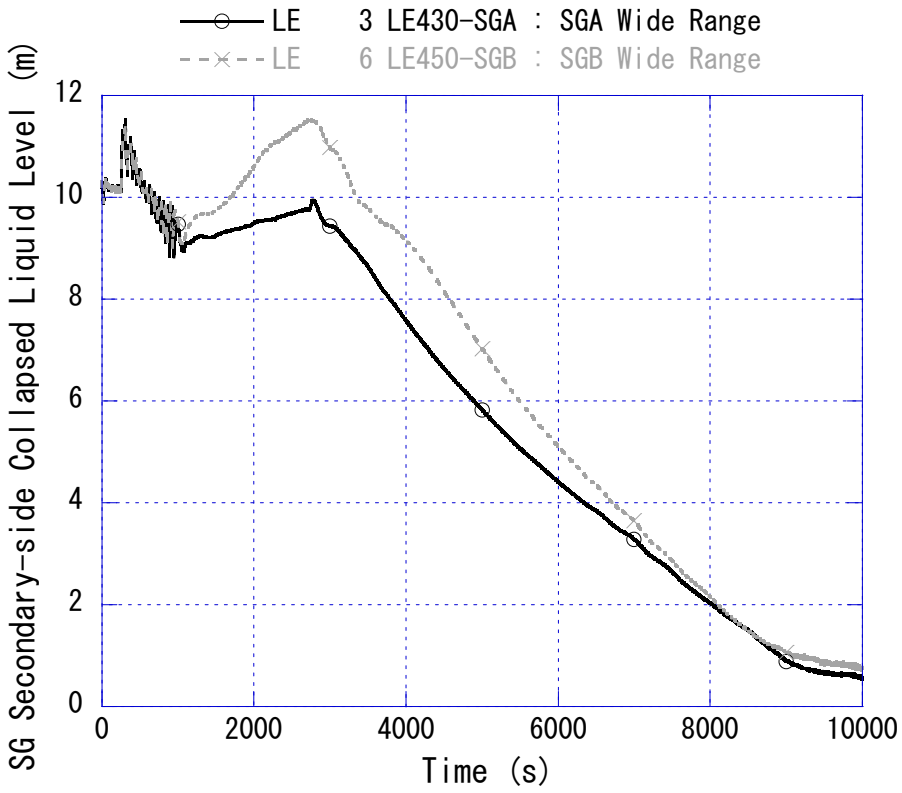

Fig. 4-8 SG secondary-side collapsed liquid level

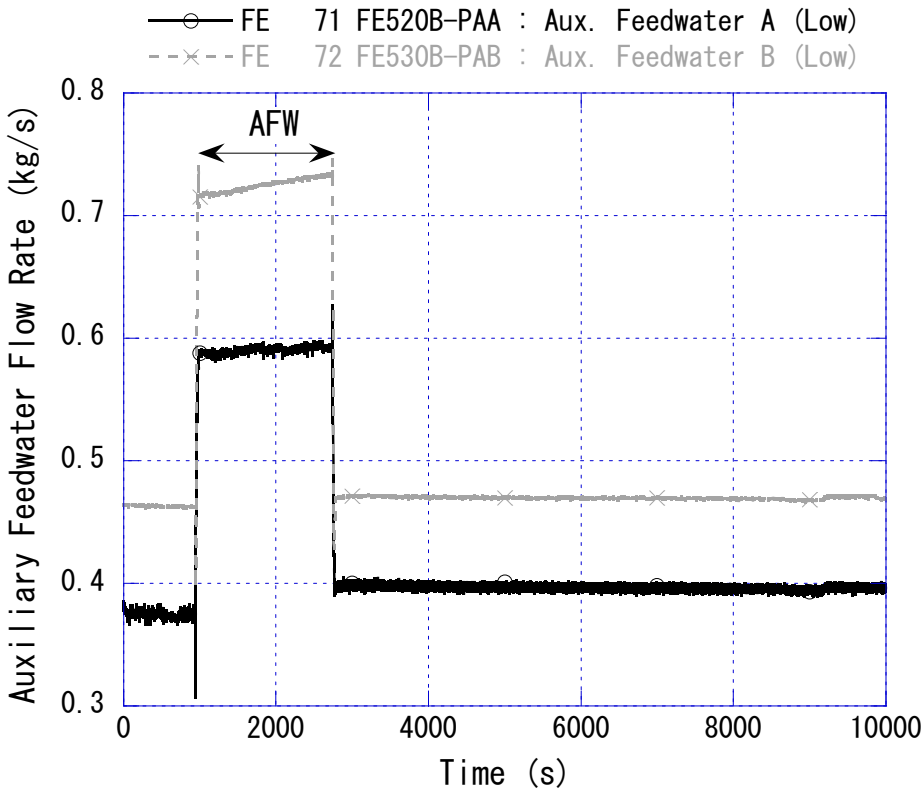

Fig. 4-9 Auxiliary feedwater flow rate

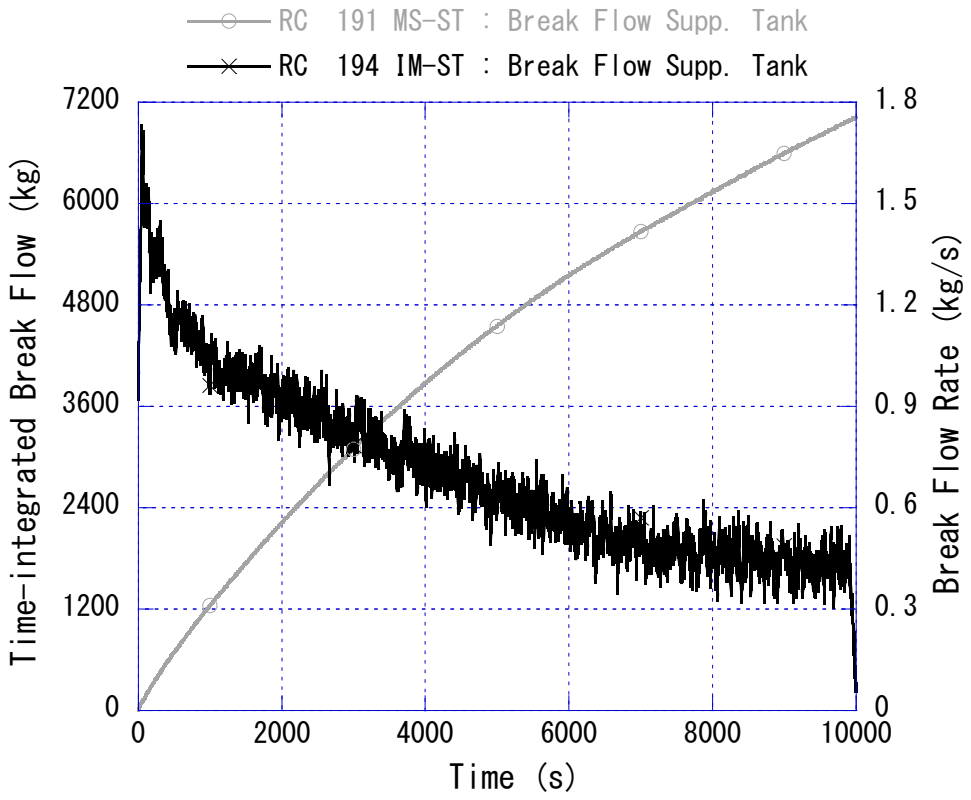

Fig. 4-10 Time-integrated break flow and break flow rate

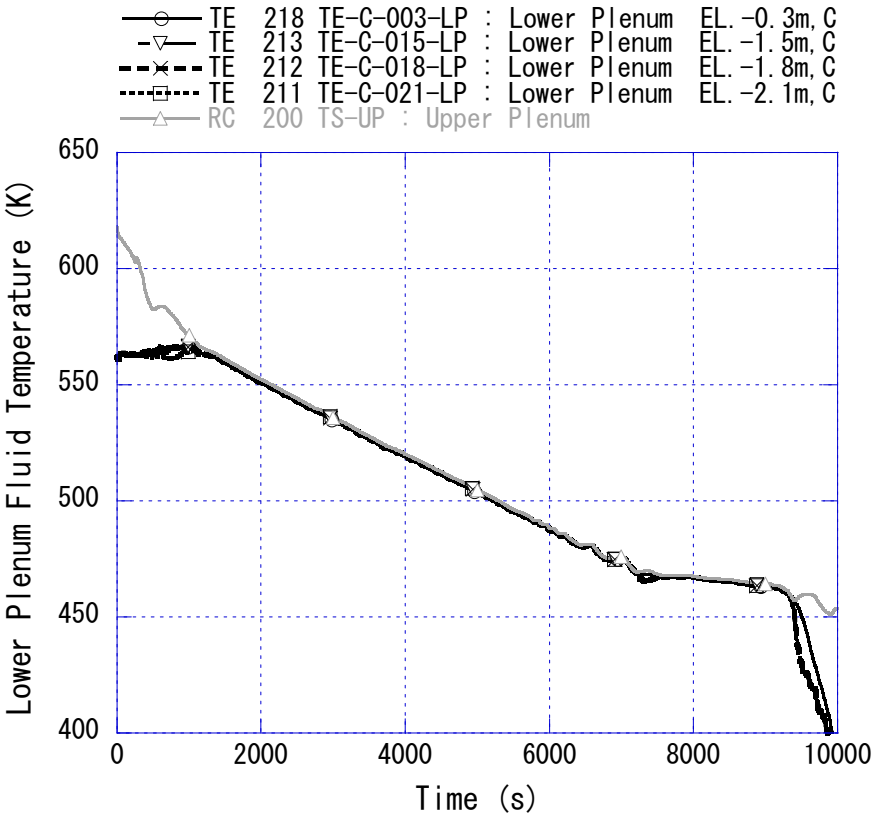

Fig. 4-11 Lower plenum fluid temperature

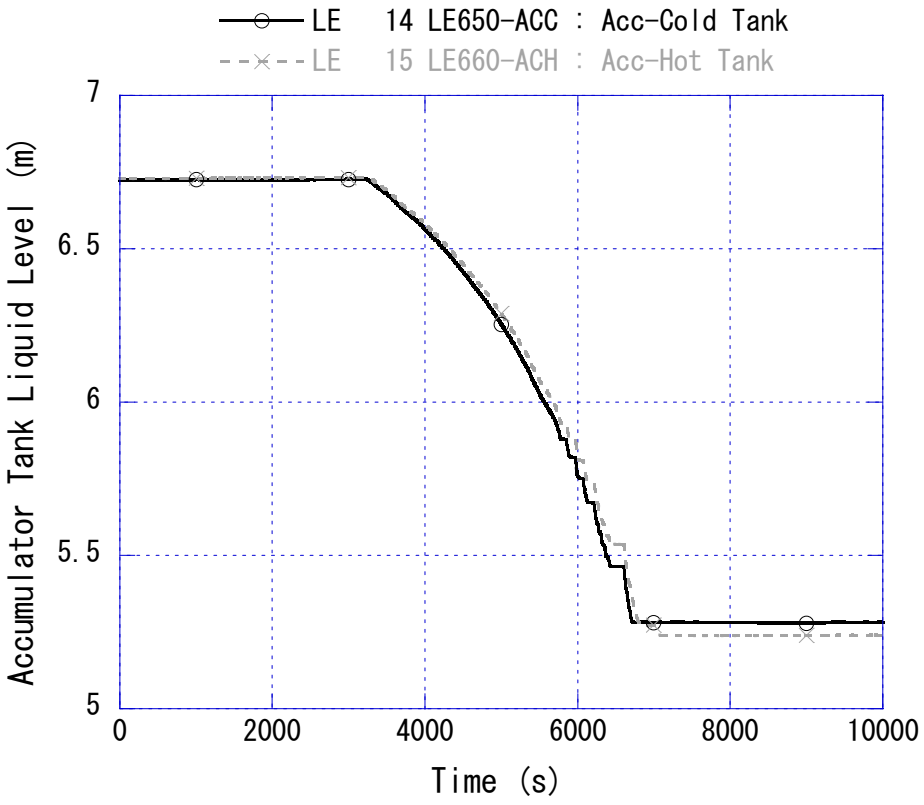

Fig. 4-12 Liquid level in accumulator tank

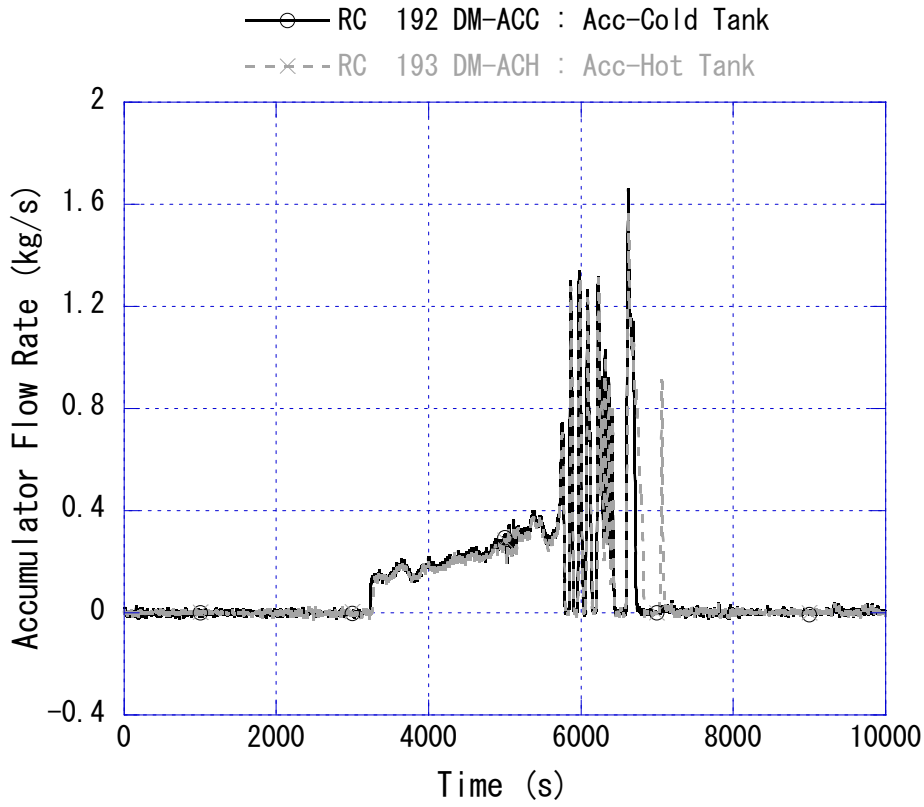

Fig. 4-13 Coolant injection flow rate from accumulator tank (0 to 10000 s)

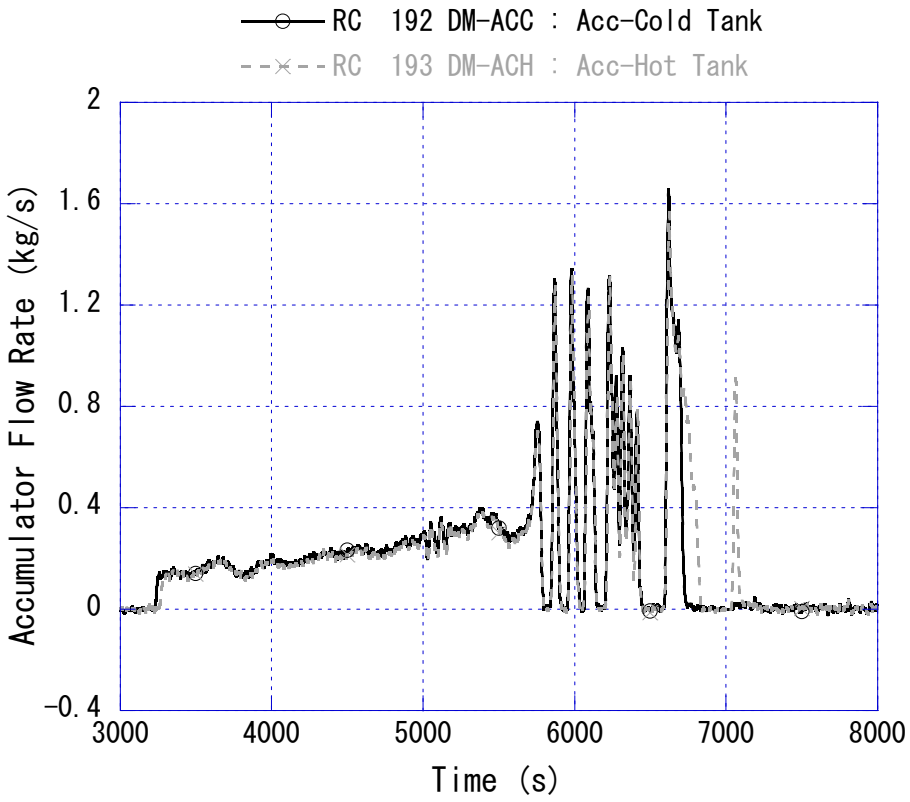

Fig. 4-14 Coolant injection flow rate from accumulator tank (3000 to 8000 s)

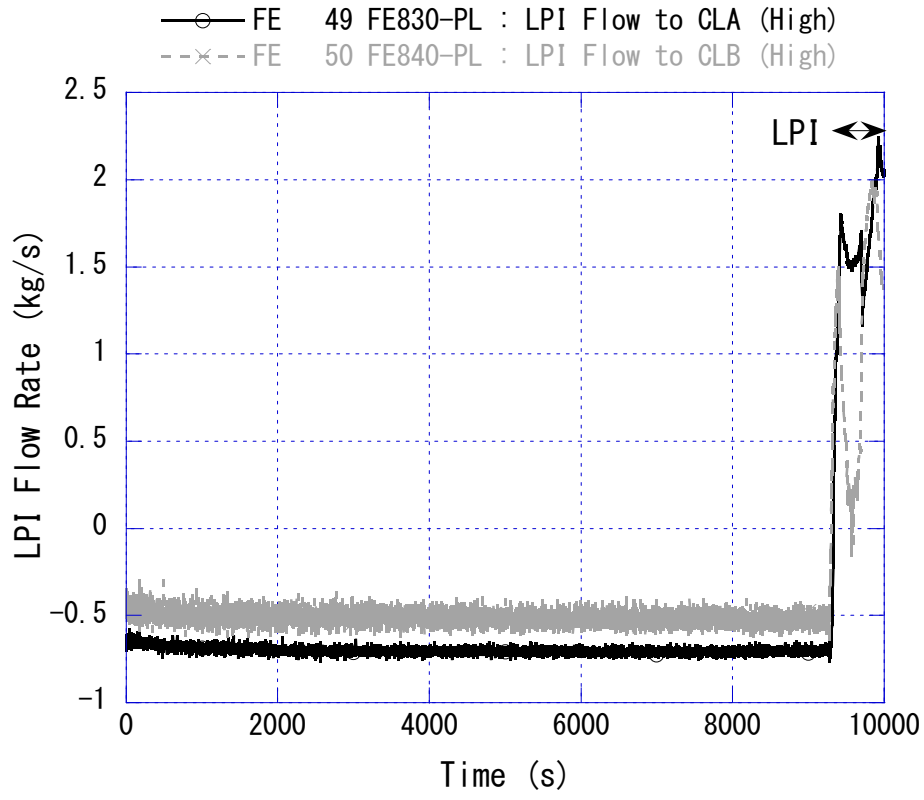

Fig. 4-15 Coolant injection flow rate from LPI system

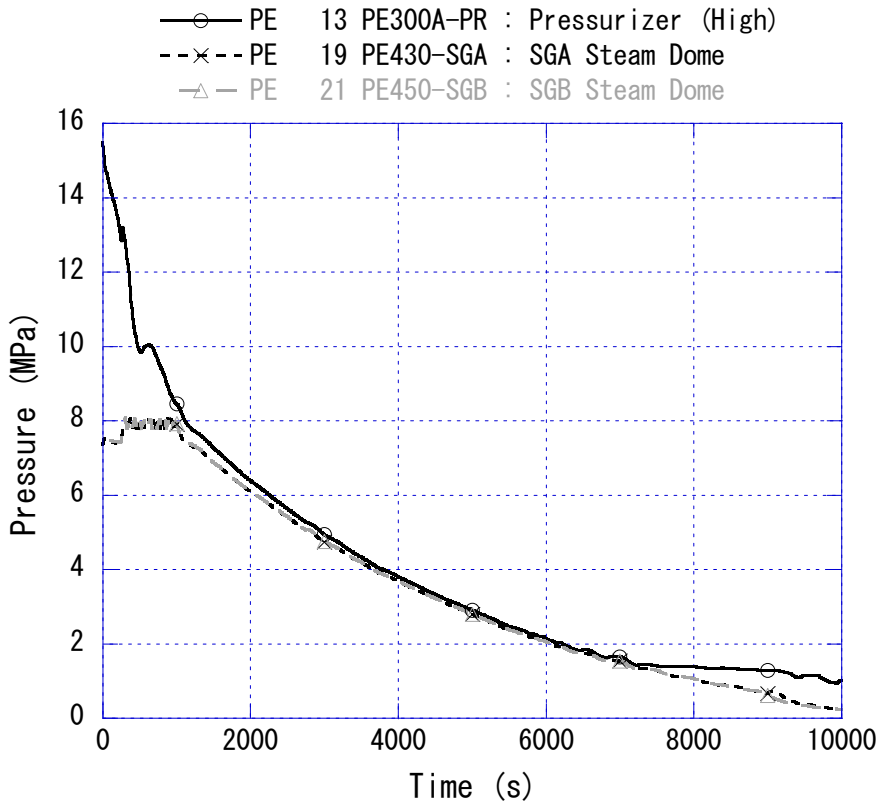

Fig. 4-16 Primary and secondary pressures

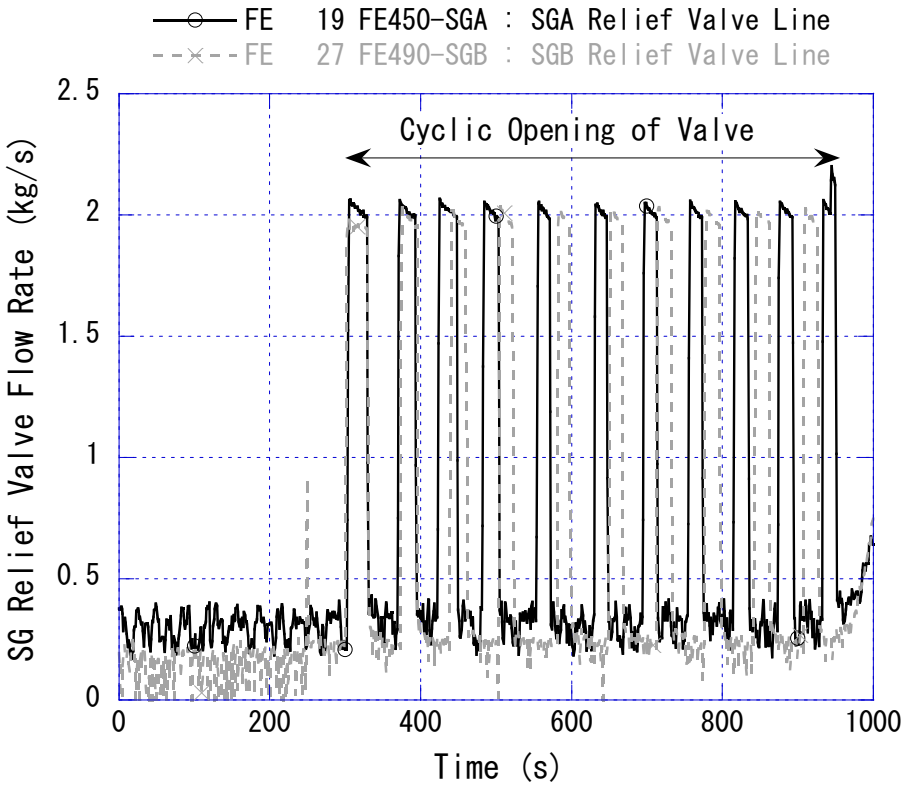

Fig. 4-17 SG relief valve flow rate

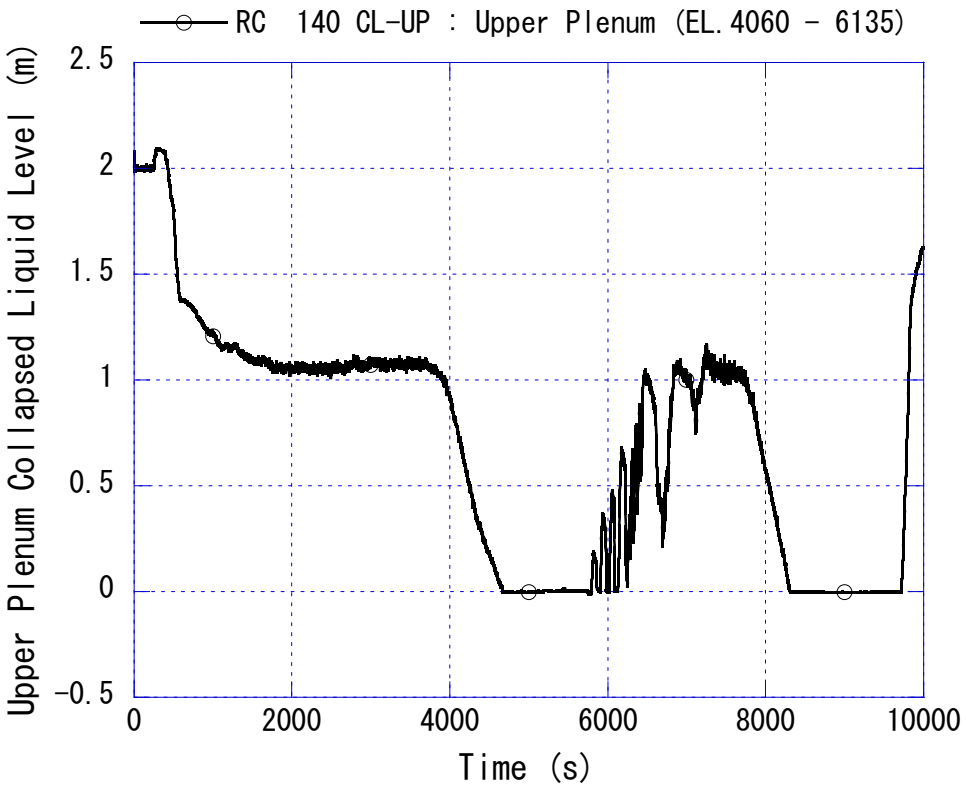

Fig. 4-18 Upper plenum collapsed liquid level (0 to 10000 s)

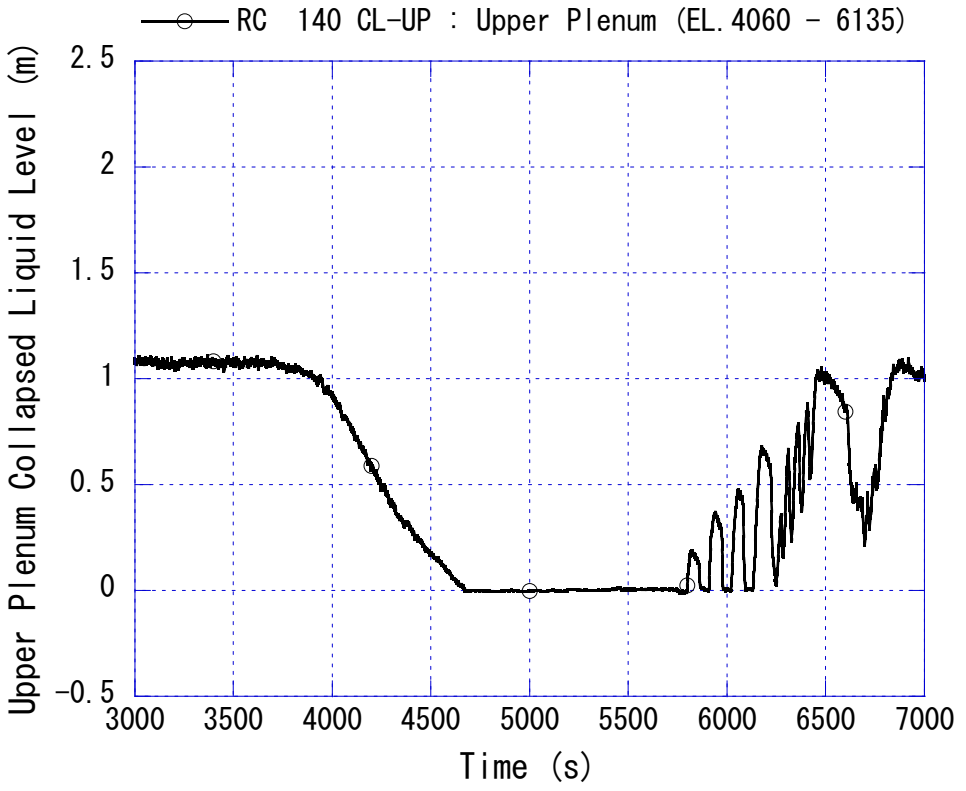

Fig. 4-19 Upper plenum collapsed liquid level (3000 to 7000 s)

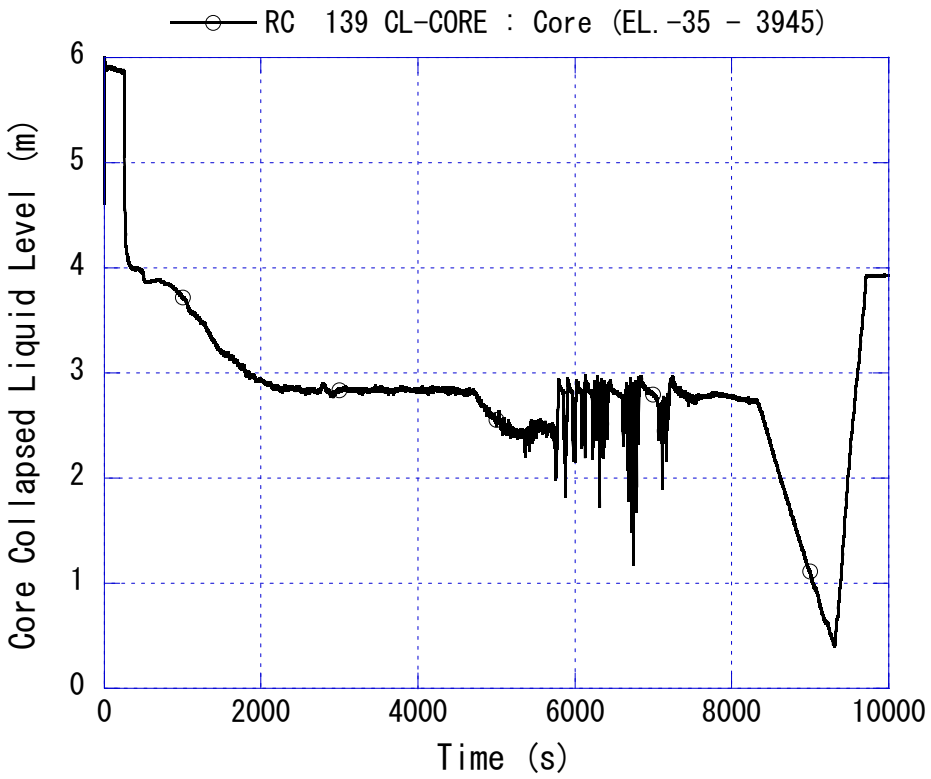

Fig. 4-20 Core collapsed liquid level (0 to 10000 s)

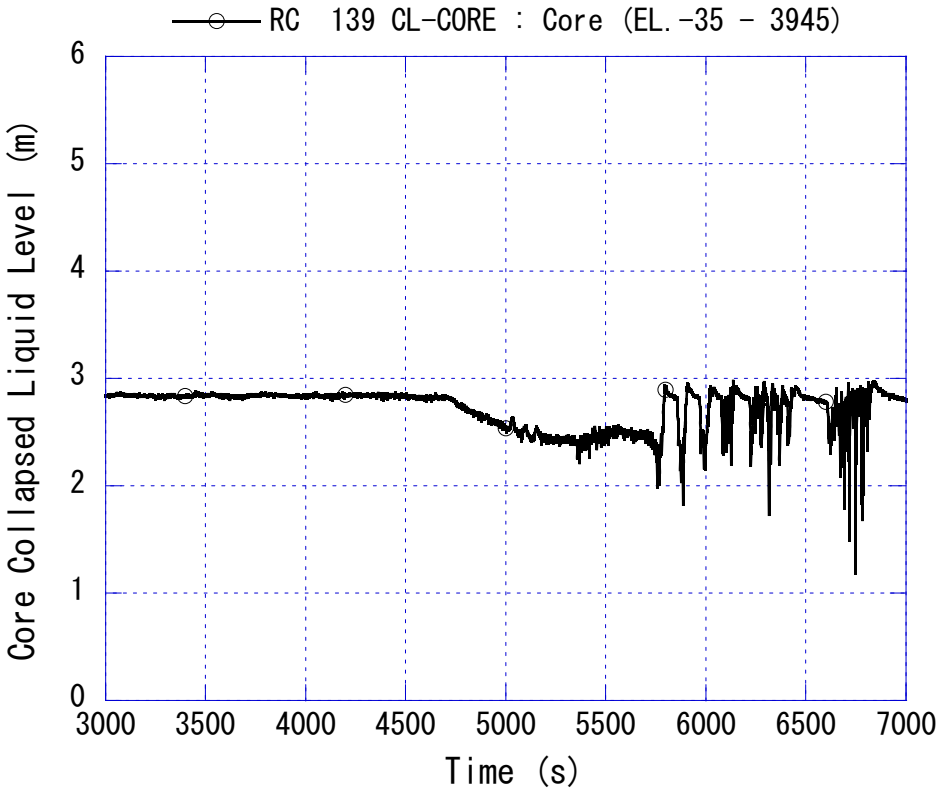

Fig. 4-21 Core collapsed liquid level (3000 to 7000 s)

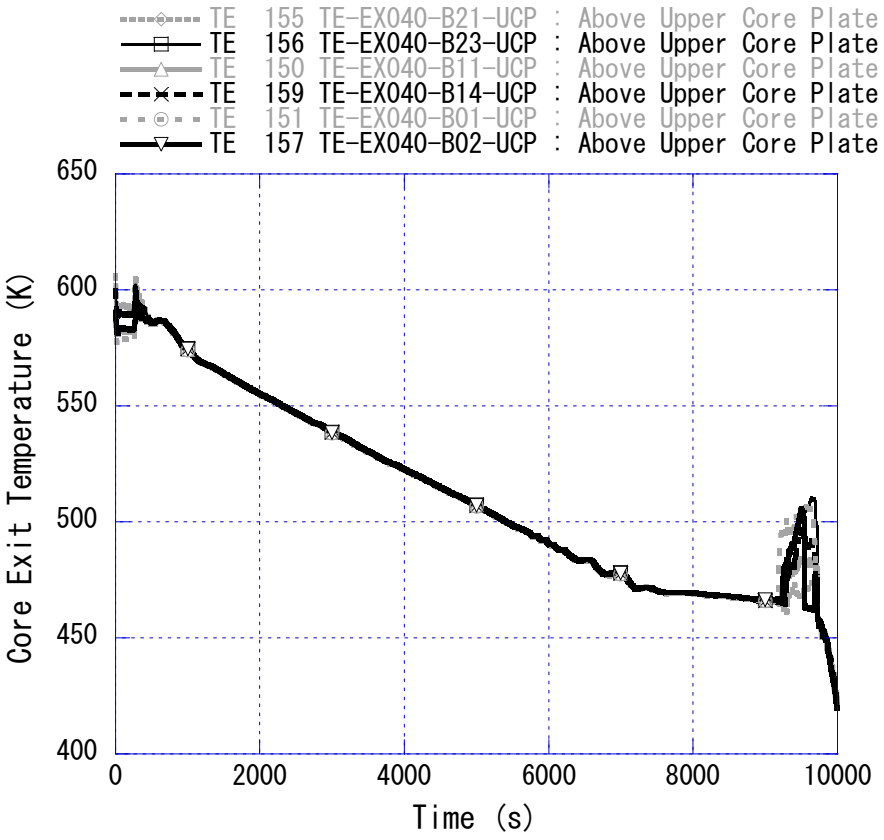

Fig. 4-22 Typical core exit temperatures (0 to 10000 s)

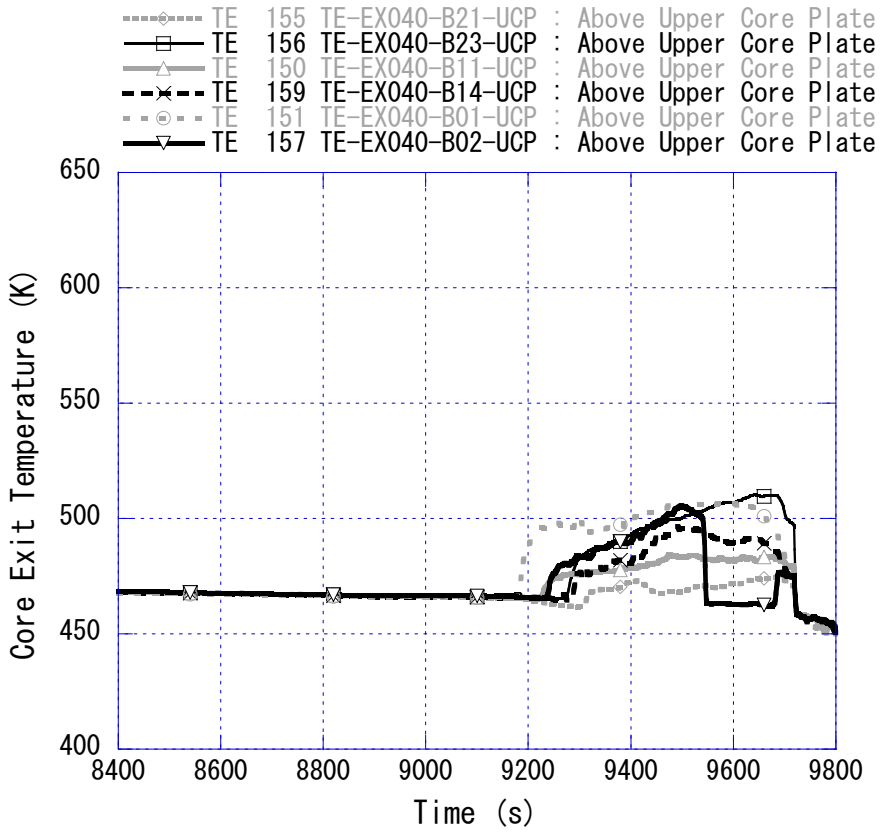

Fig. 4-23 Typical core exit temperatures (8400 to 9800 s)

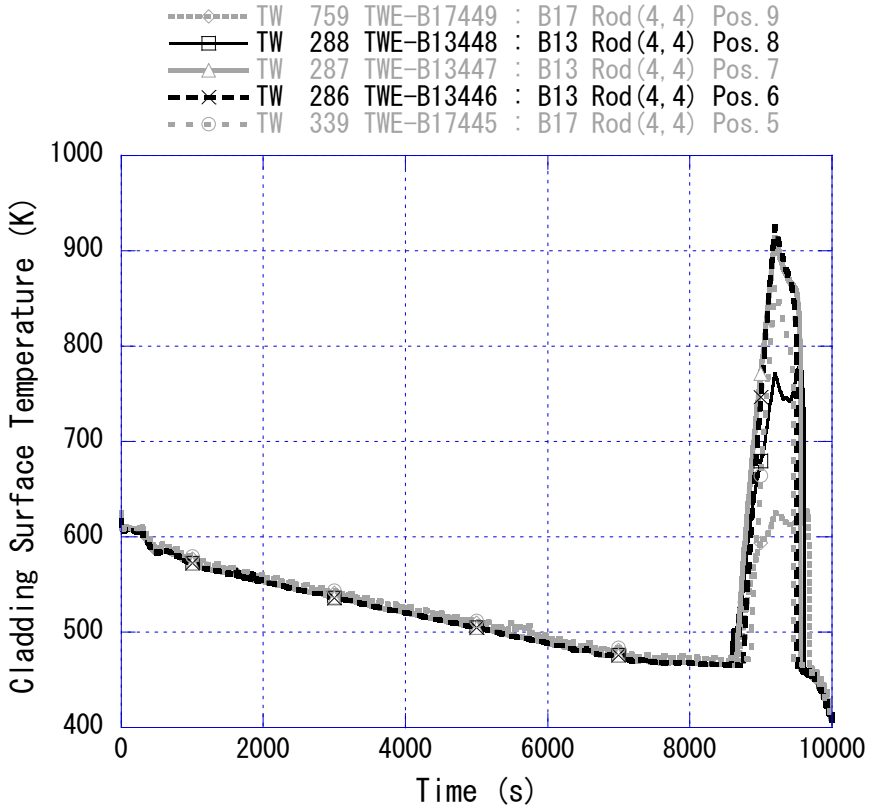

Fig. 4-24 Typical cladding surface temperatures at Positions 9-5 (0 to 10000 s)

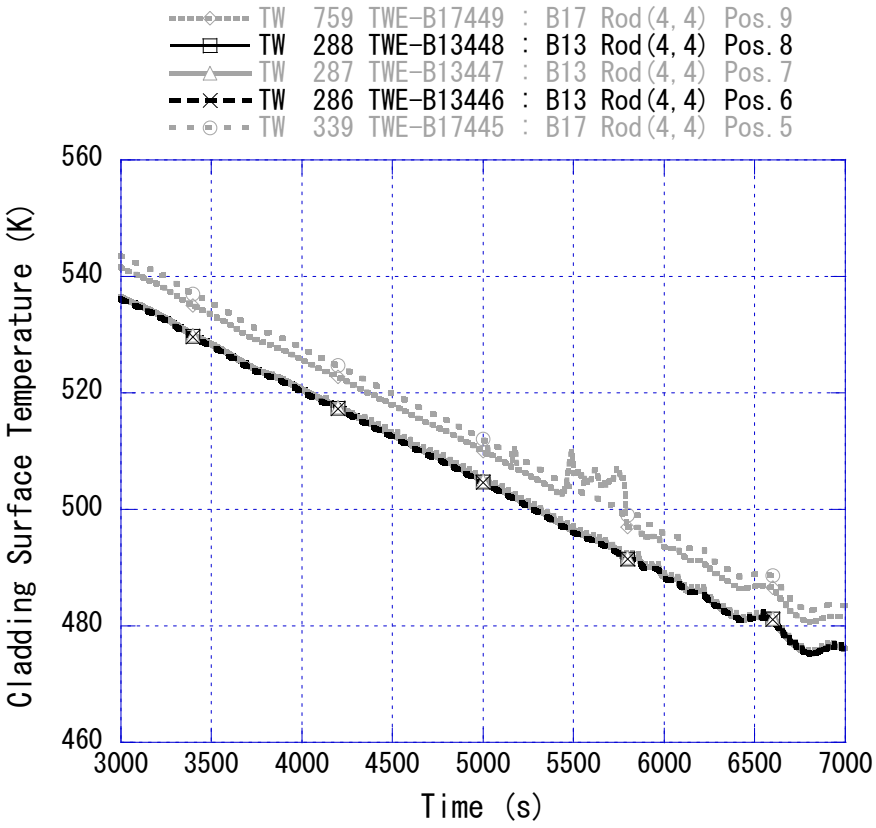

Fig. 4-25 Typical cladding surface temperatures at Positions 9-5 (3000 to 7000 s)

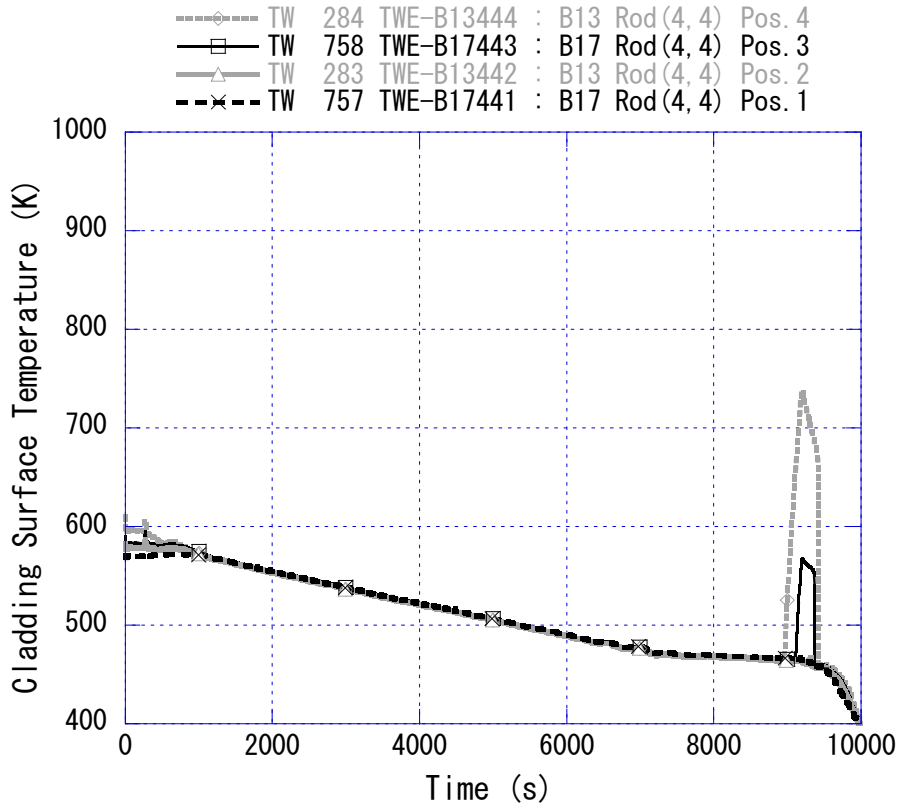

Fig. 4-26 Typical cladding surface temperatures at Positions 4-1 (0 to 10000 s)

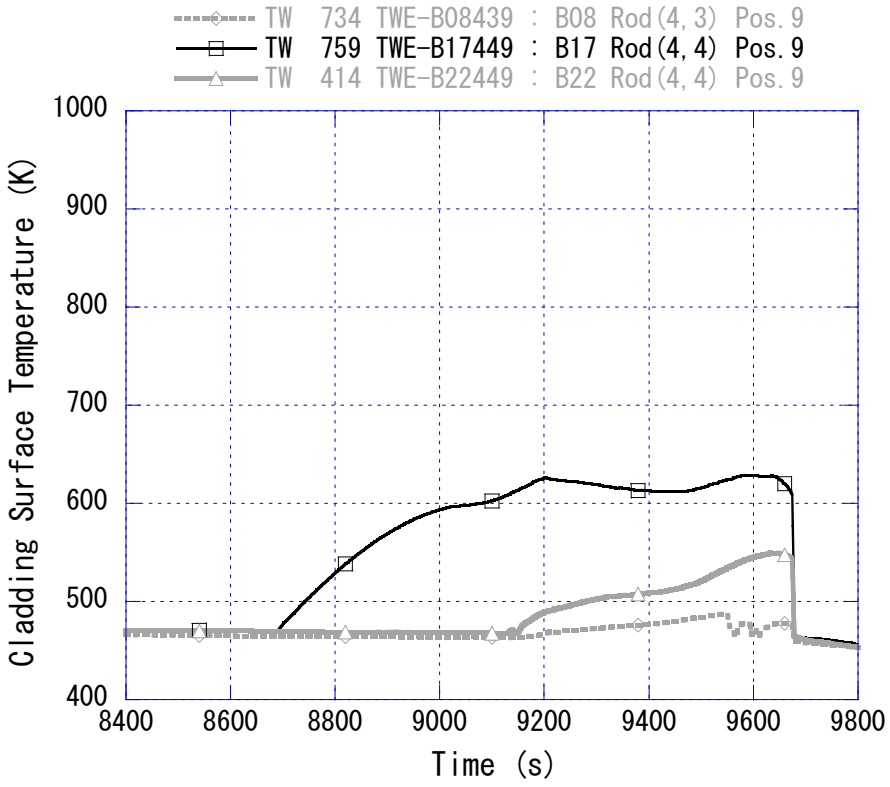

Fig. 4-27 Cladding surface temperatures at Position 9 (8400 to 9800 s)

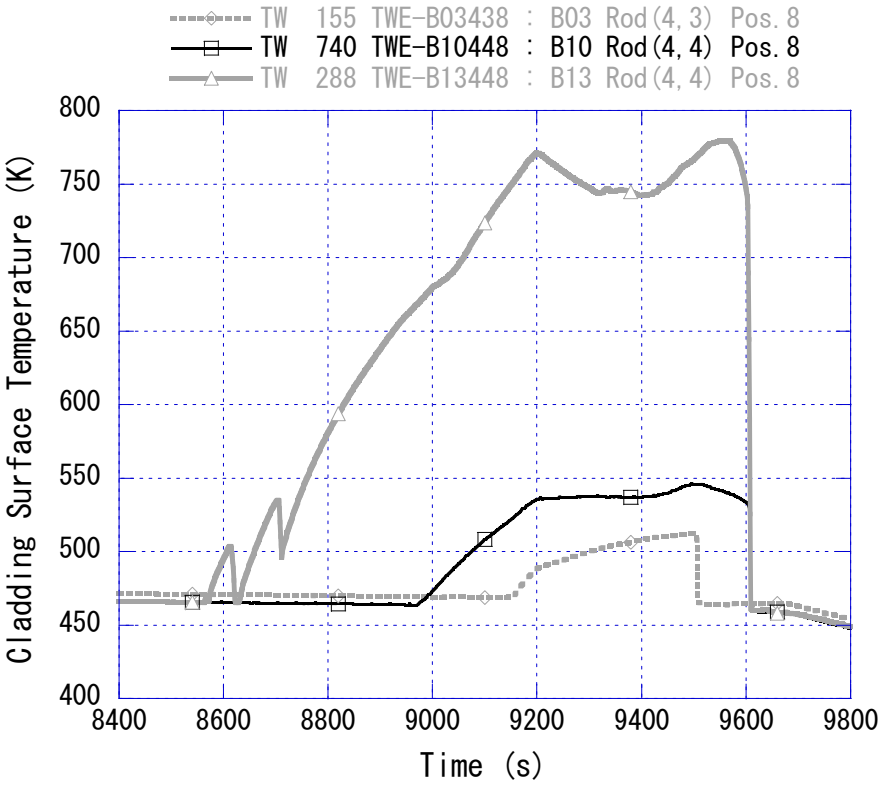

Fig. 4-28 Cladding surface temperatures at Position 8 (8400 to 9800 s)

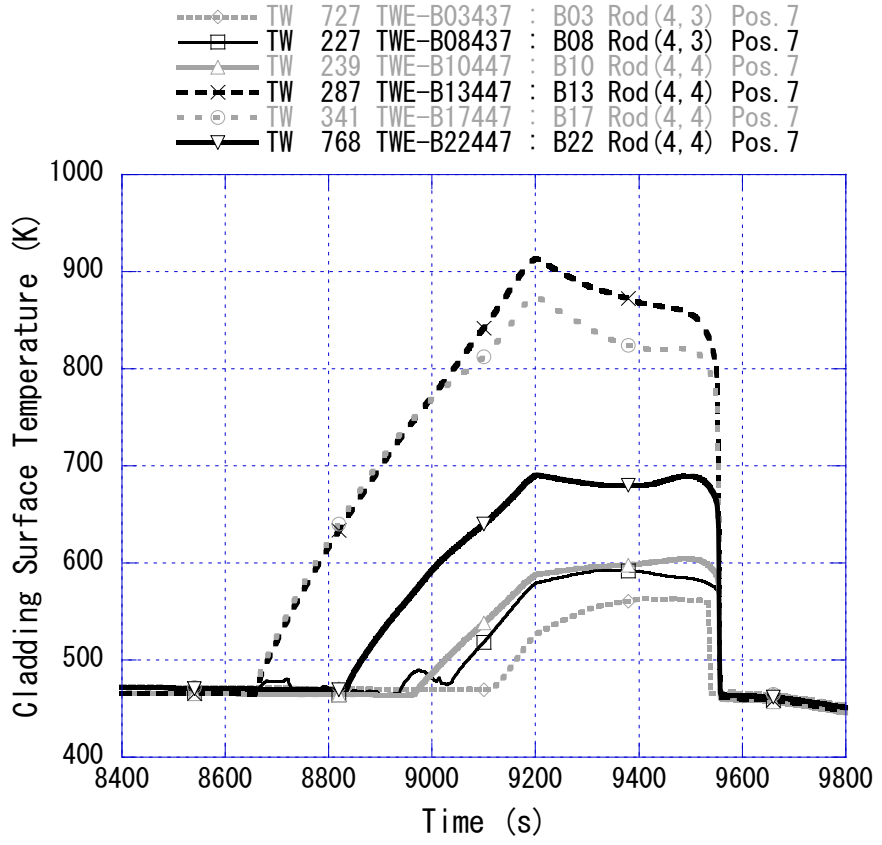

Fig. 4-29 Cladding surface temperatures at Position 7 (8400 to 9800 s)

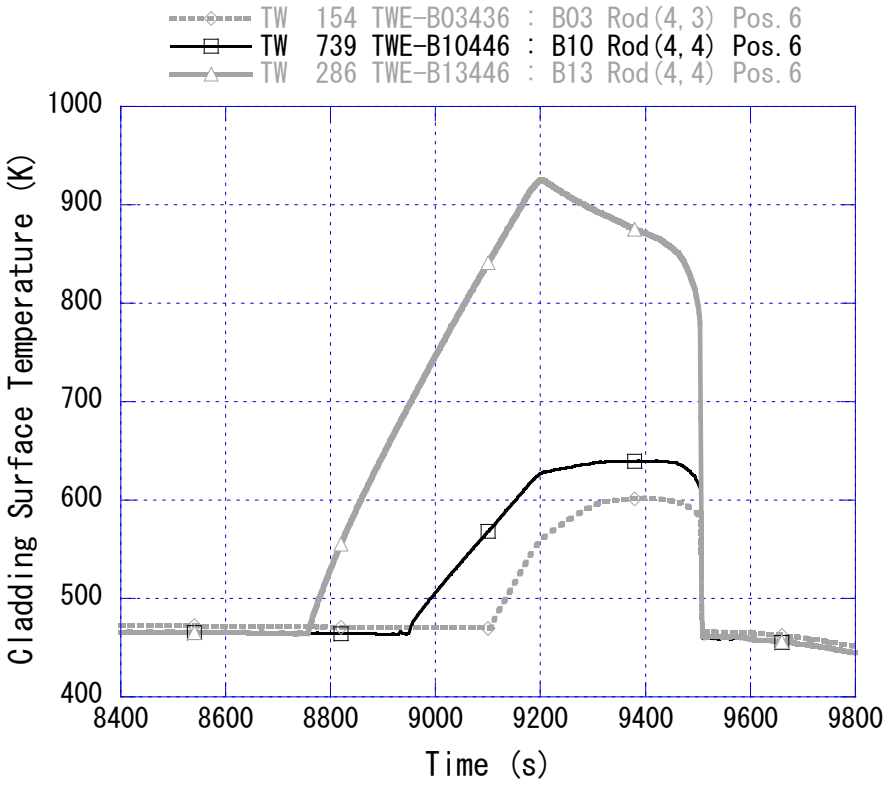

Fig. 4-30 Cladding surface temperatures at Position 6 (8400 to 9800 s)

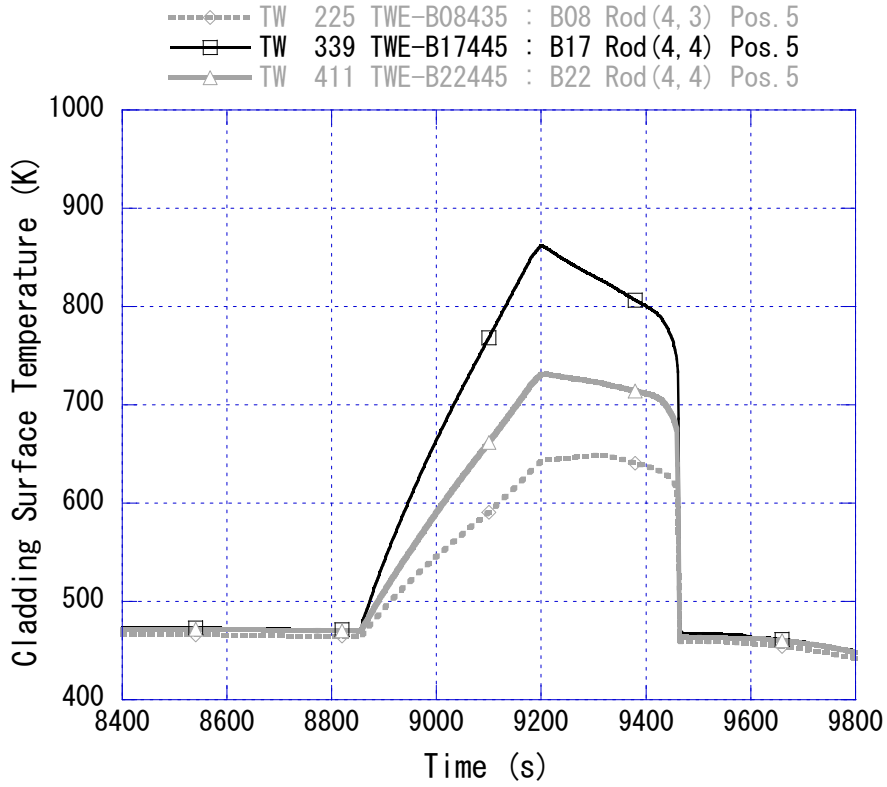

Fig. 4-31 Cladding surface temperatures at Position 5 (8400 to 9800 s)

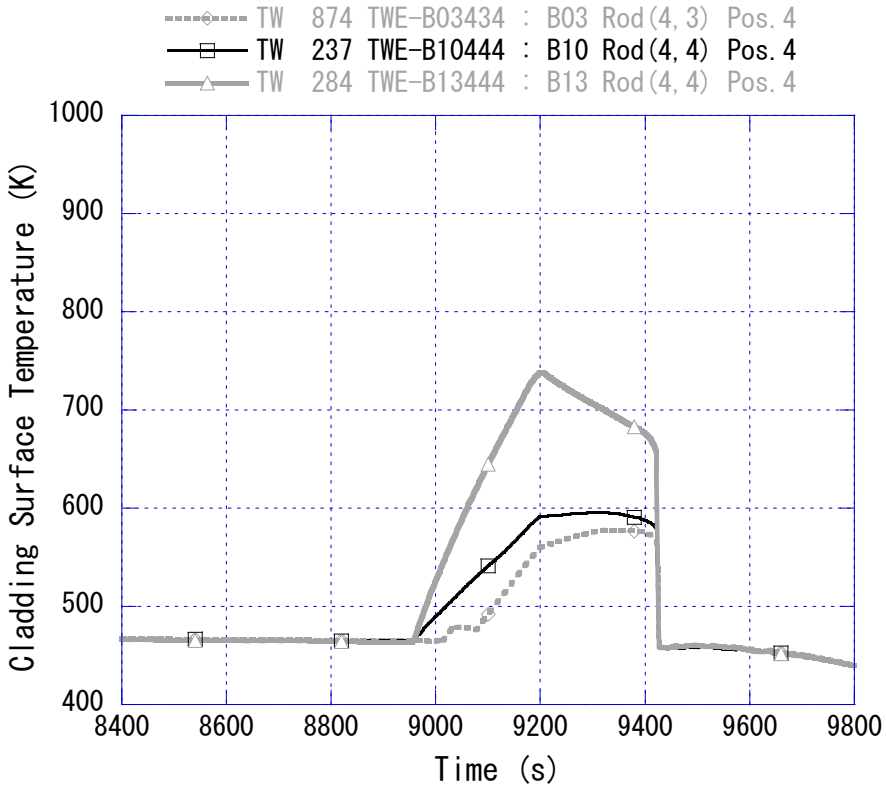

Fig. 4-32 Cladding surface temperatures at Position 4 (8400 to 9800 s)

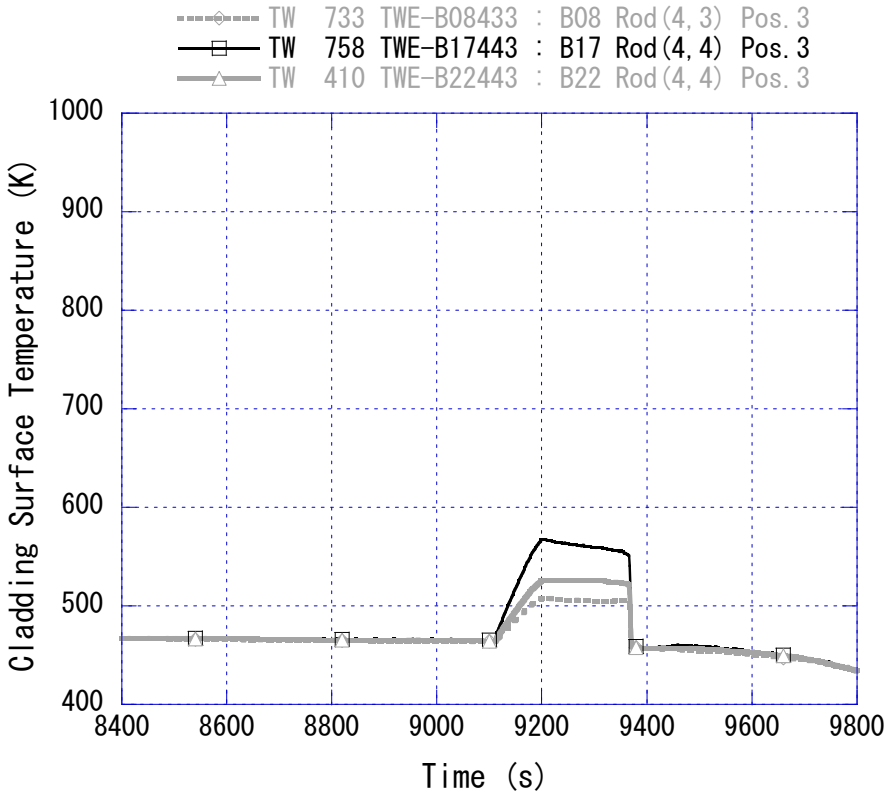

Fig. 4-33 Cladding surface temperatures at Position 3 (8400 to 9800 s)

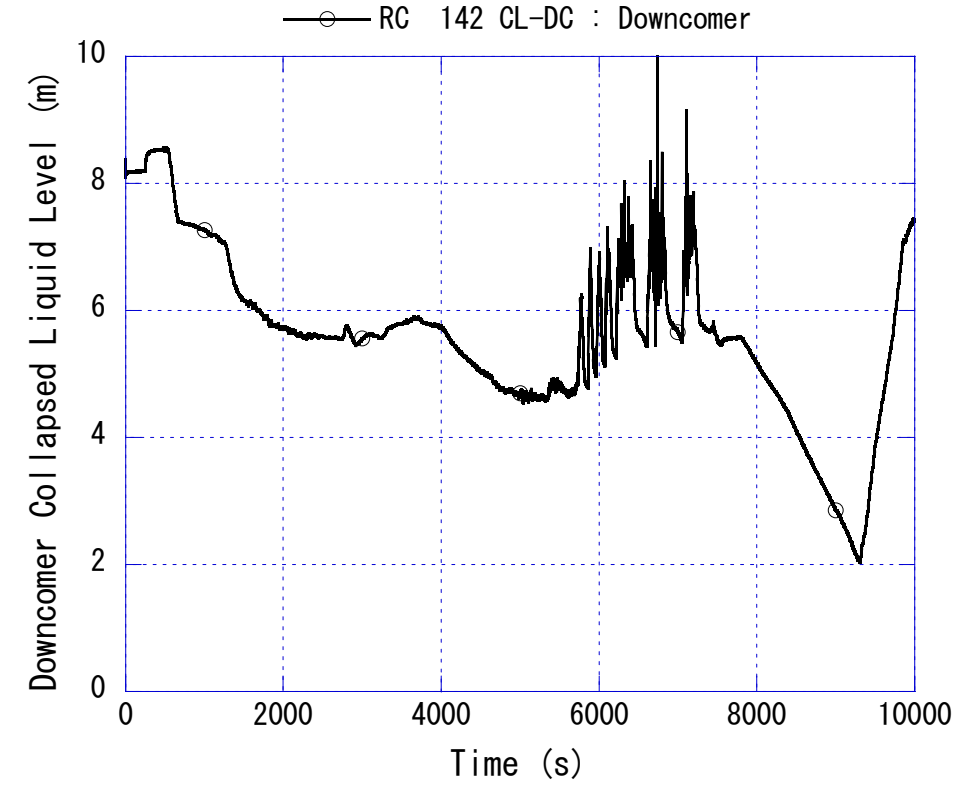

Fig. 4-34 Downcomer collapsed liquid level

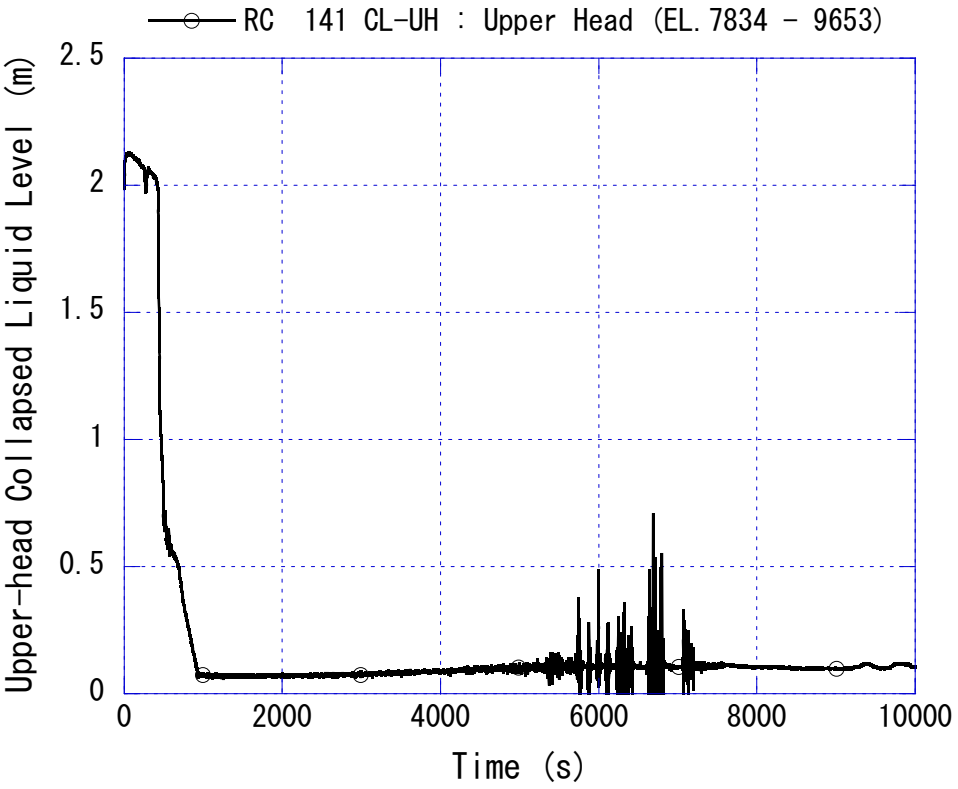

Fig. 4-35 Upper-head collapsed liquid level

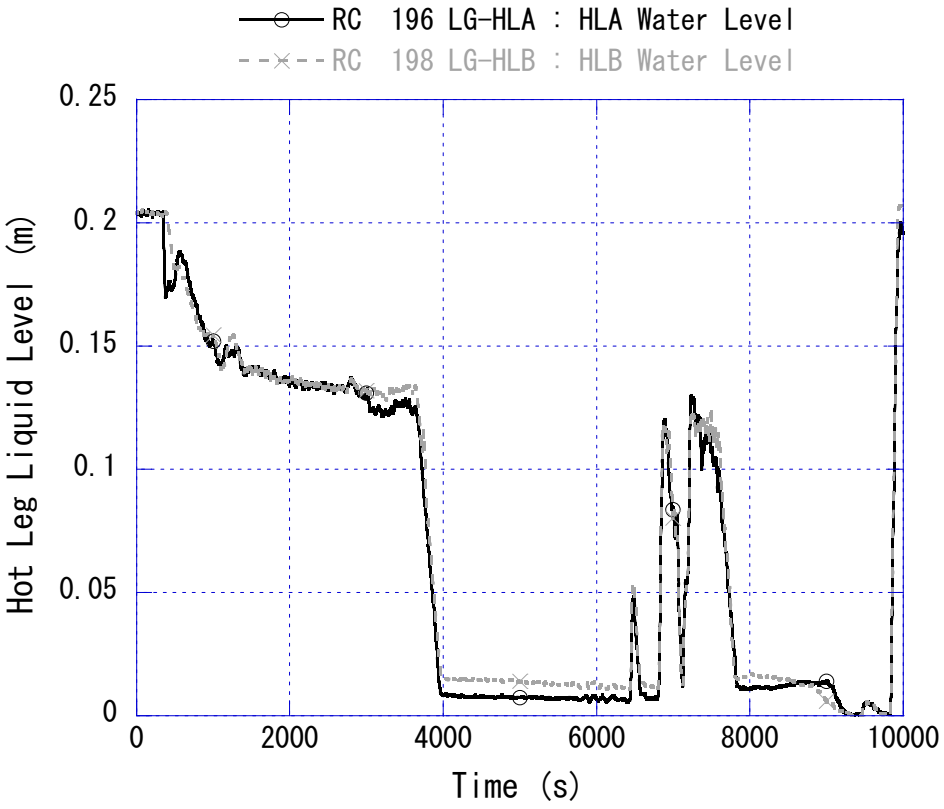

Fig. 4-36 Hot leg liquid level

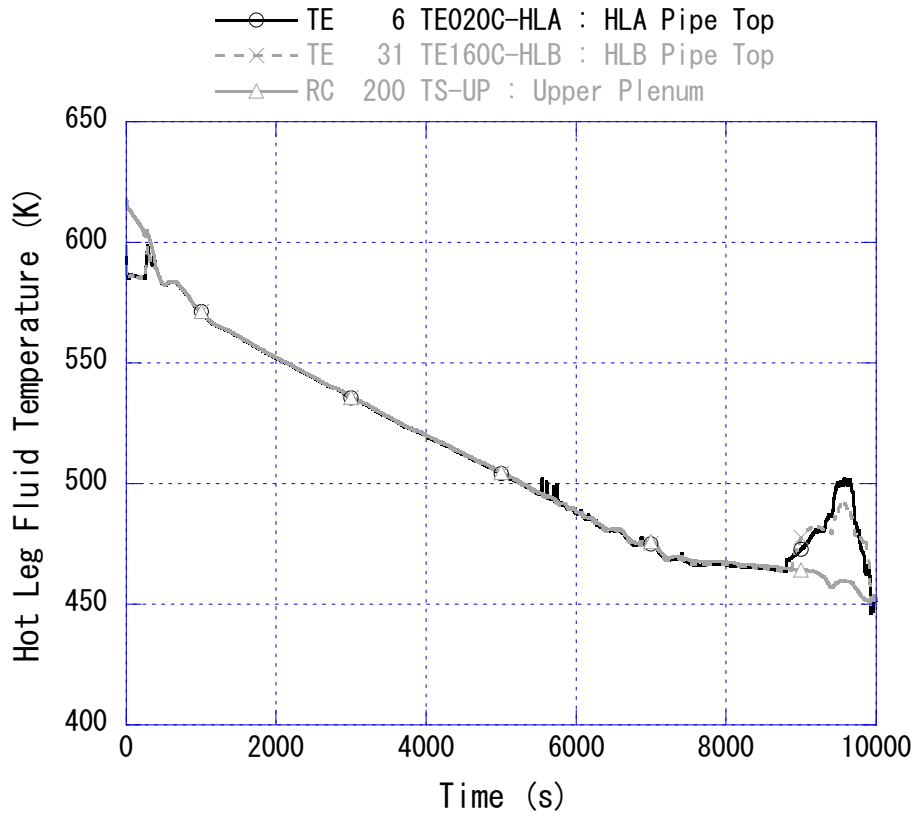

Fig. 4-37 Hot leg fluid temperature

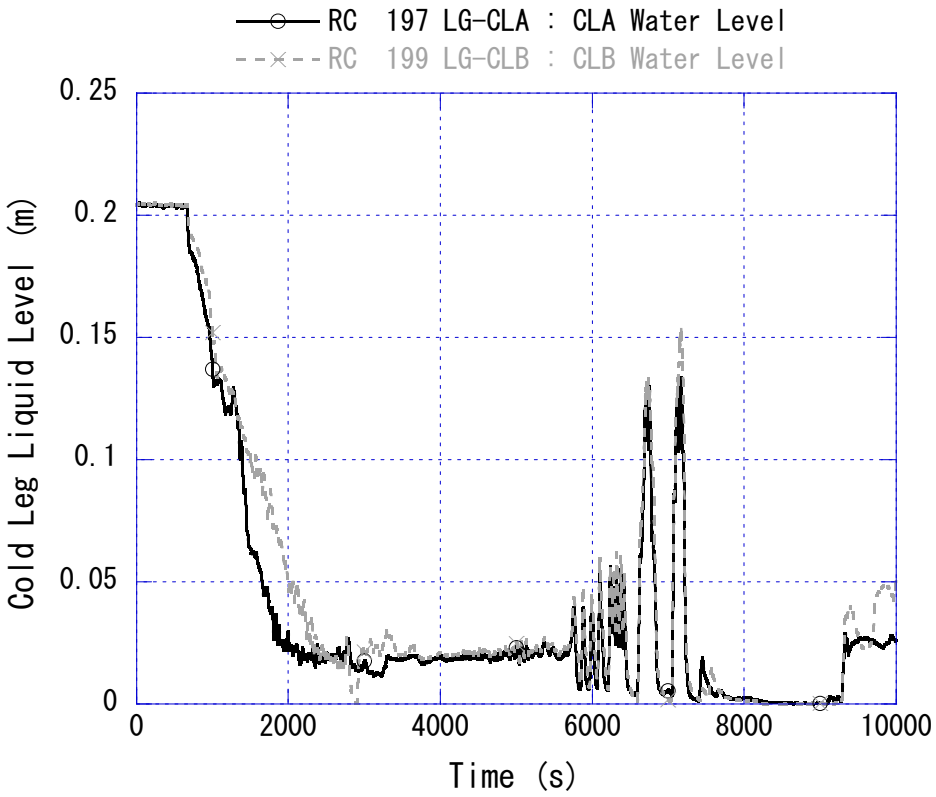

Fig. 4-38 Cold leg liquid level

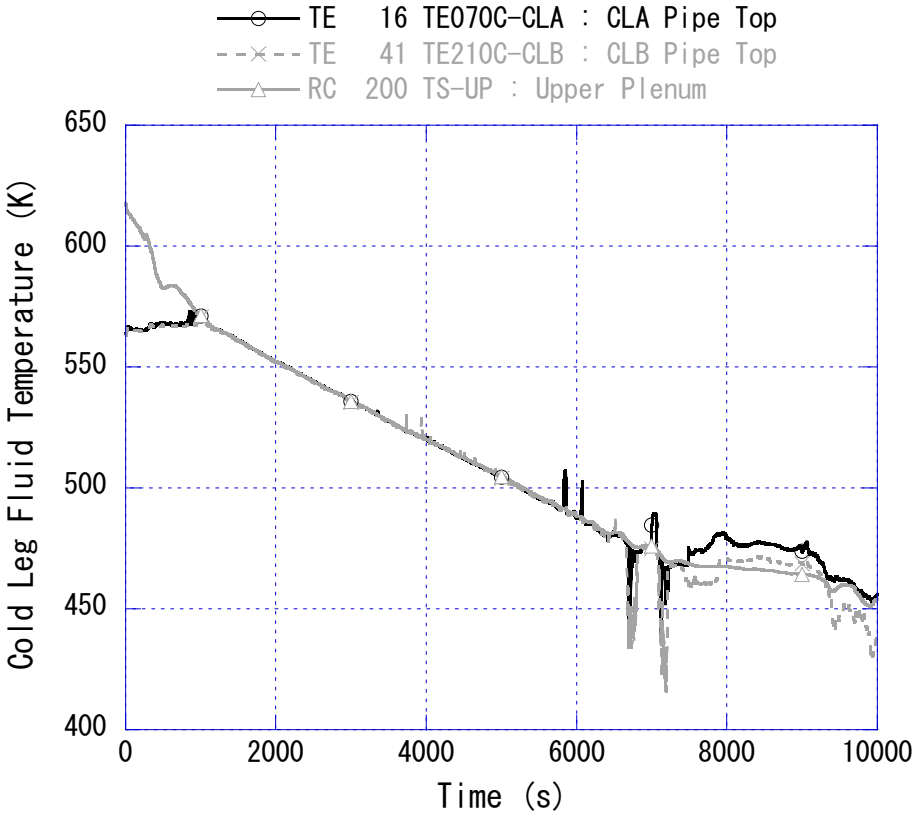

Fig. 4-39 Cold leg fluid temperature

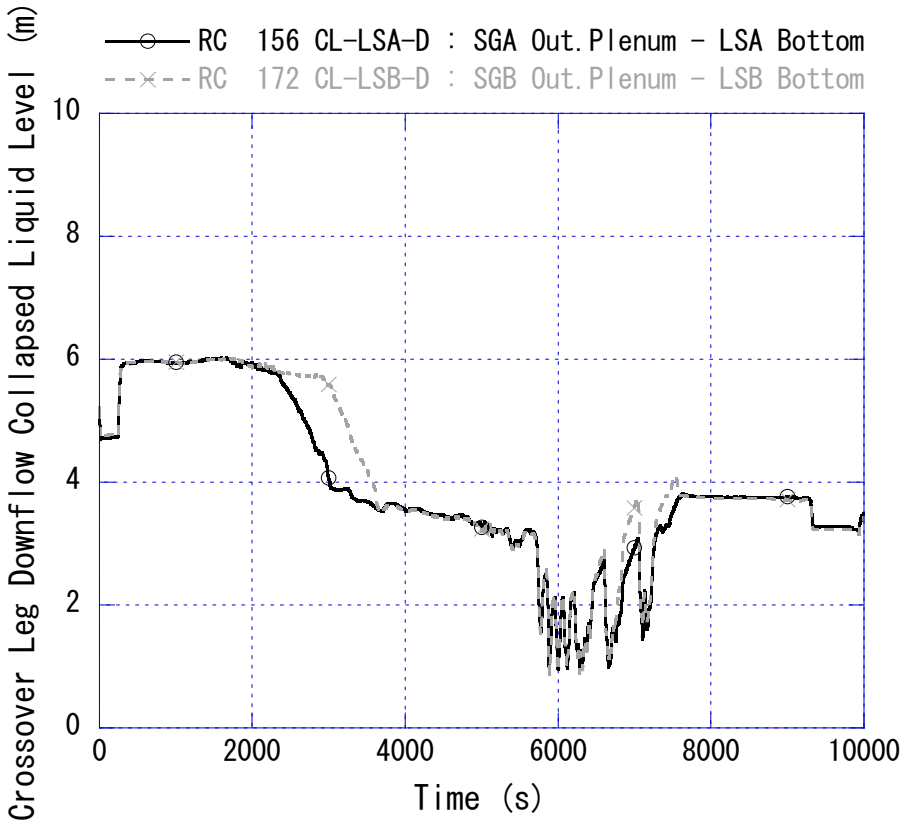

Fig. 4-40 Crossover leg downflow-side collapsed liquid level

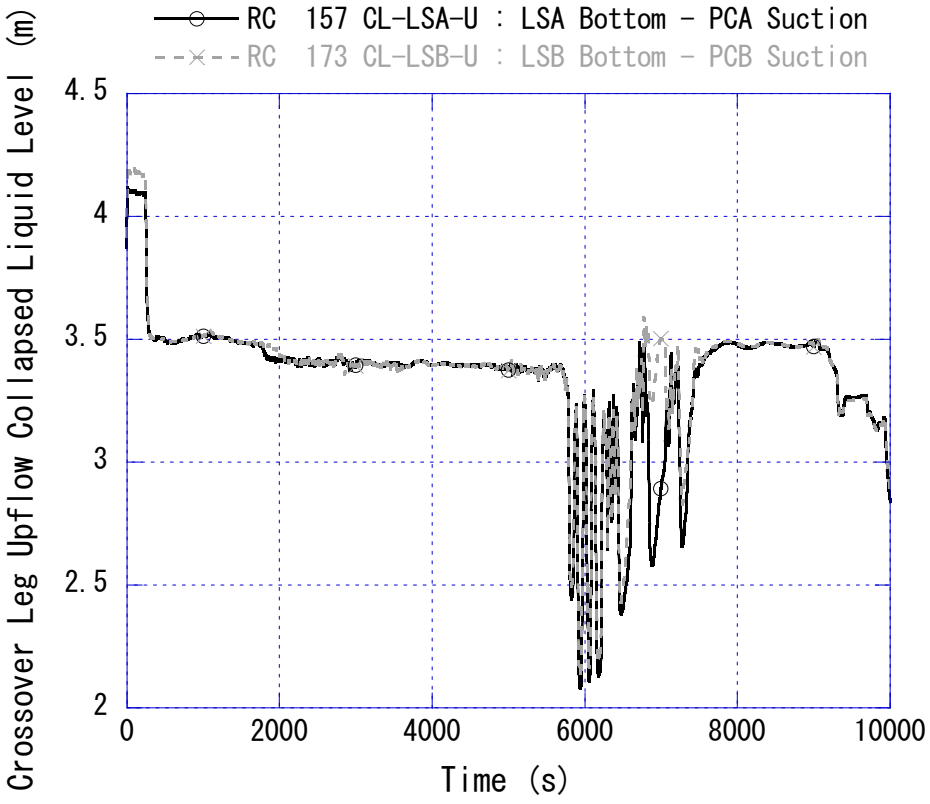

Fig. 4-41 Crossover leg upflow-side collapsed liquid level

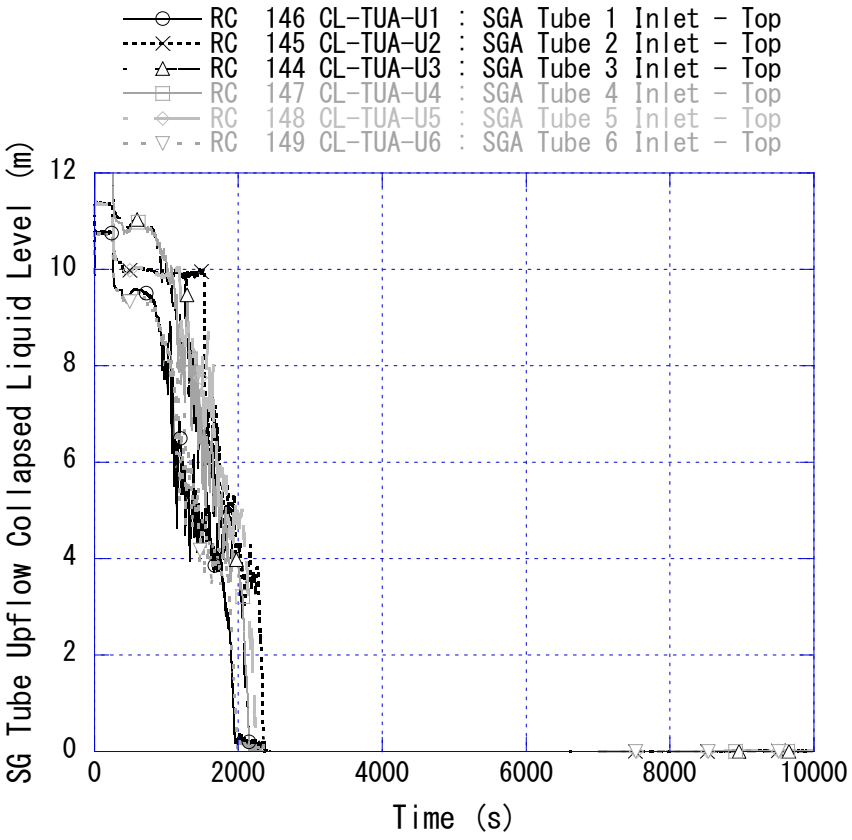

Fig. 4-42 SG U-tube upflow-side collapsed liquid level in loop with pressurizer

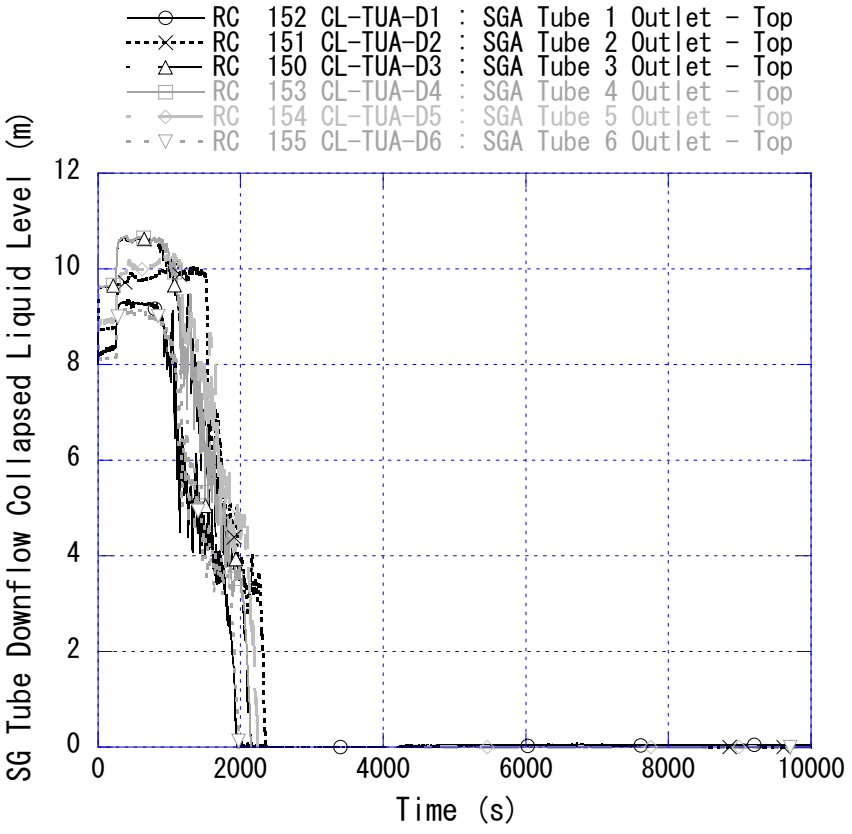

Fig. 4-43 SG U-tube downflow-side collapsed liquid level in loop with pressurizer

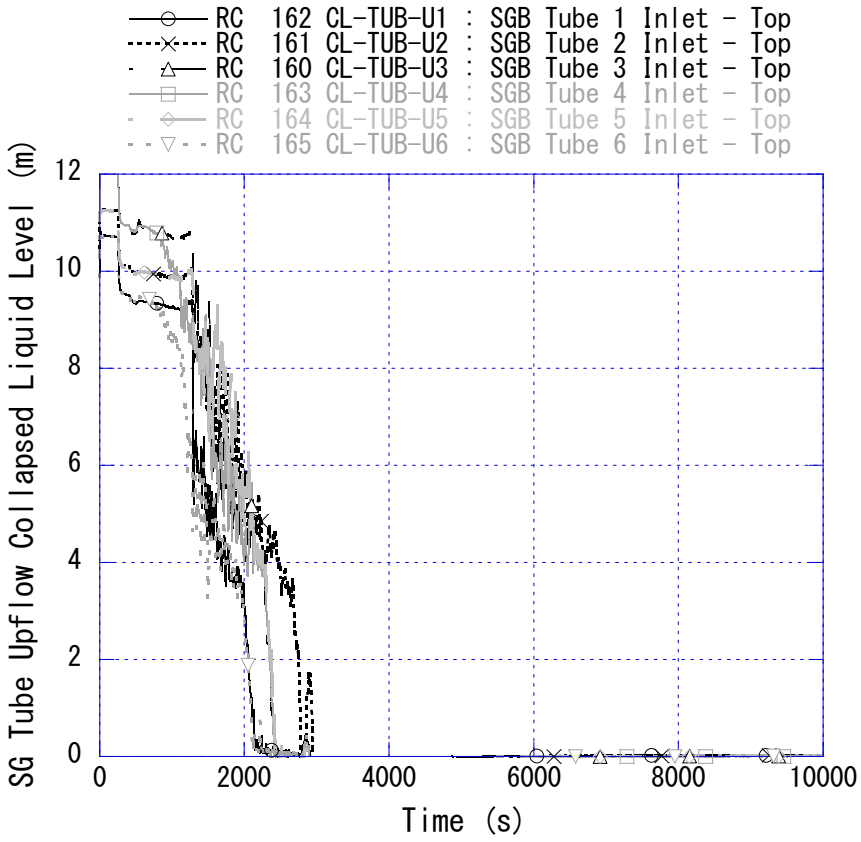

Fig. 4-44 SG U-tube upflow-side collapsed liquid level in loop without pressurizer

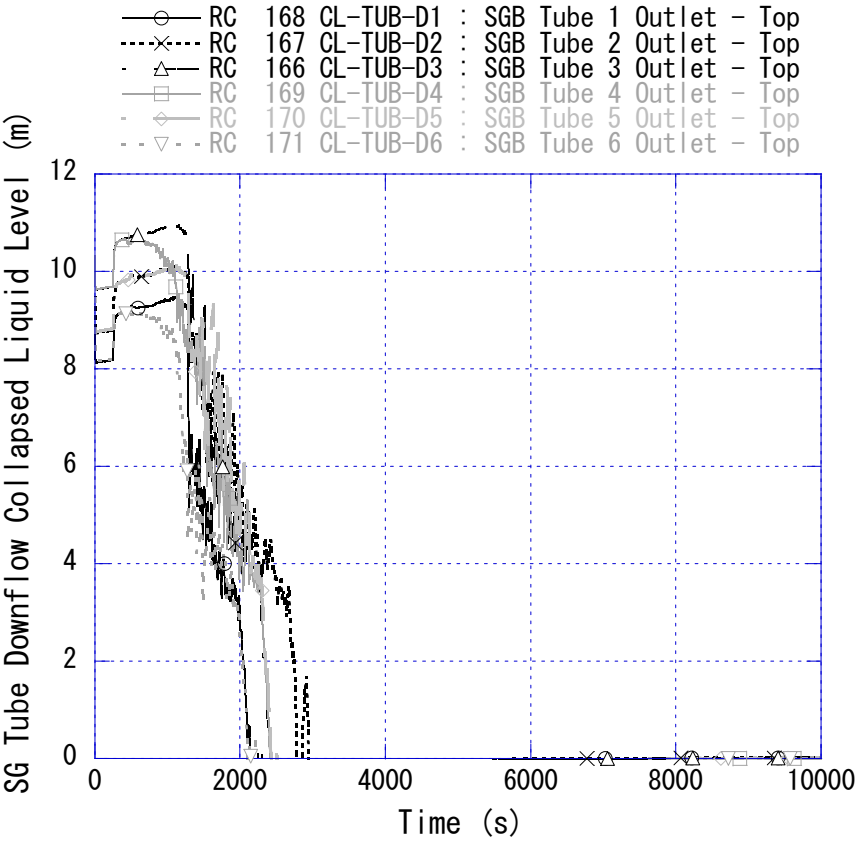

Fig. 4-45 SG U-tube downflow-side collapsed liquid level in loop without pressurizer

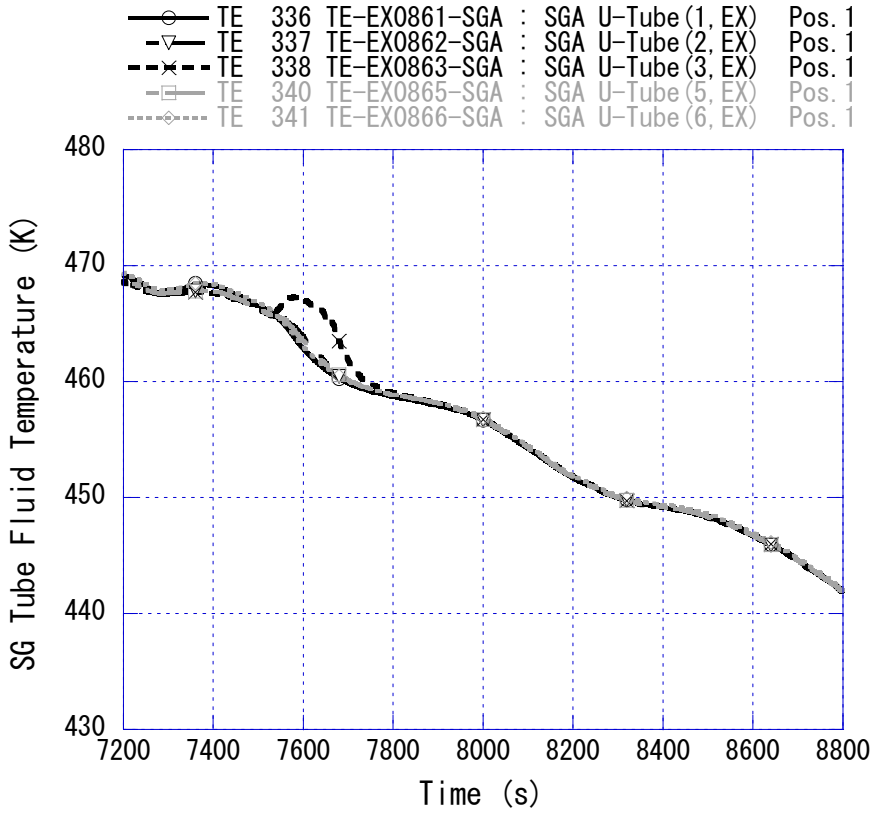

Fig. 4-46 SG U-tube downflow-side fluid temperature in loop with pressurizer

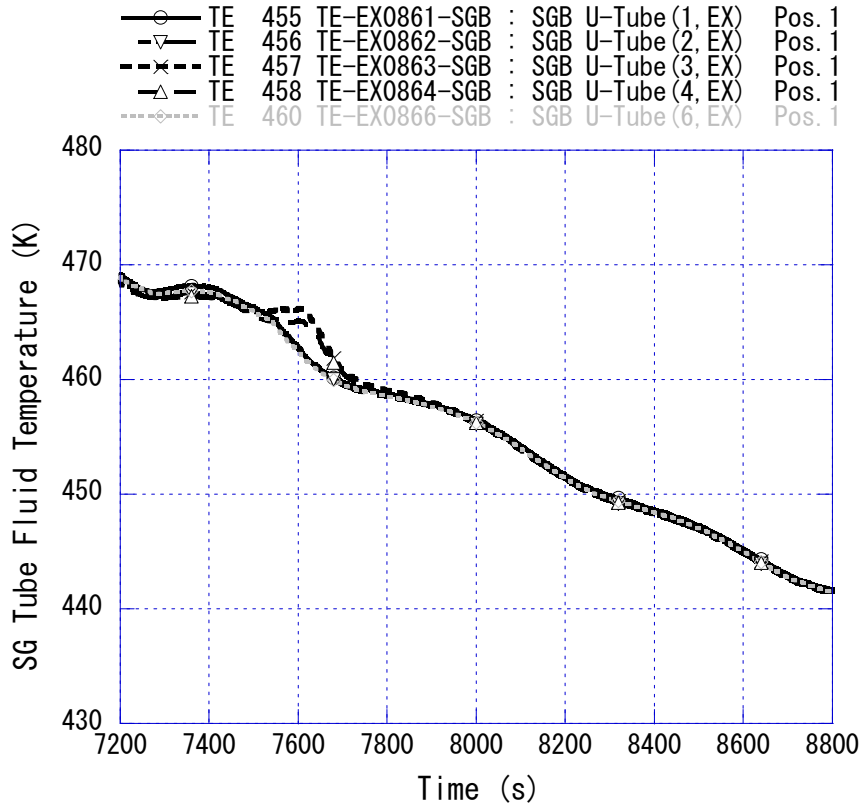

Fig. 4-47 SG U-tube downflow-side fluid temperature in loop without pressurizer

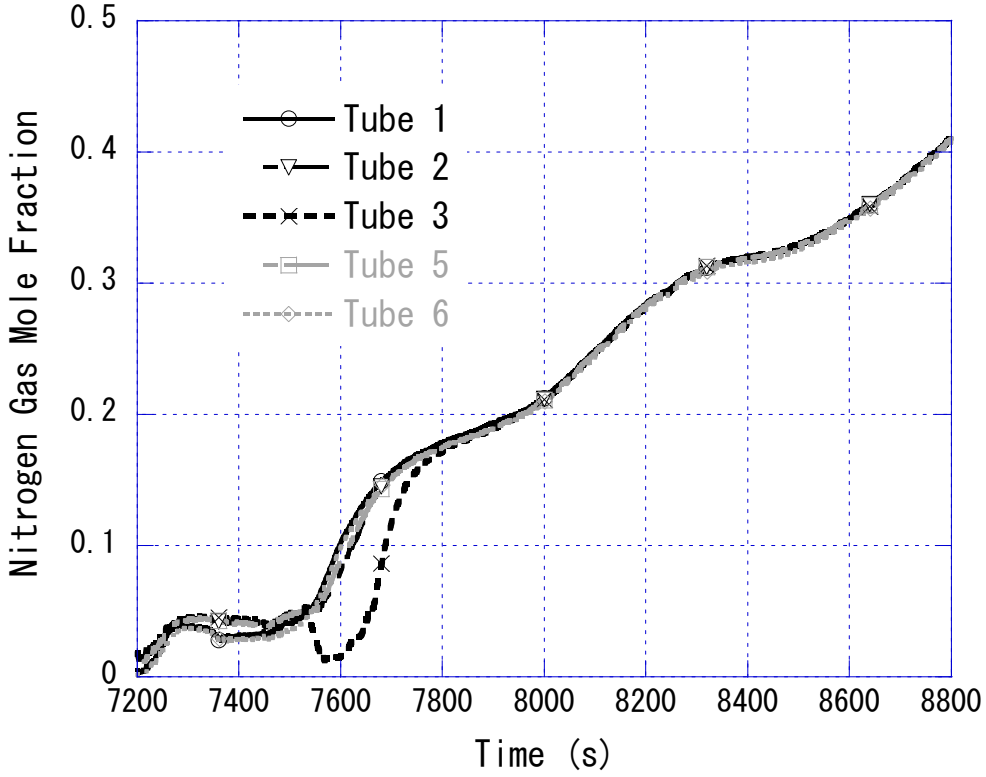

Fig. 4-48 Nitrogen gas mole fraction of SG U-tube in loop with pressurizer

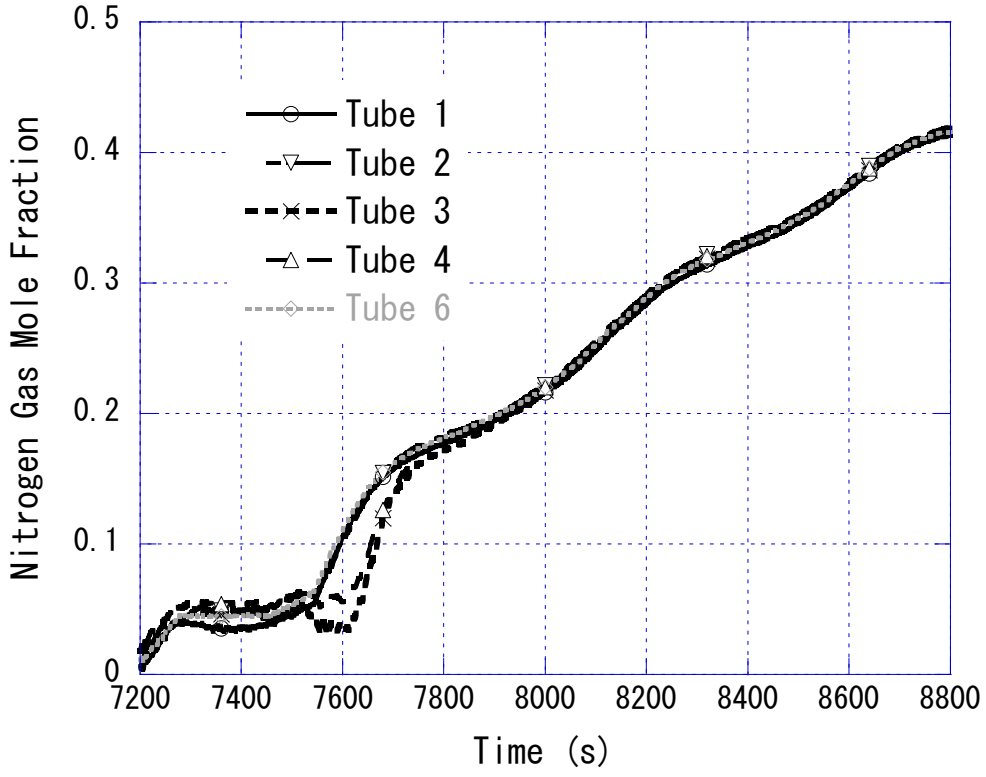

Fig. 4-49 Nitrogen gas mole fraction of SG U-tube in loop without pressurizer

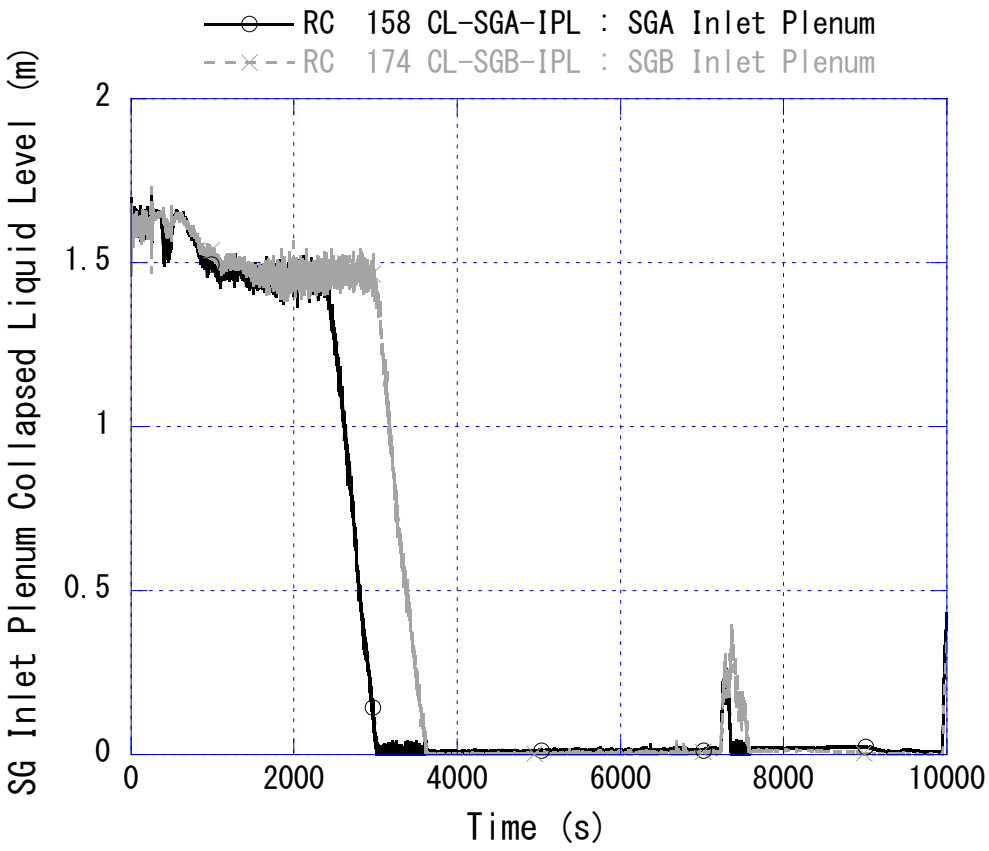

Fig. 4-50 SG inlet plenum collapsed liquid level

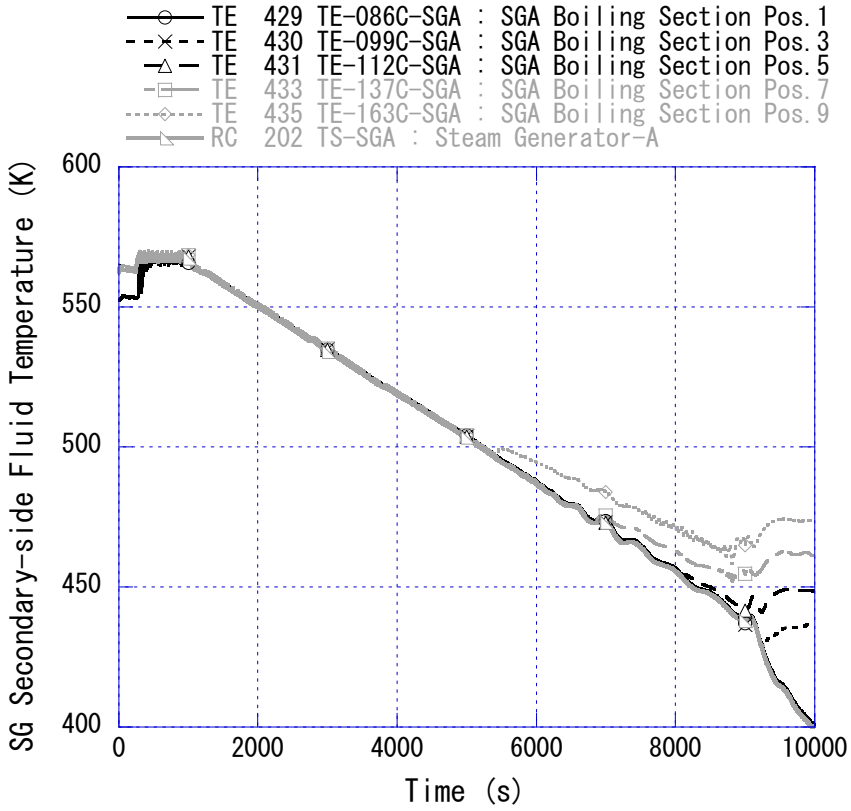

Fig. 4-51 SG secondary-side fluid temperature in loop with pressurizer

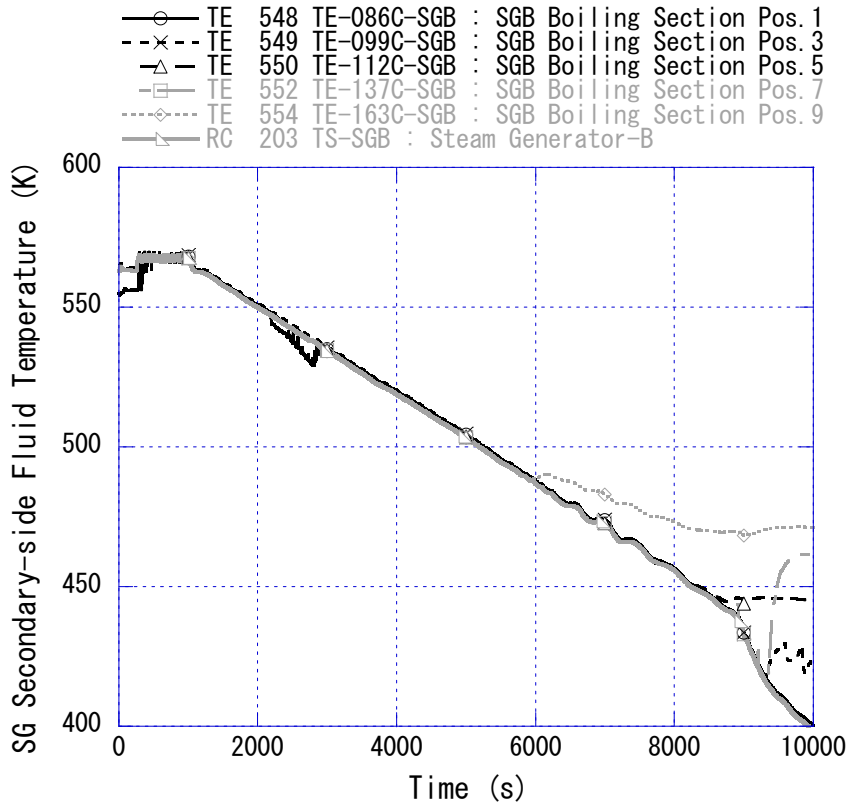

Fig. 4-52 SG secondary-side fluid temperature in loop without pressurizer

5. Summary

A ROSA/LSTF experiment named SB-PV-03 was carried out on November 19, 2002, simulating a PWR 0.2% pressure vessel bottom SBLOCA. The test assumptions were made such as unavailability of HPI system of ECCS and non-condensable gas (nitrogen gas) inflow to the primary system from ACC tanks of ECCS. Secondary-side depressurization of both SGs as an AM action to attain the depressurization rate of 55 K/h in the primary system was undertaken 10 min after a SI signal generation, and went on thereafter. AFW was supplied for 30 min into the secondary-side of both SGs with some delay after the initiation of the AM action. The AM action effectiveness was examined under the impact of nitrogen gas ingress from the ACC tanks. Further, the influence of a difference in the AFW flow rate on the SG secondary-side collapsed liquid level was surveyed. Major consequences are summarized as follows;

(1) The AM action took effect on the intended primary depressurization, which caused the activation of the ACC system. The liquid level recovery was oscillative in the core because coolant was intermittently fed from the ACC system into both cold legs. Accordingly, there was a small drop in the core liquid level.

(2) After the ACC tanks began to discharge nitrogen gas into the primary system, the pressure difference between the primary and SG secondary sides became larger due to degradation in the condensation heat transfer in the SG U-tubes.

(3) The liquid level difference in the secondary-side of both SGs was the largest at the end of the AFW injection, and declined gradually afterwards. The SG secondary-side was not voided throughout the experiment, which gave rise to successive heat removal from the SG secondary-side system.

(4) A large increase occurred in cladding surface temperature of simulated fuel rods during reflux condensation in the SG U-tubes under nitrogen gas influx. Automatic core power reduction procedure to protect the LSTF core was initiated when the maximum cladding surface temperature exceeded the pre-determined value of 908 K. The peak cladding temperature was 925 K. During the core uncovery, by contrast, the CET was increased to 510 K, which did not exceed the initial value.

(5) After the automatic core power reduction, LPI system of ECCS started the coolant injection into both cold legs. Resultantly, the core was entirely quenched owing to the liquid level recovery in the core.

(6) After the continuous core cooling was confirmed because of the coolant injection from the LPI system, the experiment came to an end.

Acknowledgement

The author would like to thank Messrs. I. Ohtsu and A. Ohwada of Japan Atomic Energy Agency for performing the LSTF SB-PV-03 test as well as Miss K. Toyoda of Frontier System Co., Ltd. for manipulating the experimental data. The author is grateful to Messrs. L. Dennhardt and S. Schollenberger of Framatome GmbH for their useful comments to improve the manuscript.

References

[1] USNRC, Leakage from Reactor Pressure Vessel Lower Head Penetrations and Reactor Coolant Pressure Boundary Integrity, NRC Bulletin 2003-02, OMB Control 3150-0012, 2003.

[2] Kukita, Y., Asaka, H., Nakamura, H., Tasaka, K., Pressurized water reactor core instrument tube ruptures: experimental simulation at the ROSA-IV LSTF, Nuclear Engineering and Design, 120(2-3), 1990, pp. 249-257.

[3] Kukita, Y., Anoda, Y., Tasaka, K., Summary of ROSA-IV LSTF first-phase test program – Integral simulation of PWR small-break LOCAs and transients –, Nuclear Engineering and Design, 131(1), 1991, pp. 101-111.

[4] Asaka, H., Anoda, Y., Kukita, Y., Ohtsu, I., Secondary-side depressurization during PWR cold-leg small break LOCAs based on ROSA-V/LSTF experiments and analyses, Journal of Nuclear Science and Technology, 35(12), 1998, pp. 905-915.

[5] NEA, Final Integration Report of OECD/NEA ROSA Project 2005-2009, NEA/CSNI/R(2013)1, 2013, 99p.

[6] Takeda, T., RELAP5 Analyses of ROSA/LSTF experiments on AM measures during PWR vessel bottom small-break LOCAs with gas inflow, International Journal of Nuclear Energy, Article ID 803470, 2014, 17p.

[7] The ROSA-V Group, ROSA-V Large Scale Test Facility (LSTF) System Description for the Third and Fourth Simulated Fuel Assemblies, JAERI-Tech 2003-037, 2003, 479p.

[8] NRA, Analyses of Events for the Evaluation of the Effectiveness of Measures against Severe Core Damage (PWR), NTEC-2014-1001, 2014, 141p., (in Japanese).

[9] Yoshida, Y., Risk of Japanese PWR plants by shutting off forced core cooling in an accident requiring safety injection system, Nuclear Engineering and Design, 368, Article ID 110822, 2020, 6p.

[10] Umminger, K., Dennhardt, L., Schollenberger, S., Schoen, B., Integral test facility PKL: experimental PWR accident investigation, Science and Technology of Nuclear Installations, Article ID 891056, 2012, 16p.

[11] NEA, Solving Thermal Hydraulic Safety Issues for Current and New Pressurized Water Reactor Design Concepts: Primary Coolant Loop Test Facility (PKL2) Project – Final Report, NEA/CSNI/R(2017)6, 2017, 84p.

[12] NEA, Final Integration Report of Rig-of-Safety Assessment (ROSA-2) Project – 2009-2012, NEA/CSNI/R(2016)10, 2017, 217p.

[13] Takeda, T., ROSA/LSTF test and RELAP5 code analyses on PWR hot leg small-break LOCA with accident management measure based on core exit temperature and PKL counterpart test, Annals of Nuclear Energy, 121, 2018, pp. 594-606.

[14] Takeda, T., Data Report of ROSA/LSTF Experiment SB-CL-32 – 1% Cold Leg Break LOCA with SG Depressurization and No Gas Inflow –, JAEA-Data/Code 2014-021, 2014, 59p.

[15] Takeda, T., Ohtsu, I., ROSA/LSTF test and RELAP5 analyses on PWR cold leg small-break LOCA with accident management measure and PKL counterpart test, Nuclear Engineering and Technology, 49, 2017, pp. 928-940.

[16] NEA, Summary and Conclusions of the Joint PKL3-ATLAS Workshop on Analytical Activities, NEA/CSNI/R(2017)10, 2017, 29p.

[17] Takeda, T., Data Report of ROSA/LSTF Experiment SB-HL-12 – 1% Hot Leg Break LOCA with SG Depressurization and Gas Inflow –, JAEA-Data/Code 2015-022, 2016, 58p.

[18] Takeda, T., Ohtsu, I., Uncertainty analysis of ROSA/LSTF test by RELAP5 code and PKL counterpart test concerning PWR hot leg break LOCAs, Nuclear Engineering and Technology, 50, 2018, pp. 829-841.

[19] Takeda, T., Data Report of ROSA/LSTF Experiment SB-PV-09 – 1.9% Pressure Vessel Top Break LOCA with SG Depressurization and Gas Inflow –, JAEA-Data/Code 2021-006, 2021, 61p.

[20] Hyvärinen, J., Riikonen, V., Telkkä, J., et al., Creating the foundations for safe nuclear power in Finland – Thermal hydraulics, safety analyses, safety justification methods research at the LUT University, 2000–2023, Nuclear Engineering and Design, 419, Article ID 112935, 2024, 26p.

[21] Zuber, N., Problems in modeling small break LOCA, Technical Report, NUREG-0724, 1980.

[22] Kumamaru, H., Tasaka, K., Recalculation of simulated post-scram core power decay curve for use in ROSA-IV/LSTF experiments on PWR small-break LOCAs and transients, JAERI-M 90-142, 1990, 63p.

Appendix A Available Experimental Data List

Table A-1 shows the list of available experimental data qualified as “Good” for LSTF SB-PV-03 (Run ID designated to be SP3). This table contains Sequential No., Function ID., Tag Name, measurement location, range, unit, and uncertainty. The alphabetical prefix of the Function ID. and Tag Name is explained as follows;

(1) TE, fluid temperature,

(2) DT, differential temperature,

(3) TW, heater rod and structure temperature,

(4) FE, flow rate measured with conventional (differential pressure) flow meters,

(5) PE, pressure,

(6) MI, miscellaneous instrumented-signal (power, pump rotation speed, etc.),

(7) LE, liquid level,

(8) DP, differential pressure,

(9) DE, fluid density measured with gamma-ray densitometer,

(10) RC, two-phase flow data calculated with DE and others.

Table A-1 List of available experimental data for LSTF SB-PV-03

SEQ No.	Function ID.	Tagname	Location	Range		Unit	Uncertainty	
				LO	HI		±ABS.	±%FR
1	TE 1	TE010A-HLA	HLA Vessel-Side CPT	270	720	K	2.75	0.61
2	TE 2	TE010B-HLA	HLA Vessel-Side CPT	270	720	K	2.75	0.61
3	TE 3	TE010C-HLA	HLA Vessel-Side CPT	270	720	K	2.75	0.61
4	TE 4	TE010D-HLA	HLA Vessel-Side CPT	270	720	K	2.75	0.61
5	TE 5	TE010E-HLA	HLA Vessel-Side CPT	270	720	K	2.75	0.61
6	TE 6	TE020C-HLA	HLA Pipe Top	270	720	K	2.75	0.61
7	TE 7	TE020D-HLA	HLA Pipe Bottom	270	720	K	2.75	0.61
8	TE 8	TE030C-HLA	HLA Pipe Top	270	720	K	2.75	0.61
9	TE 10	TE040A-HLA	HLA SG-Side CPT	270	720	K	2.75	0.61
10	TE 11	TE040B-HLA	HLA SG-Side CPT	270	720	K	2.75	0.61
11	TE 12	TE040C-HLA	HLA SG-Side CPT	270	720	K	2.75	0.61
12	TE 13	TE040D-HLA	HLA SG-Side CPT	270	720	K	2.75	0.61
13	TE 14	TE040E-HLA	HLA SG-Side CPT	270	720	K	2.75	0.61
14	TE 15	TE050C-LSA	LSA Upflow Leg	270	720	K	2.75	0.61
15	TE 16	TE070C-CLA	CLA Pipe Top	270	720	K	2.75	0.61
16	TE 17	TE070D-CLA	CLA Pipe Bottom	270	720	K	2.75	0.61
17	TE 18	TE080C-CLA	CLA Pipe Top	270	720	K	2.75	0.61
18	TE 20	TE090A-CLA	CLA Vessel-Side CPT	270	720	K	2.75	0.61
19	TE 21	TE090B-CLA	CLA Vessel-Side CPT	270	720	K	2.75	0.61
20	TE 22	TE090C-CLA	CLA Vessel-Side CPT	270	720	K	2.75	0.61
21	TE 23	TE090D-CLA	CLA Vessel-Side CPT	270	720	K	2.75	0.61
22	TE 24	TE090E-CLA	CLA Vessel-Side CPT	270	720	K	2.75	0.61
23	TE 25	TE100-HLA	HLA-CLA Average	270	720	K	2.75	0.61
24	TE 27	TE150B-HLB	HLB Vessel-Side CPT	270	720	K	2.75	0.61
25	TE 28	TE150C-HLB	HLB Vessel-Side CPT	270	720	K	2.75	0.61
26	TE 29	TE150D-HLB	HLB Vessel-Side CPT	270	720	K	2.75	0.61
27	TE 30	TE150E-HLB	HLB Vessel-Side CPT	270	720	K	2.75	0.61
28	TE 31	TE160C-HLB	HLB Pipe Top	270	720	K	2.75	0.61
29	TE 32	TE160D-HLB	HLB Pipe Bottom	270	720	K	2.75	0.61
30	TE 33	TE170C-HLB	HLB Pipe Top	270	720	K	2.75	0.61
31	TE 35	TE180A-HLB	HLB SG-Side CPT	270	720	K	2.75	0.61
32	TE 36	TE180B-HLB	HLB SG-Side CPT	270	720	K	2.75	0.61
33	TE 37	TE180C-HLB	HLB SG-Side CPT	270	720	K	2.75	0.61
34	TE 38	TE180D-HLB	HLB SG-Side CPT	270	720	K	2.75	0.61
35	TE 39	TE180E-HLB	HLB SG-Side CPT	270	720	K	2.75	0.61
36	TE 40	TE190C-LSB	LSB Upflow Leg	270	720	K	2.75	0.61
37	TE 41	TE210C-CLB	CLB Pipe Top	270	720	K	2.75	0.61
38	TE 42	TE210D-CLB	CLB Pipe Bottom	270	720	K	2.75	0.61
39	TE 43	TE220C-CLB	CLB Pipe Top	270	720	K	2.75	0.61
40	TE 46	TE230B-CLB	CLB Vessel-Side CPT	270	720	K	2.75	0.61
41	TE 47	TE230C-CLB	CLB Vessel-Side CPT	270	720	K	2.75	0.61
42	TE 48	TE230D-CLB	CLB Vessel-Side CPT	270	720	K	2.75	0.61
43	TE 49	TE230E-CLB	CLB Vessel-Side CPT	270	720	K	2.75	0.61
44	TE 50	TE240-HLB	HLB-CLB Average	270	720	K	2.75	0.61
45	TE 52	TE280C-PR	PZR Surge Line	270	720	K	2.75	0.61
46	TE 55	TE430-SGA	SGA Feedwater Line	270	670	K	2.63	0.66
47	TE 56	TE440-SGA	SGA Main Steam Line	270	670	K	2.63	0.66
48	TE 57	TE450-SGA	SGA Relief Valve Line	270	670	K	2.63	0.66
49	TE 59	TE470-SGB	SGB Feedwater Line	270	670	K	2.63	0.66
50	TE 60	TE480-SGB	SGB Main Steam Line	270	670	K	2.63	0.66
51	TE 61	TE490-SGB	SGB Relief Valve Line	270	670	K	2.63	0.66
52	TE 63	TE510-SH	MSL Steam Header	270	670	K	2.63	0.66
53	TE 64	TE520-JC	JC Hot Water	270	670	K	2.63	0.66
54	TE 65	TE530-JC	PF Suction Line	270	670	K	2.63	0.66
55	TE 66	TE540-JC	JC Spray Water	270	670	K	2.63	0.66
56	TE 67	TE550-JC	JC Steam Vent Line	270	670	K	2.63	0.66
57	TE 68	TE431-SGA	SGA Downcomer A	270	670	K	2.63	0.66
58	TE 69	TE432-SGA	SGA Downcomer B	270	670	K	2.63	0.66
59	TE 70	TE433-SGA	SGA Downcomer C	270	670	K	2.63	0.66
60	TE 71	TE434-SGA	SGA Downcomer D	270	670	K	2.63	0.66
61	TE 72	TE471-SGB	SGB Downcomer A	270	670	K	2.63	0.66
62	TE 73	TE472-SGB	SGB Downcomer B	270	670	K	2.63	0.66
63	TE 74	TE473-SGB	SGB Downcomer C	270	670	K	2.63	0.66
64	TE 75	TE474-SGB	SGB Downcomer D	270	670	K	2.63	0.66
65	TE 76	TE560C-BU	Break Upstream	270	720	K	2.63	0.66
66	TE 77	TE560D-BU	Break Upstream	270	720	K	2.63	0.66
67	TE 78	TE570C-BU	RSV Spool Piece, Outlet Side	270	720	K	2.63	0.66
68	TE 79	TE570D-BU	RSV Spool Piece, Outlet Side	270	720	K	2.63	0.66
69	TE 80	TE580C-BU	Break Orif. Upstream Top	270	720	K	2.63	0.66
70	TE 81	TE580D-BU	Break Orif. Upstream Bottom	270	720	K	2.63	0.66
71	TE 82	TE590C-BU	Break Orif. Downstream Top	270	720	K	2.63	0.66
72	TE 83	TE590D-BU	Break Orif. Downstream Bottom	270	720	K	2.63	0.66
73	TE 84	TE600-ST	ST Inlet Line	270	470	K	2.30	1.15
74	TE 85	TE610-ST	ST Top Region	270	470	K	2.30	1.15
75	TE 86	TE620-ST	ST Middle Region	270	470	K	2.30	1.15
76	TE 87	TE630-ST	ST Bottom Region	270	470	K	2.30	1.15
77	TE 88	TE640-ST	ST Spray Line	270	470	K	2.30	1.15
78	TE 89	TE650-ACC	Acc-Cold Tank Bottom	270	470	K	2.30	1.15
79	TE 90	TE660-ACC	Acc-Cold Tank Top	270	470	K	2.30	1.15
80	TE 91	TE670-ACC	Acc-Cold Line to CLA	270	470	K	2.30	1.15
81	TE 94	TE700-ACH	Acc-Hot Tank Top	270	570	K	2.42	0.81

Table A-1 (Cont'd)

SEQ No.	Function ID.	Tagname	Location	Range		Unit	Uncertainty	
				LO	HI		±ABS.	±%FR
82	TE 96	TE720-ACH	Acc-Hot Line to CLB	270	570	K	2.42	0.81
83	TE 97	TE730-HLA	HLA ECCS Nozzle	270	670	K	2.63	0.66
84	TE 98	TE740-LSA	LSA ECCS Nozzle	270	670	K	2.63	0.66
85	TE 99	TE750-CLA	CLA ECCS Nozzle	270	670	K	2.63	0.66
86	TE 100	TE760-HLB	HKB ECCS Nozzle	270	670	K	2.63	0.66
87	TE 101	TE770-LSB	LSB ECCS Nozzle	270	670	K	2.63	0.66
88	TE 102	TE780-CLB	CLB ECCS Nozzle	270	670	K	2.63	0.66
89	TE 103	TE790-PV	PV Bottom ECCS Nozzle	270	670	K	2.63	0.66
90	TE 104	TE800-PV	PV Top ECCS Nozzle	270	670	K	2.63	0.66
91	TE 106	TE820-PL	RHR Inlet Region	270	670	K	2.63	0.66
92	TE 107	TE830-PL	RHR Outlet Region	270	670	K	2.63	0.66
93	TE 108	TE840-PL	RHR Injection Line	270	670	K	2.63	0.66
94	TE 112	TE880-RWST	RWST Lower Region	270	370	K	2.37	2.37
95	TE 113	TE890-RWST	RWST Middle Region	270	370	K	2.37	2.37
96	TE 115	TE-E066F-PV	Upper Head Bottom	270	970	K	3.49	0.50
97	TE 117	TE-E075F-PV	Upper Head Middle	270	970	K	3.49	0.50
98	TE 118	TE-W075F-PV	Upper Head Middle	270	970	K	3.49	0.50
99	TE 119	TE-E081F-PV	Upper Head Top	270	970	K	3.49	0.50
100	TE 120	TE-W081F-PV	Upper Head Top	270	970	K	3.49	0.50
101	TE 121	TE-E080H-PV	CR Guide Tube Top	270	970	K	3.49	0.50
102	TE 122	TE-W080H-PV	CR Guide Tube Top	270	970	K	3.49	0.50
103	TE 123	TE-E049F-PV	Upper Plenum Bottom	270	970	K	3.49	0.50
104	TE 125	TE-E055F-PV	Upper Plenum Middle	270	970	K	3.49	0.50
105	TE 126	TE-W055F-PV	Upper Plenum Middle	270	970	K	3.49	0.50
106	TE 127	TE-E060F-PV	Upper Plenum Top	270	970	K	3.49	0.50
107	TE 128	TE-W060F-PV	Upper Plenum Top	270	970	K	3.49	0.50
108	TE 129	TE-IN038-B09-UCP	Below Upper Core Plate	270	970	K	3.49	0.50
109	TE 130	TE-IN038-B11-UCP	Below Upper Core Plate	270	970	K	3.49	0.50
110	TE 131	TE-IN038-B01-UCP	Below Upper Core Plate	270	970	K	3.49	0.50
111	TE 132	TE-IN038-B03-UCP	Below Upper Core Plate	270	970	K	3.49	0.50
112	TE 133	TE-IN038-B05-UCP	Below Upper Core Plate	270	970	K	3.49	0.50
113	TE 134	TE-IN038-B07-UCP	Below Upper Core Plate	270	970	K	3.49	0.50
114	TE 135	TE-IN038-B21-UCP	Below Upper Core Plate	270	970	K	3.49	0.50
115	TE 136	TE-IN038-B23-UCP	Below Upper Core Plate	270	970	K	3.49	0.50
116	TE 137	TE-IN038-B02-UCP	Below Upper core Plate	270	970	K	3.49	0.50
117	TE 138	TE-IN038-B06-UCP	Below Upper Core Plate	270	970	K	3.49	0.50
118	TE 139	TE-IN038-B14-UCP	Below Upper Core Plate	270	970	K	3.49	0.50
119	TE 140	TE-IN038-B15-UCP	Below Upper Core Plate	270	970	K	3.49	0.50
120	TE 141	TE-IN038-B18-UCP	Below Upper Core Plate	270	970	K	3.49	0.50
121	TE 142	TE-IN038-B19-UCP	Below Upper Core Plate	270	970	K	3.49	0.50
122	TE 143	TE-IN038-B10-UCP	Below Upper Core Plate	270	970	K	3.49	0.50
123	TE 144	TE-IN038-B12-UCP	Below Upper Core Plate	270	970	K	3.49	0.50
124	TE 145	TE-IN038-B04-UCP	Below Upper Core Plate	270	970	K	3.49	0.50
125	TE 146	TE-IN038-B08-UCP	Below Upper Core Plate	270	970	K	3.49	0.50
126	TE 149	TE-EX040-B09-UCP	Above Upper Core Plate	270	970	K	3.49	0.50
127	TE 150	TE-EX040-B11-UCP	Above Upper Core Plate	270	970	K	3.49	0.50
128	TE 151	TE-EX040-B01-UCP	Above Upper Core Plate	270	970	K	3.49	0.50
129	TE 152	TE-EX040-B03-UCP	Above Upper Core Plate	270	970	K	3.49	0.50
130	TE 153	TE-EX040-B05-UCP	Above Upper Core Plate	270	970	K	3.49	0.50
131	TE 154	TE-EX040-B07-UCP	Above Upper Core Plate	270	970	K	3.49	0.50
132	TE 155	TE-EX040-B21-UCP	Above Upper Core Plate	270	970	K	3.49	0.50
133	TE 156	TE-EX040-B23-UCP	Above Upper Core Plate	270	970	K	3.49	0.50
134	TE 157	TE-EX040-B02-UCP	Above Upper Core Plate	270	970	K	3.49	0.50
135	TE 158	TE-EX040-B06-UCP	Above Upper Core Plate	270	970	K	3.49	0.50
136	TE 159	TE-EX040-B14-UCP	Above Upper Core Plate	270	970	K	3.49	0.50
137	TE 160	TE-EX040-B15-UCP	Above Upper Core Plate	270	970	K	3.49	0.50
138	TE 161	TE-EX040-B18-UCP	Above Upper Core Plate	270	970	K	3.49	0.50
139	TE 162	TE-EX040-B19-UCP	Above Upper Core Plate	270	970	K	3.49	0.50
140	TE 163	TE-EX040-B10-UCP	Above Upper Core Plate	270	970	K	3.49	0.50
141	TE 164	TE-EX040-B12-UCP	Above Upper Core Plate	270	970	K	3.49	0.50
142	TE 165	TE-EX040-B04-UCP	Above Upper Core Plate	270	970	K	3.49	0.50
143	TE 166	TE-EX040-B08-UCP	Above Upper Core Plate	270	970	K	3.49	0.50
144	TE 167	TE-EX040-B22-UCP	Above Upper Core Plate	270	970	K	3.49	0.50
145	TE 168	TE-EX040-B24-UCP	Above Upper Core Plate	270	970	K	3.49	0.50
146	TE 193	TE-N000C-DC	Downcomer EL.0.0m,North	270	720	K	2.75	0.61
147	TE 194	TE-S000C-DC	Downcomer EL.0.0m,South	270	720	K	2.75	0.61
148	TE 196	TE-W000C-DC	Downcomer EL.0.0m,West	270	720	K	2.75	0.61
149	TE 197	TE-N018C-DC	Downcomer EL.1.8m,North	270	720	K	2.75	0.61
150	TE 199	TE-E018C-DC	Downcomer EL.1.8m,East	270	720	K	2.75	0.61
151	TE 200	TE-W018C-DC	Downcomer EL.1.8m,West	270	720	K	2.75	0.61
152	TE 201	TE-N036C-DC	Downcomer EL.3.6m,North	270	720	K	2.75	0.61
153	TE 202	TE-S036C-DC	Downcomer EL.3.6m,South	270	720	K	2.75	0.61
154	TE 203	TE-E036C-DC	Downcomer EL.3.6m,East	270	720	K	2.75	0.61
155	TE 204	TE-W036C-DC	Downcomer EL.3.6m,West	270	720	K	2.75	0.61
156	TE 206	TE-S060C-DC	Downcomer EL.6.0m,South	270	720	K	2.75	0.61
157	TE 208	TE-W060C-DC	Downcomer EL.6.0m,West	270	720	K	2.75	0.61
158	TE 209	TE-N055C-DC	Downcomer EL.5.5m,North	270	720	K	2.75	0.61
159	TE 210	TE-S055C-DC	Downcomer EL.5.5m,South	270	720	K	2.75	0.61
160	TE 211	TE-C-021-LP	Lower Plenum EL.-2.1m,C	270	720	K	2.75	0.61
161	TE 212	TE-C-018-LP	Lower Plenum EL.-1.8m,C	270	720	K	2.75	0.61
162	TE 213	TE-C-015-LP	Lower Plenum EL.-1.5m,C	270	720	K	3.73	0.83
163	TE 216	TE-C-006-LP	Lower Plenum EL.-0.6m,C	270	720	K	2.75	0.61

Table A-1 (Cont'd)

SEQ No.	Function ID.	Tagname	Location	Range		Unit	Uncertainty	
				LO	HI		±ABS.	±%FR
164	TE 217	TE-C-005-LP	Lower Plenum EL.-0.5m,C	270	720	K	2.75	0.61
165	TE 218	TE-C-003-LP	Lower Plenum EL.-0.3m,C	270	720	K	2.75	0.61
166	TE 220	TE-B18622	B18 Rod(6,2) Pos.2,Fluid	270	970	K	3.49	0.50
167	TE 221	TE-B18623	B18 Rod(6,2) Pos.3,Fluid	270	970	K	3.49	0.50
168	TE 222	TE-B18624	B18 Rod(6,2) Pos.4,Fluid	270	970	K	3.49	0.50
169	TE 223	TE-B18625	B18 Rod(6,2) Pos.5,Fluid	270	970	K	3.49	0.50
170	TE 226	TE-B18628	B18 Rod(6,2) Pos.8,Fluid	270	970	K	3.49	0.50
171	TE 227	TE-B18629	B18 Rod(6,2) Pos.9,Fluid	270	970	K	3.49	0.50
172	TE 256	TE-B09663	B09 Rod(6,6) Pos.3,Fluid	270	970	K	3.69	0.53
173	TE 257	TE-B09665	B09 Rod(6,6) Pos.5,Fluid	270	970	K	3.69	0.53
174	TE 258	TE-B09666	B09 Rod(6,6) Pos.6,Fluid	270	970	K	3.69	0.53
175	TE 260	TE-B09669	B09 Rod(6,6) Pos.9,Fluid	270	970	K	3.69	0.53
176	TE 277	TE-B14267	B14 Rod(2,6) Pos.7,Fluid	270	970	K	3.49	0.50
177	TE 279	TE-B15261	B15 Rod(2,6) Pos.1,Fluid	270	970	K	4.31	0.62
178	TE 280	TE-B15263	B15 Rod(2,6) Pos.3,Fluid	270	970	K	4.31	0.62
179	TE 281	TE-B15265	B15 Rod(2,6) Pos.5,Fluid	270	970	K	4.31	0.62
180	TE 282	TE-B15266	B15 Rod(2,6) Pos.6,Fluid	270	970	K	4.31	0.62
181	TE 283	TE-B15267	B15 Rod(2,6) Pos.7,Fluid	270	970	K	3.69	0.53
182	TE 284	TE-B15269	B15 Rod(2,6) Pos.9,Fluid	270	970	K	3.69	0.53
183	TE 291	TE-B15262	B15 Rod(2,6) Pos.2,Fluid	270	970	K	4.31	0.62
184	TE 292	TE-B15264	B15 Rod(2,6) Pos.4,Fluid	270	970	K	4.31	0.62
185	TE 293	TE-B15268	B15 Rod(2,6) Pos.8,Fluid	270	970	K	3.69	0.53
186	TE 294	TE-B23221	B23 Rod(2,2) Pos.1,Fluid	270	970	K	3.69	0.53
187	TE 295	TE-B23223	B23 Rod(2,2) Pos.3,Fluid	270	970	K	3.69	0.53
188	TE 296	TE-B23225	B23 Rod(2,2) Pos.5,Fluid	270	970	K	3.69	0.53
189	TE 297	TE-B23226	B23 Rod(2,2) Pos.6,Fluid	270	970	K	3.69	0.53
190	TE 298	TE-B23227	B23 Rod(2,2) Pos.7,Fluid	270	970	K	3.69	0.53
191	TE 299	TE-B23229	B23 Rod(2,2) Pos.9,Fluid	270	970	K	3.69	0.53
192	TE 300	TE-B20661	B20 Rod(6,6) Pos.1,Fluid	270	970	K	3.69	0.53
193	TE 301	TE-B20662	B20 Rod(6,6) Pos.2,Fluid	270	970	K	3.69	0.53
194	TE 302	TE-B20663	B20 Rod(6,6) Pos.3,Fluid	270	970	K	3.69	0.53
195	TE 303	TE-B20664	B20 Rod(6,6) Pos.4,Fluid	270	970	K	3.69	0.53
196	TE 305	TE-B20666	B20 Rod(6,6) Pos.6,Fluid	270	970	K	3.69	0.53
197	TE 306	TE-B20667	B20 Rod(6,6) Pos.7,Fluid	270	970	K	0.00	0.00
198	TE 307	TE-B20668	B20 Rod(6,6) Pos.8,Fluid	270	970	K	3.69	0.53
199	TE 308	TE-B20669	B20 Rod(6,6) Pos.9,Fluid	270	970	K	0.00	0.00
200	TE 309	TE-B22661	B22 Rod(6,6) Pos.1,Fluid	270	970	K	4.31	0.62
201	TE 310	TE-B22662	B22 Rod(6,6) Pos.2,Fluid	270	970	K	4.31	0.62
202	TE 311	TE-B22663	B22 Rod(6,6) Pos.3,Fluid	270	970	K	4.31	0.62
203	TE 312	TE-B22664	B22 Rod(6,6) Pos.4,Fluid	270	970	K	4.31	0.62
204	TE 313	TE-B22665	B22 Rod(6,6) Pos.5,Fluid	270	970	K	4.31	0.62
205	TE 314	TE-B22666	B22 Rod(6,6) Pos.6,Fluid	270	970	K	4.31	0.62
206	TE 315	TE-B22667	B22 Rod(6,6) Pos.7,Fluid	270	970	K	4.31	0.62
207	TE 316	TE-B22668	B22 Rod(6,6) Pos.8,Fluid	270	970	K	4.31	0.62
208	TE 317	TE-B22669	B22 Rod(6,6) Pos.9,Fluid	270	970	K	4.31	0.62
209	TE 318	TE-B24621	B24 Rod(6,2) Pos.1,Fluid	270	970	K	3.69	0.53
210	TE 319	TE-B24623	B24 Rod(6,2) Pos.3,Fluid	270	970	K	3.69	0.53
211	TE 320	TE-B24625	B24 Rod(6,2) Pos.5,Fluid	270	970	K	3.69	0.53
212	TE 321	TE-B24626	B24 Rod(6,2) Pos.6,Fluid	270	970	K	3.69	0.53
213	TE 322	TE-B24627	B24 Rod(6,2) Pos.7,Fluid	270	970	K	3.69	0.53
214	TE 323	TE-B24629	B24 Rod(6,2) Pos.9,Fluid	270	970	K	3.69	0.53
215	TE 324	TE-IN0641-SGA	SGA Inlet Plenum	270	720	K	2.75	0.61
216	TE 325	TE-IN0642-SGA	SGA Inlet Plenum	270	720	K	2.75	0.61
217	TE 326	TE-IN0643-SGA	SGA Inlet Plenum	270	720	K	2.75	0.61
218	TE 330	TE-IN0861-SGA	SGA U-Tube(1,IN) Pos.1	270	720	K	2.75	0.61
219	TE 331	TE-IN0862-SGA	SGA U-Tube(2,IN) Pos.1	270	720	K	2.75	0.61
220	TE 332	TE-IN0863-SGA	SGA U-Tube(3,IN) Pos.1	270	720	K	2.75	0.61
221	TE 333	TE-IN0864-SGA	SGA U-Tube(4,IN) Pos.1	270	720	K	2.75	0.61
222	TE 334	TE-IN0865-SGA	SGA U-Tube(5,IN) Pos.1	270	720	K	2.75	0.61
223	TE 335	TE-IN0866-SGA	SGA U-Tube(6,IN) Pos.1	270	720	K	2.75	0.61
224	TE 336	TE-EX0861-SGA	SGA U-Tube(1,EX) Pos.1	270	720	K	2.75	0.61
225	TE 337	TE-EX0862-SGA	SGA U-Tube(2,EX) Pos.1	270	720	K	2.75	0.61
226	TE 338	TE-EX0863-SGA	SGA U-Tube(3,EX) Pos.1	270	720	K	2.75	0.61
227	TE 340	TE-EX0865-SGA	SGA U-Tube(5,EX) Pos.1	270	720	K	2.75	0.61
228	TE 341	TE-EX0866-SGA	SGA U-Tube(6,EX) Pos.1	270	720	K	2.75	0.61
229	TE 344	TE-IN0933-SGA	SGA U-Tube(3,IN) Pos.2	270	720	K	2.75	0.61
230	TE 345	TE-IN0934-SGA	SGA U-Tube(4,IN) Pos.2	270	720	K	2.75	0.61
231	TE 347	TE-IN0936-SGA	SGA U-Tube(6,IN) Pos.2	270	720	K	2.75	0.61
232	TE 348	TE-IN0991-SGA	SGA U-Tube(1,IN) Pos.3	270	720	K	2.75	0.61
233	TE 349	TE-EX0991-SGA	SGA U-Tube(1,EX) Pos.3	270	720	K	2.75	0.61
234	TE 350	TE-IN0992-SGA	SGA U-Tube(2,IN) Pos.3	270	720	K	2.75	0.61
235	TE 351	TE-EX0992-SGA	SGA U-Tube(2,IN) Pos.3	270	720	K	2.75	0.61
236	TE 352	TE-IN0993-SGA	SGA U-Tube(3,IN) Pos.3	270	720	K	2.75	0.61
237	TE 353	TE-EX0993-SGA	SGA U-Tube(3,EX) Pos.3	270	720	K	2.75	0.61
238	TE 354	TE-IN0994-SGA	SGA U-Tube(4,IN) Pos.3	270	720	K	2.75	0.61
239	TE 355	TE-EX0994-SGA	SGA U-Tube(4,EX) Pos.3	270	720	K	2.75	0.61
240	TE 356	TE-IN0995-SGA	SGA U-Tube(5,IN) Pos.3	270	720	K	2.75	0.61
241	TE 358	TE-IN0996-SGA	SGA U-Tube(6,IN) Pos.3	270	720	K	2.75	0.61
242	TE 359	TE-EX0996-SGA	SGA U-Tube(6,EX) Pos.3	270	720	K	2.75	0.61
243	TE 360	TE-IN1051-SGA	SGA U-Tube(1,IN) Pos.4	270	720	K	2.75	0.61
244	TE 361	TE-IN1052-SGA	SGA U-Tube(2,IN) Pos.4	270	720	K	2.75	0.61
245	TE 362	TE-IN1053-SGA	SGA U-Tube(3,IN) Pos.4	270	720	K	2.75	0.61

Table A-1 (Cont'd)

SEQ No.	Function ID.	Tagname	Location	Range		Unit	Uncertainty	
				LO	HI		±ABS.	±%FR
246	TE 363	TE-IN1054-SGA	SGA U-Tube(4,IN) Pos.4	270	720	K	2.75	0.61
247	TE 364	TE-IN1055-SGA	SGA U-Tube(5,IN) Pos.4	270	720	K	2.75	0.61
248	TE 365	TE-IN1056-SGA	SGA U-Tube(6,IN) Pos.4	270	720	K	2.75	0.61
249	TE 366	TE-IN1121-SGA	SGA U-Tube(1,IN) Pos.5	270	720	K	2.75	0.61
250	TE 367	TE-EX1121-SGA	SGA U-Tube(1,EX) Pos.5	270	720	K	2.75	0.61
251	TE 368	TE-IN1122-SGA	SGA U-Tube(2,IN) Pos.5	270	720	K	2.75	0.61
252	TE 369	TE-EX1122-SGA	SGA U-Tube(2,EX) Pos.5	270	720	K	2.75	0.61
253	TE 372	TE-IN1124-SGA	SGA U-Tube(4,IN) Pos.5	270	720	K	2.75	0.61
254	TE 373	TE-EX1124-SGA	SGA U-Tube(4,EX) Pos.5	270	720	K	2.75	0.61
255	TE 374	TE-IN1125-SGA	SGA U-Tube(5,IN) Pos.5	270	720	K	2.75	0.61
256	TE 376	TE-IN1126-SGA	SGA U-Tube(6,IN) Pos.5	270	720	K	2.75	0.61
257	TE 377	TE-EX1126-SGA	SGA U-Tube(6,EX) Pos.5	270	720	K	2.75	0.61
258	TE 378	TE-IN1251-SGA	SGA U-Tube(1,IN) Pos.6	270	720	K	2.75	0.61
259	TE 379	TE-EX1251-SGA	SGA U-Tube(1,EX) Pos.6	270	720	K	2.75	0.61
260	TE 380	TE-IN1252-SGA	SGA U-Tube(2,IN) Pos.6	270	720	K	2.75	0.61
261	TE 381	TE-EX1252-SGA	SGA U-Tube(2,EX) Pos.6	270	720	K	2.75	0.61
262	TE 382	TE-IN1253-SGA	SGA U-Tube(3,IN) Pos.6	270	720	K	2.75	0.61
263	TE 383	TE-EX1253-SGA	SGA U-Tube(3,EX) Pos.6	270	720	K	2.75	0.61
264	TE 384	TE-IN1254-SGA	SGA U-Tube(4,IN) Pos.6	270	720	K	2.75	0.61
265	TE 385	TE-EX1254-SGA	SGA U-Tube(4,EX) Pos.6	270	720	K	2.75	0.61
266	TE 387	TE-EX1255-SGA	SGA U-Tube(5,EX) Pos.6	270	720	K	2.75	0.61
267	TE 389	TE-EX1256-SGA	SGA U-Tube(6,EX) Pos.6	270	720	K	2.75	0.61
268	TE 390	TE-IN1371-SGA	SGA U-Tube(1,IN) Pos.7	270	720	K	2.75	0.61
269	TE 392	TE-IN1372-SGA	SGA U-Tube(2,IN) Pos.7	270	720	K	2.75	0.61
270	TE 393	TE-EX1372-SGA	SGA U-Tube(2,EX) Pos.7	270	720	K	2.75	0.61
271	TE 395	TE-EX1373-SGA	SGA U-Tube(3,EX) Pos.7	270	720	K	2.75	0.61
272	TE 396	TE-IN1374-SGA	SGA U-Tube(4,IN) Pos.7	270	720	K	2.75	0.61
273	TE 397	TE-EX1374-SGA	SGA U-Tube(4,EX) Pos.7	270	720	K	2.75	0.61
274	TE 399	TE-EX1375-SGA	SGA U-Tube(5,EX) Pos.7	270	720	K	2.75	0.61
275	TE 400	TE-IN1376-SGA	SGA U-Tube(6,IN) Pos.7	270	720	K	2.75	0.61
276	TE 401	TE-EX1376-SGA	SGA U-Tube(6,EX) Pos.7	270	720	K	2.75	0.61
277	TE 402	TE-IN1501-SGA	SGA U-Tube(1,IN) Pos.8	270	720	K	2.75	0.61
278	TE 403	TE-EX1501-SGA	SGA U-Tube(1,EX) Pos.8	270	720	K	2.75	0.61
279	TE 404	TE-IN1502-SGA	SGA U-Tube(2,IN) Pos.8	270	720	K	2.75	0.61
280	TE 405	TE-EX1502-SGA	SGA U-Tube(2,EX) Pos.8	270	720	K	2.75	0.61
281	TE 406	TE-IN1503-SGA	SGA U-Tube(3,IN) Pos.8	270	720	K	2.75	0.61
282	TE 407	TE-EX1503-SGA	SGA U-Tube(3,EX) Pos.8	270	720	K	2.75	0.61
283	TE 408	TE-IN1504-SGA	SGA U-Tube(4,IN) Pos.8	270	720	K	2.75	0.61
284	TE 409	TE-EX1504-SGA	SGA U-Tube(4,EX) Pos.8	270	720	K	2.75	0.61
285	TE 410	TE-IN1505-SGA	SGA U-Tube(5,IN) Pos.8	270	720	K	2.75	0.61
286	TE 412	TE-IN1506-SGA	SGA U-Tube(6,IN) Pos.8	270	720	K	2.75	0.61
287	TE 414	TE-IN1632-SGA	SGA U-Tube(2,IN) Pos.9	270	720	K	2.75	0.61
288	TE 415	TE-EX1632-SGA	SGA U-Tube(2,EX) Pos.9	270	720	K	2.75	0.61
289	TE 416	TE-IN1633-SGA	SGA U-Tube(3,IN) Pos.9	270	720	K	2.75	0.61
290	TE 417	TE-EX1633-SGA	SGA U-Tube(3,EX) Pos.9	270	720	K	2.75	0.61
291	TE 418	TE-IN1634-SGA	SGA U-Tube(4,IN) Pos.9	270	720	K	2.75	0.61
292	TE 419	TE-EX1634-SGA	SGA U-Tube(4,EX) Pos.9	270	720	K	2.75	0.61
293	TE 420	TE-IN1635-SGA	SGA U-Tube(5,IN) Pos.9	270	720	K	2.75	0.61
294	TE 422	TE-IN1701-SGA	SGA U-Tube(1,IN) Pos.10	270	720	K	2.75	0.61
295	TE 424	TE-IN1782-SGA	SGA U-Tube(2,IN) Pos.10	270	720	K	2.75	0.61
296	TE 426	TE-IN1863-SGA	SGA U-Tube(3,IN) Pos.11	270	720	K	2.75	0.61
297	TE 427	TE-IN1864-SGA	SGA U-Tube(4,IN) Pos.11	270	720	K	2.75	0.61
298	TE 429	TE-086C-SGA	SGA Boiling Section Pos.1	270	670	K	2.63	0.66
299	TE 430	TE-099C-SGA	SGA Boiling Section Pos.3	270	670	K	2.63	0.66
300	TE 431	TE-112C-SGA	SGA Boiling Section Pos.5	270	670	K	2.63	0.66
301	TE 432	TE-125C-SGA	SGA Boiling Section Pos.6	270	670	K	2.63	0.66
302	TE 433	TE-137C-SGA	SGA Boiling Section Pos.7	270	670	K	2.63	0.66
303	TE 434	TE-150C-SGA	SGA Boiling Section Pos.8	270	670	K	2.63	0.66
304	TE 435	TE-163C-SGA	SGA Boiling Section Pos.9	270	670	K	2.63	0.66
305	TE 436	TE-178C-SGA	SGA Boiling Section Pos.10	270	670	K	2.63	0.66
306	TE 437	TE-192F-SGA	SGA Boiling Section	270	670	K	2.63	0.66
307	TE 438	TE-208F-SGA	SGA Separator	270	670	K	2.63	0.66
308	TE 439	TE-192C-SGA	SGA Downcomer	270	670	K	2.63	0.66
309	TE 440	TE-208C-SGA	SGA Downcomer	270	670	K	2.63	0.66
310	TE 441	TE-223C-SGA	SGA Steam Dome	270	670	K	2.63	0.66
311	TE 442	TE-245C-SGA	SGA Steam Dome	270	670	K	2.63	0.66
312	TE 443	TE-IN0641-SGB	SGB Inlet Plenum	270	720	K	2.75	0.61
313	TE 444	TE-IN0642-SGB	SGB Inlet Plenum	270	720	K	2.75	0.61
314	TE 445	TE-IN0643-SGB	SGB Inlet Plenum	270	720	K	2.75	0.61
315	TE 449	TE-IN0861-SGB	SGB U-Tube(1,IN) Pos.1	270	720	K	2.75	0.61
316	TE 450	TE-IN0862-SGB	SGB U-Tube(2,IN) Pos.1	270	720	K	2.75	0.61
317	TE 452	TE-IN0864-SGB	SGB U-Tube(4,IN) Pos.1	270	720	K	2.75	0.61
318	TE 453	TE-IN0865-SGB	SGB U-Tube(5,IN) Pos.1	270	720	K	2.75	0.61
319	TE 454	TE-IN0866-SGB	SGB U-Tube(6,IN) Pos.1	270	720	K	2.75	0.61
320	TE 455	TE-EX0861-SGB	SGB U-Tube(1,EX) Pos.1	270	720	K	2.75	0.61
321	TE 456	TE-EX0862-SGB	SGB U-Tube(2,EX) Pos.1	270	720	K	2.75	0.61
322	TE 457	TE-EX0863-SGB	SGB U-Tube(3,EX) Pos.1	270	720	K	2.75	0.61
323	TE 458	TE-EX0864-SGB	SGB U-Tube(4,EX) Pos.1	270	720	K	2.75	0.61
324	TE 460	TE-EX0866-SGB	SGB U-Tube(6,EX) Pos.1	270	720	K	2.75	0.61
325	TE 461	TE-IN0931-SGB	SGB U-Tube(1,IN) Pos.2	270	720	K	2.75	0.61
326	TE 463	TE-IN0933-SGB	SGB U-Tube(3,IN) Pos.2	270	720	K	2.75	0.61
327	TE 464	TE-IN0934-SGB	SGB U-Tube(4,IN) Pos.2	270	720	K	2.75	0.61

Table A-1 (Cont'd)

SEQ No.	Function ID.	Tagname	Location	Range		Unit	Uncertainty	
				LO	HI		±ABS.	±%FR
328	TE 467	TE-IN0991-SGB	SGB U-Tube(1,IN) Pos.3	270	720	K	2.75	0.61
329	TE 468	TE-EX0991-SGB	SGB U-Tube(1,EX) Pos.3	270	720	K	2.75	0.61
330	TE 469	TE-IN0992-SGB	SGB U-Tube(2,IN) Pos.3	270	720	K	2.75	0.61
331	TE 470	TE-EX0992-SGB	SGB U-Tube(2,EX) Pos.3	270	720	K	2.75	0.61
332	TE 471	TE-IN0993-SGB	SGB U-Tube(3,IN) Pos.3	270	720	K	2.75	0.61
333	TE 472	TE-EX0993-SGB	SGB U-Tube(3,EX) Pos.3	270	720	K	2.75	0.61
334	TE 473	TE-IN0994-SGB	SGB U-Tube(4,IN) Pos.3	270	720	K	2.75	0.61
335	TE 474	TE-EX0994-SGB	SGB U-Tube(4,EX) Pos.3	270	720	K	2.75	0.61
336	TE 476	TE-EX0995-SGB	SGB U-Tube(5,EX) Pos.3	270	720	K	2.75	0.61
337	TE 477	TE-IN0996-SGB	SGB U-Tube(6,IN) Pos.3	270	720	K	2.75	0.61
338	TE 478	TE-EX0996-SGB	SGB U-Tube(6,EX) Pos.3	270	720	K	2.75	0.61
339	TE 479	TE-IN1051-SGB	SGB U-Tube(1,IN) Pos.4	270	720	K	2.75	0.61
340	TE 482	TE-IN1054-SGB	SGB U-Tube(4,IN) Pos.4	270	720	K	2.75	0.61
341	TE 486	TE-EX1121-SGB	SGB U-Tube(1,EX) Pos.5	270	720	K	2.75	0.61
342	TE 487	TE-IN1122-SGB	SGB U-Tube(2,IN) Pos.5	270	720	K	2.75	0.61
343	TE 488	TE-EX1122-SGB	SGB U-Tube(2,EX) Pos.5	270	720	K	2.75	0.61
344	TE 489	TE-IN1123-SGB	SGB U-Tube(3,IN) Pos.5	270	720	K	2.75	0.61
345	TE 490	TE-EX1123-SGB	SGB U-Tube(3,EX) Pos.5	270	720	K	2.75	0.61
346	TE 491	TE-IN1124-SGB	SGB U-Tube(4,IN) Pos.5	270	720	K	2.75	0.61
347	TE 492	TE-EX1124-SGB	SGB U-Tube(4,EX) Pos.5	270	720	K	2.75	0.61
348	TE 497	TE-IN1251-SGB	SGB U-Tube(1,IN) Pos.6	270	720	K	2.75	0.61
349	TE 498	TE-EX1251-SGB	SGB U-Tube(1,EX) Pos.6	270	720	K	2.75	0.61
350	TE 499	TE-IN1252-SGB	SGB U-Tube(2,IN) Pos.6	270	720	K	2.75	0.61
351	TE 502	TE-EX1253-SGB	SGB U-Tube(3,EX) Pos.6	270	720	K	2.75	0.61
352	TE 503	TE-IN1254-SGB	SGB U-Tube(4,IN) Pos.6	270	720	K	2.75	0.61
353	TE 504	TE-EX1254-SGB	SGB U-Tube(4,EX) Pos.6	270	720	K	2.75	0.61
354	TE 505	TE-IN1255-SGB	SGB U-Tube(5,IN) Pos.6	270	720	K	2.75	0.61
355	TE 506	TE-EX1255-SGB	SGB U-Tube(5,EX) Pos.6	270	720	K	2.75	0.61
356	TE 507	TE-IN1256-SGB	SGB U-Tube(6,IN) Pos.6	270	720	K	2.75	0.61
357	TE 508	TE-EX1256-SGB	SGB U-Tube(6,EX) Pos.6	270	720	K	2.75	0.61
358	TE 510	TE-EX1371-SGB	SGB U-Tube(1,EX) Pos.7	270	720	K	2.75	0.61
359	TE 511	TE-IN1372-SGB	SGB U-Tube(2,IN) Pos.7	270	720	K	2.75	0.61
360	TE 514	TE-EX1373-SGB	SGB U-Tube(3,EX) Pos.7	270	720	K	2.75	0.61
361	TE 515	TE-IN1374-SGB	SGB U-Tube(4,IN) Pos.7	270	720	K	2.75	0.61
362	TE 516	TE-EX1374-SGB	SGB U-Tube(4,EX) Pos.7	270	720	K	2.75	0.61
363	TE 517	TE-IN1375-SGB	SGB U-Tube(5,IN) Pos.7	270	720	K	2.75	0.61
364	TE 518	TE-EX1375-SGB	SGB U-Tube(5,EX) Pos.7	270	720	K	2.75	0.61
365	TE 519	TE-IN1376-SGB	SGB U-Tube(6,IN) Pos.7	270	720	K	2.75	0.61
366	TE 520	TE-EX1376-SGB	SGB U-Tube(6,EX) Pos.7	270	720	K	2.75	0.61
367	TE 523	TE-IN1502-SGB	SGB U-Tube(2,IN) Pos.8	270	720	K	2.75	0.61
368	TE 525	TE-IN1503-SGB	SGB U-Tube(3,IN) Pos.8	270	720	K	2.75	0.61
369	TE 526	TE-EX1503-SGB	SGB U-Tube(3,EX) Pos.8	270	720	K	2.75	0.61
370	TE 527	TE-IN1504-SGB	SGB U-Tube(4,IN) Pos.8	270	720	K	2.75	0.61
371	TE 528	TE-EX1504-SGB	SGB U-Tube(4,EX) Pos.8	270	720	K	2.75	0.61
372	TE 529	TE-IN1505-SGB	SGB U-Tube(5,IN) Pos.8	270	720	K	2.75	0.61
373	TE 530	TE-EX1505-SGB	SGB U-Tube(5,EX) Pos.8	270	720	K	2.75	0.61
374	TE 532	TE-EX1506-SGB	SGB U-Tube(6,EX) Pos.8	270	720	K	2.75	0.61
375	TE 533	TE-IN1632-SGB	SGB U-Tube(2,IN) Pos.9	270	720	K	2.75	0.61
376	TE 534	TE-EX1632-SGB	SGB U-Tube(2,EX) Pos.9	270	720	K	2.75	0.61
377	TE 535	TE-IN1633-SGB	SGB U-Tube(3,IN) Pos.9	270	720	K	2.75	0.61
378	TE 536	TE-EX1633-SGB	SGB U-Tube(3,EX) Pos.9	270	720	K	2.75	0.61
379	TE 537	TE-IN1634-SGB	SGB U-Tube(4,IN) Pos.9	270	720	K	2.75	0.61
380	TE 538	TE-EX1634-SGB	SGB U-Tube(4,EX) Pos.9	270	720	K	2.75	0.61
381	TE 539	TE-IN1635-SGB	SGB U-Tube(5,IN) Pos.9	270	720	K	2.75	0.61
382	TE 540	TE-EX1635-SGB	SGB U-Tube(5,EX) Pos.9	270	720	K	2.75	0.61
383	TE 544	TE-IN1785-SGB	SGB U-Tube(5,IN) Pos.10	270	720	K	2.75	0.61
384	TE 545	TE-IN1863-SGB	SGB U-Tube(3,IN) Pos.11	270	720	K	2.75	0.61
385	TE 546	TE-IN1864-SGB	SGB U-Tube(4,IN) Pos.11	270	720	K	2.75	0.61
386	TE 548	TE-086C-SGB	SGB Boiling Section Pos.1	270	670	K	2.63	0.66
387	TE 549	TE-099C-SGB	SGB Boiling Section Pos.3	270	670	K	2.63	0.66
388	TE 550	TE-112C-SGB	SGB Boiling Section Pos.5	270	670	K	2.63	0.66
389	TE 551	TE-125C-SGB	SGB Boiling Section Pos.6	270	670	K	2.63	0.66
390	TE 552	TE-137C-SGB	SGB Boiling Section Pos.7	270	670	K	2.63	0.66
391	TE 553	TE-150C-SGB	SGB Boiling Section Pos.8	270	670	K	2.63	0.66
392	TE 554	TE-163C-SGB	SGB Boiling Section Pos.9	270	670	K	2.63	0.66
393	TE 555	TE-178C-SGB	SGB Boiling Section Pos.10	270	670	K	2.63	0.66
394	TE 556	TE-192F-SGB	SGB Boiling Section	270	670	K	2.63	0.66
395	TE 557	TE-208F-SGB	SGB Separator	270	670	K	2.63	0.66
396	TE 558	TE-192C-SGB	SGB Downcomer	270	670	K	2.63	0.66
397	TE 559	TE-208C-SGB	SGB Downcomer	270	670	K	2.63	0.66
398	TE 560	TE-223C-SGB	SGB Steam Dome	270	670	K	2.63	0.66
399	TE 561	TE-245C-SGB	SGB Steam Dome	270	670	K	2.63	0.29
400	TE 595	TE724-ACH	Acc-Hot Line to CLB	270	570	K	2.42	0.81
401	TE 607	TE011B-HLA	HLA Spool Piece Side	270	720	K	2.75	0.61
402	TE 609	TE012C-HLA	HLA Spool Piece Top	270	720	K	2.75	0.61
403	TE 610	TE012D-HLA	HLA Spool Piece Bottom	270	720	K	2.75	0.61
404	TE 615	TE052-LSA	LSA Spool Piece	270	720	K	2.75	0.61
405	TE 619	TE072C-CLA	CLA Spool Piece Top	270	720	K	2.75	0.61
406	TE 620	TE072D-CLA	CLA Spool Piece Bottom	270	720	K	2.75	0.61
407	TE 624	TE152C-HLB	HLB Spool Piece Top	270	720	K	2.75	0.61
408	TE 625	TE152D-HLB	HLB Spool Piece Bottom	270	720	K	2.75	0.61
409	TE 628	TE191C-LSB	LSB Spool Piece East	270	720	K	2.75	0.61

Table A-1 (Cont'd)

SEQ No.	Function ID.	Tagname	Location	Range		Unit	Uncertainty	
				LO	HI		±ABS.	±%FR
410	TE 630	TE192-LSB	LSB Spool Piece	270	720	K	2.75	0.61
411	TE 634	TE212C-CLB	CLB Spool Piece Top	270	720	K	2.75	0.61
412	TE 635	TE212D-CLB	CLB Spool Piece Bottom	270	720	K	2.75	0.61
413	TE 644	TE571C-BU	RSV Spool Piece, Inlet Side	270	720	K	2.75	0.61
414	TE 645	TE571D-BU	RSV Spool Piece, Inlet Side	270	720	K	2.75	0.61
415	TE 651	TE591C-BU	Break Spool Piece	270	720	K	2.75	0.61
416	TE 652	TE591D-BU	Break Spool Piece	270	720	K	2.75	0.61
417	TE 662	TE-N-006-DC	PV Downcomer DTT North	270	720	K	2.75	0.61
418	TE 663	TE-S-006-DC	PV Downcomer DTT South	270	720	K	2.75	0.61
419	TE 664	TE-E-006-DC	PV Downcomer DTT East	270	720	K	2.75	0.61
420	TE 665	TE-W-006-DC	PV Downcomer DTT West	270	720	K	2.75	0.61
421	TE 707	TE-121E-UHDP	PLR-UH-9 Oil Outlet	270	720	K	2.75	0.61
422	TE 709	TE-121B-UHDP	PLR-UH-9 EL. 7.6m	270	720	K	2.75	0.61
423	TE 710	TE-121C-UHDP	PLR-UH-9 EL. 8.2m	270	720	K	2.75	0.61
424	TE 711	TE-E071C-DC	Downcomer EL.7.1m,East	270	720	K	2.75	0.61
425	TE 712	TE-W071C-DC	Downcomer EL.7.1m,West	270	720	K	2.75	0.61
426	TE 713	TE-E067C-DC	Downcomer EL.6.7m,East	270	720	K	2.75	0.61
427	TE 715	TE-951-CS	Oil Inlet-Main	270	720	K	2.75	0.61
428	TE 716	TE-952-CS	Oil Outlet-Main	270	720	K	2.75	0.61
429	TE 718	TE-B05221	B05 Rod(2,2) Pos.1,Fluid	270	970	K	3.69	0.53
430	TE 719	TE-B05223	B05 Rod(2,2) Pos.3,Fluid	270	970	K	3.69	0.53
431	TE 720	TE-B05225	B05 Rod(2,2) Pos.5,Fluid	270	970	K	3.69	0.53
432	TE 721	TE-B05226	B05 Rod(2,2) Pos.6,Fluid	270	970	K	3.69	0.53
433	TE 723	TE-B05229	B05 Rod(2,2) Pos.9,Fluid	270	970	K	3.69	0.53
434	TE 724	TE-B07221	B07 Rod(2,2) Pos.1,Fluid	270	1470	K	5.31	0.44
435	TE 725	TE-B07223	B07 Rod(2,2) Pos.3,Fluid	270	1470	K	5.31	0.44
436	TE 726	TE-B07225	B07 Rod(2,2) Pos.5,Fluid	270	1470	K	5.31	0.44
437	TE 727	TE-B07226	B07 Rod(2,2) Pos.6,Fluid	270	1470	K	5.31	0.44
438	TE 728	TE-B07227	B07 Rod(2,2) Pos.7,Fluid	270	1470	K	5.31	0.44
439	TE 729	TE-B07229	B07 Rod(2,2) Pos.9,Fluid	270	1470	K	5.31	0.44
440	TE 730	TE-EX0650-SGA	SGA Outlet Plenum	270	720	K	2.75	0.61
441	TE 731	TE-EX0680-SGA	SGA Outlet Plenum	270	720	K	2.75	0.61
442	TE 732	TE-EX0720-SGA	SGA Outlet Plenum	270	720	K	2.75	0.61
443	TE 733	TE-EX0650-SGB	SGB Outlet Plenum	270	720	K	2.75	0.61
444	TE 734	TE-EX0680-SGB	SGB Outlet Plenum	270	720	K	2.75	0.61
445	TE 735	TE-EX0720-SGB	SGB Outlet Plenum	270	720	K	2.75	0.61
446	TE 739	TE275C-PR	PZR Spray Inlet Nozzle	270	720	K	2.75	0.61
447	TE 752	TE293-ACH	Acc-Hot Top Gas Line	270	720	K	2.75	0.61
448	TE 780	TE687X-ACH	Acc-Hot Tank Fluid DL.6570	270	720	K	2.75	0.61
449	TE 854	TE-NP053F-PV	PV UP North Peri. EL.5299	270	630	K	3.05	0.85
450	TE 855	TE-NP055F-PV	PV UP North Peri. EL.5503	270	630	K	3.05	0.85
451	TE 856	TE-NP057F-PV	PV UP North Peri. EL.5706	270	630	K	3.05	0.85
452	TE 857	TE-NP059F-PV	PV UP North Peri. EL.5938	270	630	K	3.05	0.85
453	TE 858	TE-EP047F-PV	PV UP East Peri. EL.4672	270	630	K	3.05	0.85
454	TE 859	TE-EP053F-PV	PV UP East Peri. EL.5299	270	630	K	3.05	0.85
455	TE 860	TE-EP055F-PV	PV UP East Peri. EL.5503	270	630	K	3.05	0.85
456	TE 861	TE-EP057F-PV	PV UP East Peri. EL.5706	270	630	K	3.05	0.85
457	TE 862	TE-EP059F-PV	PV UP East Peri. EL.5938	270	630	K	3.05	0.85
458	TE 863	TE-SP047F-PV	PV UP South Peri. EL.4672	270	630	K	3.05	0.85
459	TE 864	TE-SP053F-PV	PV UP South Peri. EL.5299	270	630	k	3.05	0.85
460	TE 865	TE-SP055F-PV	PV UP South Peri. EL.5503	270	630	K	3.05	0.85
461	TE 866	TE-SP057F-PV	PV UP South Peri. EL.5706	270	630	K	3.05	0.85
462	TE 867	TE-SP059F-PV	PV UP South Peri. EL.5938	270	630	K	3.05	0.85
463	TE 868	TE-WP047F-PV	PV UP West Peri. EL.4672	270	630	K	3.05	0.85
464	TE 869	TE-WP053F-PV	PV UP West Peri. EL.5299	270	630	K	3.05	0.85
465	TE 870	TE-WP055F-PV	PV UP West Peri. EL.5503	270	630	K	3.05	0.85
466	TE 871	TE-WP057F-PV	PV UP West Peri. EL.5706	270	630	K	3.05	0.85
467	TE 872	TE-WP059F-PV	PV UP West Peri. EL.5938	270	630	K	3.05	0.85
468	TE 873	TE-EM053F-PV	PV UP East Middle EL.5299	270	630	K	3.05	0.85
469	TE 874	TE-EM057F-PV	PV UP East Middle EL.5706	270	630	K	3.05	0.85
470	TE 875	TE-WM053F-PV	PV UP West Middle EL.5299	270	630	K	3.05	0.85
471	TE 876	TE-WM057F-PV	PV UP West Middle EL.5706	270	630	K	3.05	0.85
472	TE 877	TE-WC047F-PV	PV UP West Center EL.4672	270	630	K	3.05	0.85
473	TE 878	TE-WC053F-PV	PV UP West Center EL.5299	270	630	K	3.05	0.85
474	TE 879	TE-WC055F-PV	PV UP West Center EL.5503	270	630	K	3.05	0.85
475	TE 880	TE-WC057F-PV	PV UP West Center EL.5706	270	630	K	3.05	0.85
476	TE 881	TE-WC059F-PV	PV UP West Center EL.5938	270	630	K	3.05	0.85
477	TE 882	TE-EC047F-PV	PV UP East Center EL.4672	270	630	K	3.05	0.85
478	TE 883	TE-EC053F-PV	PV UP East Center EL.5299	270	630	K	3.05	0.85
479	TE 884	TE-EC055F-PV	PV UP East Center EL.5503	270	630	K	3.05	0.85
480	TE 885	TE-EC057F-PV	PV UP East Center EL.5706	270	630	K	3.05	0.85
481	TE 886	TE-EC059F-PV	PV UP East Center EL.5938	270	630	K	3.05	0.85
482	TE 888	TE-E037C-DC	DC East EL.3662	270	630	K	3.05	0.85
483	TE 891	TE-W037C-DC	DC West EL.3662	270	630	K	3.05	0.85
484	TE 893	TE-EN040C-DC	DC East-North EL.4037	270	630	K	3.05	0.85
485	TE 894	TE-E040C-DC	DC East EL.4037	270	630	K	3.05	0.85
486	TE 895	TE-ES040C-DC	DC East-South EL.4037	270	630	K	3.05	0.85
487	TE 896	TE-WN040C-DC	DC West-North EL.4037	270	630	K	3.05	0.85
488	TE 897	TE-W040C-DC	DC West EL.4037	270	630	K	3.05	0.85
489	TE 898	TE-WS040C-DC	DC West-South EL.4037	270	630	K	3.05	0.85
490	TE 899	TE-W042C-DC	DC West EL.4210	270	630	K	3.05	0.85
491	TE 900	TE-E042C-DC	DC East EL.4210	270	630	K	3.05	0.85

Table A-1 (Cont'd)

SEQ No.	Function ID.	Tagname	Location	Range		Unit	Uncertainty	
				LO	HI		±ABS.	±%FR
492	TE 901	TE-SW045C-DC	DC South-West EL.4497	270	630	K	3.05	0.85
493	TE 902	TE-NE045C-DC	DC North-East EL.4497	270	630	K	3.05	0.85
494	TE 903	TE-N045C-DC	DC North EL.4497	270	630	K	3.05	0.85
495	TE 904	TE-NW045C-DC	DC North-West EL.4497	270	630	K	3.05	0.85
496	TE 905	TE-S045C-DC	DC South EL.4497	270	630	K	3.05	0.85
497	TE 906	TE-SE045C-DC	DC South-East EL.4497	270	630	K	3.05	0.85
498	TE 907	TE-NE051C-DC	DC North-East EL.5074	270	630	K	3.05	0.85
499	TE 908	TE-N051C-DC	DC North EL.5074	270	630	K	3.05	0.85
500	TE 909	TE-NW051C-DC	DC North-West EL.5074	270	630	K	3.05	0.85
501	TE 910	TE-SW051C-DC	DC South-West EL.5074	270	630	K	3.05	0.85
502	TE 912	TE-SE051C-DC	DC South-East EL.5074	270	630	K	3.05	0.85
503	TE 913	TE-N054C-DC	DC North EL.5363	270	630	K	3.05	0.85
504	TE 914	TE-S054C-DC	DC South EL.5363	270	630	K	3.05	0.85
505	TE 921	HTE-C046-PV	Heated TC, EL.4597	270	1270	K	4.55	0.46
506	TE 922	TE-C046-PV	HTC Fluid, EL.4597	270	1270	K	4.55	0.46
507	TE 924	TE-C051-PV	HTC Fluid, EL.5102	270	1270	K	4.55	0.46
508	TE 925	TE-C056-PV	HTC Fluid, EL.5606	270	1270	K	4.55	0.46
509	TE 926	HTE-C056-PV	Heated TC, EL.5606	270	1270	K	4.55	0.46
510	TE 958	TE194A-PR	PZR DL.2025	270	720	K	2.75	0.61
511	TE 960	TE194C-PR	PZR DL.5995	270	720	K	2.75	0.61
512	TE 961	TE194D-PR	PZR DL.7965	270	720	K	2.75	0.61
513	TE 962	TE194E-PR	PZR DL.9795	270	720	K	2.75	0.61
514	TE 963	TE194F-PR	PZR DL.11321	270	720	K	2.75	0.61
515	TE 964	TE-PR2	PZR HT	270	1470	K	5.31	0.44
516	TE 965	TE677-ACC	Acc-Cold Tank Fluid DL.6450	270	720	K	2.75	0.61
517	TE 1089	TE910-CWT	Cooling Water Tank	270	370	K	2.37	2.37
518	TE 1092	TE960-AIR	Atmospheric Temperature	170	370	K	2.30	1.15
519	TE 1093	TE961-AIR	Room Temperature	170	370	K	2.30	1.15
520	TE 1094	TC030D-HLA	HLA Fluid at Pipe Bottom	273	673	K	2.63	0.66
521	TE 1095	TC170D-HLB	HLB Fluid at Pipe Bottom	273	673	K	2.63	0.66
522	TE 1096	TC080D-CLA	CLA Fluid at Pipe Bottom	273	673	K	2.63	0.66
523	TE 1097	TC220D-CLB	CLB Fluid at Pipe Bottom	273	673	K	2.63	0.66
524	TE 1098	TC194B-PR	PZR Fluid	273	673	K	2.63	0.66
525	TE 1099	TC223D-SGA	SGA Steam Dome	273	673	K	2.63	0.66
526	TE 1100	TC223D-SGB	SGB Steam Dome	273	673	K	2.63	0.66
527	TE 1101	TC-E000C-DC	Douncomer EL.0.0m,East	273	673	K	2.63	0.66
528	TE 1102	TC-E060C-DC	Downcomer EL.6.0m,East	273	673	K	2.63	0.66
529	TE 1123	TE687A-ACH	Acc-Hot Tank Fluid DL.10	270	720	K	2.75	0.61
530	TE 1124	TE687B-ACH	Acc-Hot Tank Fluid DL.475	270	720	K	2.75	0.61
531	TE 1125	TE687C-ACH	Acc-Hot Tank Fluid DL.940	270	720	K	2.75	0.61
532	TE 1126	TE687D-ACH	Acc-Hot Tank Fluid DL.1405	270	720	K	2.75	0.61
533	TE 1127	TE687E-ACH	Acc-Hot Tank Fluid DL.1870	270	720	K	2.75	0.61
534	TE 1128	TE687F-ACH	Acc-Hot Tank Fluid DL.2335	270	720	K	2.75	0.61
535	TE 1129	TE687G-ACH	Acc-Hot Tank Fluid DL.2800	270	720	K	2.75	0.61
536	TE 1130	TE687H-ACH	Acc-Hot Tank Fluid DL.3265	270	720	K	2.75	0.61
537	TE 1131	TE687I-ACH	Acc-Hot Tank Fluid DL.3275	270	720	K	2.75	0.61
538	TE 1132	TE687J-ACH	Acc-Hot Tank Fluid DL.3285	270	720	K	2.75	0.61
539	TE 1133	TE687K-ACH	Acc-Hot Tank Fluid DL.3295	270	720	K	2.75	0.61
540	TE 1134	TE687L-ACH	Acc-Hot Tank Fluid DL.3305	270	720	K	2.75	0.61
541	TE 1135	TE687M-ACH	Acc-Hot Tank Fluid DL.3315	270	720	K	2.75	0.61
542	TE 1136	TE687N-ACH	Acc-Hot Tank Fluid DL.3325	270	720	K	2.75	0.61
543	TE 1137	TE687O-ACH	Acc-Hot Tank Fluid DL.3335	270	720	K	2.75	0.61
544	TE 1138	TE687P-ACH	Acc-Hot Tank Fluid DL.3345	270	720	K	2.75	0.61
545	TE 1139	TE687Q-ACH	Acc-Hot Tank Fluid DL.3355	270	720	K	2.75	0.61
546	TE 1140	TE687R-ACH	Acc-Hot Tank Fluid DL.3820	270	720	K	2.75	0.61
547	TE 1141	TE687S-ACH	Acc-Hot Tank Fluid DL.4285	270	720	K	2.75	0.61
548	TE 1142	TE687T-ACH	Acc-Hot Tank Fluid DL.4750	270	720	K	2.75	0.61
549	TE 1143	TE687U-ACH	Acc-Hot Tank Fluid DL.5215	270	720	K	2.75	0.61
550	TE 1144	TE687V-ACH	Acc-Hot Tank Fluid DL.5680	270	720	K	2.75	0.61
551	TE 1145	TE687W-ACH	Acc-Hot Tank Fluid DL.6145	270	720	K	2.75	0.61
552	TE 1151	TE075A-CLA	CLA TC Rake	270	720	K	2.75	0.61
553	TE 1152	TE075B-CLA	CLA TC Rake	270	720	K	2.75	0.61
554	TE 1153	TE075C-CLA	CLA TC Rake	270	720	K	2.75	0.61
555	TE 1154	TE075D-CLA	CLA TC Rake	270	720	K	2.75	0.61
556	TE 1155	TE075E-CLA	CLA TC Rake	270	720	K	2.75	0.61
557	TE 1156	TE215A-CLB	CLB TC Rake	270	720	K	2.75	0.61
558	TE 1157	TE215B-CLB	CLB TC Rake	270	720	K	2.75	0.61
559	TE 1158	TE215C-CLB	CLB TC Rake	270	720	K	2.75	0.61
560	TE 1159	TE215D-CLB	CLB TC Rake	270	720	K	2.75	0.61
561	TE 1160	TE215E-CLB	CLB TC Rake	270	720	K	2.75	0.61
562	TE 1165	TE970-DIS	Dis. Gas Sampling	270	470	K	2.30	1.15
563	TE 1166	TE-H10-GAS	Air Injection Line No.1	270	370	K	2.37	2.37
564	TE 1167	TE-H20-GAS	Air Injection Line No.2	270	370	K	2.37	2.37
565	TE 1168	TE-E030C-DC	DC East EL.3000	270	720	K	2.37	0.53
566	TE 1169	TE-S030C-DC	DC South EL.3000	270	720	K	2.37	0.53
567	TE 1170	TE-W030C-DC	DC West EL.3000	270	720	K	2.37	0.53
568	TE 1171	TE-N030C-DC	DC North EL.3000	270	720	K	2.37	0.53
569	TE 1172	TE-S037C-DC	DC South EL.3662	270	720	K	2.37	0.53
570	TE 1173	TE-N037C-DC	DC North EL.3662	270	720	K	2.37	0.53
571	DT 1	DTE020A-HLA	HLA Wall I/O	-150	150	K	2.90	0.97
572	DT 2	DTE020B-HLA	HLA Wall-Fluid	-150	150	K	2.90	0.97

Table A-1 (Cont'd)

SEQ No.	Function ID.	Tagname	Location	Range		Unit	Uncertainty	
				LO	HI		±ABS.	±%FR
573	DT 3	DTE030A-HLA	HLA Wall I/O	-150	150	K	2.90	0.97
574	DT 4	DTE030B-HLA	HLA Wall-Fluid	-150	150	K	2.90	0.97
575	DT 5	DTE050A-LSA	LSA Wall I/O	-150	150	K	2.90	0.97
576	DT 6	DTE050B-LSA	LSA Wall-Fluid	-150	150	K	2.90	0.97
577	DT 7	DTE060A-PCA	PCA Wall I/O	-150	150	K	2.90	0.97
578	DT 8	DTE070A-CLA	CLA Wall I/O	-150	150	K	2.90	0.97
579	DT 9	DTE070B-CLA	CLA Wall-Fluid	-150	150	K	2.90	0.97
580	DT 10	DTE080A-CLA	CLA Wall I/O	-150	150	K	2.90	0.97
581	DT 11	DTE080B-CLA	CLA Wall-Fluid	-150	150	K	2.90	0.97
582	DT 12	DTE100-HLA	HLA-CLA	-150	150	K	2.90	0.97
583	DT 13	DTE160A-HLB	HLB Wall I/O	-150	150	K	2.90	0.97
584	DT 14	DTE160B-HLB	HLB Wall-Fluid	-150	150	K	2.90	0.97
585	DT 15	DTE170A-HLB	HLB Wall I/O	-150	150	K	2.90	0.97
586	DT 16	DTE170B-HLB	HLB Wall-Fluid	-150	150	K	2.90	0.97
587	DT 17	DTE190A-LSB	LSB Wall I/O	-150	150	K	2.90	0.97
588	DT 18	DTE190B-LSB	LSB Wall-Fluid	-150	150	K	2.90	0.97
589	DT 19	DTE200A-PCB	PCB Wall I/O	-150	150	K	2.90	0.97
590	DT 20	DTE210A-CLB	CLB Wall I/O	-150	150	K	2.90	0.97
591	DT 21	DTE210B-CLB	CLB Wall-Fluid	-150	150	K	2.90	0.97
592	DT 22	DTE220A-CLB	CLB Wall I/O	-150	150	K	2.90	0.97
593	DT 23	DTE220B-CLB	CLB Wall-Fluid	-150	150	K	2.90	0.97
594	DT 24	DTE240-HLB	HLB-CLB	-150	150	K	2.90	0.97
595	DT 25	DTE270A-PR	PZR Spray Line Wall-Fluid	-150	150	K	2.90	0.97
596	DT 26	DTE280A-PR	PZR Surge Line Wall-Fluid	-150	150	K	2.90	0.97
597	DT 27	DTE-E-015A-PV	PV Wall I/O-E at L. Plenum	-150	150	K	2.90	0.97
598	DT 28	DTE-W-015A-PV	PV Wall I/O-W at L. Plenum	-150	150	K	2.90	0.97
599	DT 29	DTE-N000A-PV	PV Wall I/O-N at DC Bottom	-150	150	K	2.90	0.97
600	DT 30	DTE-S000A-PV	PV Wall I/O-S at DC Bottom	-150	150	K	2.90	0.97
601	DT 31	DTE-E000A-PV	PV Wall I/O-E at DC Bottom	-150	150	K	2.90	0.97
602	DT 32	DTE-W000A-PV	PV Wall I/O-W at DC Bottom	-150	150	K	2.90	0.97
603	DT 33	DTE-N018A-PV	PV Wall I/O-N at DC Middle	-150	150	K	2.90	0.97
604	DT 34	DTE-S018A-PV	PV Wall I/O-S at DC Middle	-150	150	K	2.90	0.97
605	DT 35	DTE-E018A-PV	PV Wall I/O-E at DC Middle	-150	150	K	2.90	0.97
606	DT 36	DTE-W018A-PV	PV Wall I/O-W at DC Middle	-150	150	K	2.90	0.97
607	DT 37	DTE-N036A-PV	PV Wall I/O-N at Upper DC	-150	150	K	2.90	0.97
608	DT 38	DTE-S036A-PV	PV Wall I/O-S at Upper DC	-150	150	K	2.90	0.97
609	DT 39	DTE-E036A-PV	PV Wall I/O-E at Upper DC	-150	150	K	2.90	0.97
610	DT 40	DTE-W036A-PV	PV Wall I/O-W at Upper DC	-150	150	K	2.90	0.97
611	DT 41	DTE-N060A-PV	PV Wall I/O-N at DC Top	-150	150	K	2.90	0.97
612	DT 42	DTE-S060A-PV	PV Wall I/O-S at DC Top	-150	150	K	2.90	0.97
613	DT 43	DTE-E060A-PV	PV Wall I/O-E at DC Top	-150	150	K	2.90	0.97
614	DT 44	DTE-W060A-PV	PV Wall I/O-W at DC Top	-150	150	K	2.90	0.97
615	DT 45	DTE-E080A-PV	PV Wall I/O-E at DC Head	-150	150	K	2.90	0.97
616	DT 46	DTE-W080A-PV	PV Wall I/O-W at DC Head	-150	150	K	2.90	0.97
617	DT 47	DTE-N000B-PV	PV/DC Fluid at DC Bottom	-150	150	K	2.90	0.97
618	DT 48	DTE-S000B-PV	PV/DC Fluid at DC Bottom	-150	150	K	2.90	0.97
619	DT 50	DTE-W000B-PV	PV/DC Fluid at DC Bottom	-150	150	K	2.90	0.97
620	DT 51	DTE-N018B-PV	PV/DC Fluid at DC Middle	-150	150	K	2.90	0.97
621	DT 53	DTE-E018B-PV	PV/DC Fluid at DC Middle	-150	150	K	2.90	0.97
622	DT 54	DTE-W018B-PV	PV/DC Fluid at DC Middle	-150	150	K	2.90	0.97
623	DT 55	DTE-N036B-PV	PV/DC Fluid at Upper DC	-150	150	K	2.90	0.97
624	DT 56	DTE-S036B-PV	PV/DC Fluid at Upper DC	-150	150	K	2.90	0.97
625	DT 57	DTE-E036B-PV	PV/DC Fluid at Upper DC	-150	150	K	2.90	0.97
626	DT 58	DTE-W036B-PV	PV/DC Fluid at Upper DC	-150	150	K	2.90	0.97
627	DT 60	DTE-S060B-PV	PV/DC Fluid at DC Top	-150	150	K	2.90	0.97
628	DT 62	DTE-W060B-PV	PV/DC Fluid at DC Top	-150	150	K	2.90	0.97
629	DT 64	DTE-S000C-PV	CB/DC Fluid at DC Bottom	-150	150	K	2.90	0.97
630	DT 66	DTE-W000C-PV	CB/DC Fluid at DC Bottom	-150	150	K	2.90	0.97
631	DT 67	DTE-N018C-PV	CB/DC Fluid at DC Middle	-150	150	K	2.90	0.97
632	DT 69	DTE-E018C-PV	CB/DC Fluid at DC Middle	-150	150	K	2.90	0.97
633	DT 70	DTE-W018C-PV	CB/DC Fluid at DC Middle	-150	150	K	2.90	0.97
634	DT 71	DTE-N036C-PV	CB/DC Fluid at Upper DC	-150	150	K	2.90	0.97
635	DT 72	DTE-S036C-PV	CB/DC Fluid at Upper DC	-150	150	K	2.90	0.97
636	DT 73	DTE-E036C-PV	CB/DC Fluid at Upper DC	-150	150	K	2.90	0.97
637	DT 74	DTE-W036C-PV	CB/DC Fluid at Upper DC	-150	150	K	2.90	0.97
638	DT 76	DTE-S060C-PV	CB/DC Fluid at DC Top	-150	150	K	2.90	0.97
639	DT 78	DTE-W060C-PV	CB/DC Fluid at DC Top	-150	150	K	2.90	0.97
640	DT 80	DTE-S000E-PV	CB Wall I/O at DC Bottom	-150	150	K	2.90	0.97
641	DT 81	DTE-E000E-PV	CB Wall I/O at DC Bottom	-150	150	K	2.90	0.97
642	DT 82	DTE-W000E-PV	CB Wall I/O at DC Bottom	-150	150	K	2.90	0.97
643	DT 87	DTE-N018E-PV	CB Wall I/O at DC Middle	-150	150	K	2.90	0.97
644	DT 88	DTE-S018E-PV	CB Wall I/O at DC Middle	-150	150	K	2.90	0.97
645	DT 89	DTE-E018E-PV	CB Wall I/O at DC Middle	-150	150	K	2.90	0.97
646	DT 90	DTE-W018E-PV	CB Wall I/O at DC Middle	-150	150	K	2.90	0.97
647	DT 95	DTE-N036E-PV	CB Wall I/O at Upper DC	-150	150	K	2.90	0.97
648	DT 96	DTE-S036E-PV	CB Wall I/O at Upper DC	-150	150	K	2.90	0.97
649	DT 97	DTE-E036E-PV	CB Wall I/O at Upper DC	-150	150	K	2.90	0.97
650	DT 101	DTE-E049E-PV	CB Wall I/O below Nozzle	-150	150	K	2.90	0.97
651	DT 103	DTE-N060E-PV	CB Wall I/O at DC Top	-150	150	K	2.90	0.97
652	DT 104	DTE-S060E-PV	CB Wall I/O at DC Top	-150	150	K	2.90	0.97
653	DT 105	DTE-E060E-PV	CB Wall I/O at DC Top	-150	150	K	2.90	0.97
654	DT 106	DTE-W060E-PV	CB Wall I/O at DC Top	-150	150	K	2.90	0.97

Table A-1 (Cont'd)

SEQ No.	Function ID.	Tagname	Location	Range		Unit	Uncertainty	
				LO	HI		±ABS.	±%FR
655	DT 107	DTE-040-B09-UCP	Fluid DT across UCP	-150	150	K	2.90	0.97
656	DT 108	DTE-040-B11-UCP	Fluid DT across UCP	-150	150	K	2.90	0.97
657	DT 109	DTE-040-B01-UCP	Fluid DT across UCP	-150	150	K	2.90	0.97
658	DT 110	DTE-040-B03-UCP	Fluid DT across UCP	-150	150	K	2.90	0.97
659	DT 111	DTE-040-B05-UCP	Fluid DT across UCP	-150	150	K	2.90	0.97
660	DT 112	DTE-040-B07-UCP	Fluid DT across UCP	-150	150	K	2.90	0.97
661	DT 113	DTE-040-B21-UCP	Fluid DT across UCP	-150	150	K	2.90	0.97
662	DT 114	DTE-040-B23-UCP	Fluid DT across UCP	-150	150	K	2.90	0.97
663	DT 115	DTE-040-B02-UCP	Fluid DT across UCP	-150	150	K	2.90	0.97
664	DT 116	DTE-040-B15-UCP	Fluid DT across UCP	-150	150	K	2.90	0.97
665	DT 117	DTE-040-B06-UCP	Fluid DT across UCP	-150	150	K	2.90	0.97
666	DT 118	DTE-040-B14-UCP	Fluid DT across UCP	-150	150	K	2.90	0.97
667	DT 119	DTE-040-B18-UCP	Fluid DT across UCP	-150	150	K	2.90	0.97
668	DT 120	DTE-040-B19-UCP	Fluid DT across UCP	-150	150	K	2.90	0.97
669	DT 121	DTE-040-B10-UCP	Fluid DT across UCP	-150	150	K	2.90	0.97
670	DT 122	DTE-040-B12-UCP	Fluid DT across UCP	-150	150	K	2.90	0.97
671	DT 123	DTE-040-B04-UCP	Fluid DT across UCP	-150	150	K	2.90	0.97
672	DT 124	DTE-040-B08-UCP	Fluid DT across UCP	-150	150	K	2.90	0.97
673	DT 130	DTE-000-B07-LCP	In/Out Fluid across LCP	-150	150	K	1.67	0.56
674	DT 132	DTE-000-B11-LCP	In/Out Fluid across LCP	-150	150	K	1.67	0.56
675	DT 135	DTE-000-B18-LCP	In/Out Fluid across LCP	-150	150	K	1.67	0.56
676	DT 136	DTE-000-B20-LCP	In/Out Fluid across LCP	-150	150	K	1.67	0.56
677	DT 137	DTE-000-B21-LCP	In/Out Fluid across LCP	-150	150	K	1.67	0.56
678	DT 139	DTE-086A-SGA	SGA Wall I/O Pos.1	-40	40	K	2.07	2.58
679	DT 140	DTE-137A-SGA	SGA Wall I/O Pos.7	-40	40	K	2.07	2.58
680	DT 141	DTE-178A-SGA	SGA Wall I/O Pos.10	-40	40	K	2.07	2.58
681	DT 142	DTE-223A-SGA	SGA Steam Dome Wall I/O	-40	40	K	2.07	2.58
682	DT 143	DTE-IN0861-SGA	SGA U-Tube(1,IN) Pos.1	-100	100	K	2.42	1.21
683	DT 144	DTE-EX0861-SGA	SGA U-Tube(1,EX) Pos.1	-100	100	K	2.42	1.21
684	DT 145	DTE-IN0862-SGA	SGA U-Tube(2,IN) Pos.1	-100	100	K	2.42	1.21
685	DT 146	DTE-EX0862-SGA	SGA U-Tube(2,EX) Pos.1	-100	100	K	2.42	1.21
686	DT 147	DTE-IN0863-SGA	SGA U-Tube(3,IN) Pos.1	-100	100	K	2.42	1.21
687	DT 148	DTE-EX0863-SGA	SGA U-Tube(3,EX) Pos.1	-100	100	K	2.42	1.21
688	DT 149	DTE-IN0991-SGA	SGA U-Tube(1,IN) Pos.3	-100	100	K	2.42	1.21
689	DT 150	DTE-EX0991-SGA	SGA U-Tube(1,EX) Pos.3	-100	100	K	2.42	1.21
690	DT 151	DTE-IN0992-SGA	SGA U-Tube(2,IN) Pos.3	-100	100	K	2.42	1.21
691	DT 152	DTE-EX0992-SGA	SGA U-Tube(2,EX) Pos.3	-100	100	K	2.42	1.21
692	DT 153	DTE-IN0993-SGA	SGA U-Tube(3,IN) Pos.3	-100	100	K	2.42	1.21
693	DT 154	DTE-EX0993-SGA	SGA U-Tube(3,EX) Pos.3	-100	100	K	2.42	1.21
694	DT 155	DTE-IN1121-SGA	SGA U-Tube(1,IN) Pos.5	-100	100	K	2.42	1.21
695	DT 156	DTE-EX1121-SGA	SGA U-Tube(1,EX) Pos.5	-100	100	K	2.42	1.21
696	DT 157	DTE-IN1122-SGA	SGA U-Tube(2,IN) Pos.5	-100	100	K	2.42	1.21
697	DT 161	DTE-IN1371-SGA	SGA U-Tube(1,IN) Pos.7	-100	100	K	2.42	1.21
698	DT 163	DTE-IN1372-SGA	SGA U-Tube(2,IN) Pos.7	-100	100	K	2.42	1.21
699	DT 164	DTE-EX1372-SGA	SGA U-Tube(2,EX) Pos.7	-100	100	K	2.42	1.21
700	DT 166	DTE-EX1373-SGA	SGA U-Tube(3,EX) Pos.7	-100	100	K	2.42	1.21
701	DT 167	DTE-IN1632-SGA	SGA U-Tube(2,IN) Pos.9	-100	100	K	2.42	1.21
702	DT 168	DTE-EX1632-SGA	SGA U-Tube(2,EX) Pos.9	-100	100	K	2.42	1.21
703	DT 169	DTE-IN1633-SGA	SGA U-Tube(3,IN) Pos.9	-100	100	K	2.42	1.21
704	DT 170	DTE-EX1633-SGA	SGA U-Tube(3,EX) Pos.9	-100	100	K	2.42	1.21
705	DT 171	DTE-IN1701-SGA	SGA U-Tube(1,IN) Pos.10	-100	100	K	2.42	1.21
706	DT 172	DTE-IN1782-SGA	SGA U-Tube(2,IN) Pos.10	-100	100	K	2.42	1.21
707	DT 173	DTE-IN1863-SGA	SGA U-Tube(3,IN) Pos.11	-100	100	K	2.42	1.21
708	DT 174	DTE-086A-SGB	SGB Wall I/O Pos.1	-40	40	K	2.07	2.58
709	DT 175	DTE-137A-SGB	SGB Wall I/O Pos.7	-40	40	K	2.07	2.58
710	DT 176	DTE-178A-SGB	SGB Wall I/O Pos.10	-40	40	K	2.07	2.58
711	DT 177	DTE-223A-SGB	SGB Steam Dome Wall I/O	-40	40	K	2.07	2.58
712	DT 178	DTE-IN0861-SGB	SGB U-Tube(1,IN) Pos.1	-100	100	K	2.42	1.21
713	DT 179	DTE-EX0861-SGB	SGB U-Tube(1,EX) Pos.1	-100	100	K	2.42	1.21
714	DT 180	DTE-IN0862-SGB	SGB U-Tube(2,IN) Pos.1	-100	100	K	2.42	1.21
715	DT 181	DTE-EX0862-SGB	SGB U-Tube(2,EX) Pos.1	-100	100	K	2.42	1.21
716	DT 182	DTE-IN0863-SGB	SGB U-Tube(3,IN) Pos.1	-100	100	K	2.42	1.21
717	DT 183	DTE-EX0863-SGB	SGB U-Tube(3,EX) Pos.1	-100	100	K	2.42	1.21
718	DT 184	DTE-IN0991-SGB	SGB U-Tube(1,IN) Pos.3	-100	100	K	2.42	1.21
719	DT 185	DTE-EX0991-SGB	SGB U-Tube(1,EX) Pos.3	-100	100	K	2.42	1.21
720	DT 186	DTE-IN0992-SGB	SGB U-Tube(2,IN) Pos.3	-100	100	K	2.42	1.21
721	DT 187	DTE-EX0992-SGB	SGB U-Tube(2,EX) Pos.3	-100	100	K	2.42	1.21
722	DT 188	DTE-IN0993-SGB	SGB U-Tube(3,IN) Pos.3	-100	100	K	2.42	1.21
723	DT 189	DTE-EX0993-SGB	SGB U-Tube(3,EX) Pos.3	-100	100	K	2.42	1.21
724	DT 191	DTE-EX1121-SGB	SGB U-Tube(1,EX) Pos.5	-100	100	K	2.42	1.21
725	DT 192	DTE-IN1122-SGB	SGB U-Tube(2,IN) Pos.5	-100	100	K	2.42	1.21
726	DT 193	DTE-EX1122-SGB	SGB U-Tube(2,EX) Pos.5	-100	100	K	2.42	1.21
727	DT 194	DTE-IN1123-SGB	SGB U-Tube(3,IN) Pos.5	-100	100	K	2.42	1.21
728	DT 195	DTE-EX1123-SGB	SGB U-Tube(3,EX) Pos.5	-100	100	K	2.42	1.21
729	DT 196	DTE-IN1371-SGB	SGB U-Tube(1,IN) Pos.7	-100	100	K	2.42	1.21
730	DT 197	DTE-EX1371-SGB	SGB U-Tube(1,EX) Pos.7	-100	100	K	2.42	1.21
731	DT 198	DTE-IN1372-SGB	SGB U-Tube(2,IN) Pos.7	-100	100	K	2.42	1.21
732	DT 201	DTE-EX1373-SGB	SGB U-Tube(3,EX) Pos.7	-100	100	K	2.42	1.21
733	DT 202	DTE-IN1632-SGB	SGB U-Tube(2,IN) Pos.9	-100	100	K	2.42	1.21
734	DT 203	DTE-EX1632-SGB	SGB U-Tube(2,EX) Pos.9	-100	100	K	2.42	1.21
735	DT 204	DTE-IN1633-SGB	SGB U-Tube(3,IN) Pos.9	-100	100	K	2.42	1.21
736	DT 205	DTE-EX1633-SGB	SGB U-Tube(3,EX) Pos.9	-100	100	K	2.42	1.21

Table A-1 (Cont'd)

SEQ No.	Function ID.	Tagname	Location	Range		Unit	Uncertainty	
				LO	HI		±ABS.	±%FR
737	DT 215	DTE-C046-PV	HTC Differential Temp	-150	150	K	2.90	0.97
738	DT 216	DTE-C051-PV	HTC Differential Temp	-150	150	K	2.90	0.97
739	DT 217	DTE-C056-PV	HTC Differential Temp	-150	150	K	2.90	0.97
740	TW 1	TWE020B-HLA	HLA Inner Surface	270	720	K	2.75	0.61
741	TW 2	TWE030B-HLA	HLA Inner Surface	270	720	K	2.75	0.61
742	TW 3	TWE050B-LSA	LSA Inner Surface	270	720	K	2.75	0.61
743	TW 4	TWE060B-PCA	PCA Inner Surface	270	720	K	2.75	0.61
744	TW 5	TWE070B-CLA	CLA Inner Surface	270	720	K	2.75	0.61
745	TW 6	TWE080B-CLA	CLA Inner Surface	270	720	K	2.75	0.61
746	TW 7	TWE160B-HLB	HLB Inner Surface	270	720	K	2.75	0.61
747	TW 8	TWE170B-HLB	HLB Inner Surface	270	720	K	2.75	0.61
748	TW 9	TWE190B-LSB	LSB Inner Surface	270	720	K	2.75	0.61
749	TW 10	TWE200B-PCB	PCB Inner Surface	270	720	K	2.75	0.61
750	TW 11	TWE210B-CLB	CLB Inner Surface	270	720	K	2.75	0.61
751	TW 12	TWE220B-CLB	CLB Inner Surface	270	720	K	2.75	0.61
752	TW 13	TWE280B-PR	Pressurizer Surge Line	270	720	K	2.75	0.61
753	TW 14	TWE431A-SGA	SGA Downcomer A Wall	270	670	K	2.63	0.66
754	TW 15	TWE432A-SGA	SGA Downcomer B Wall	270	670	K	2.63	0.66
755	TW 16	TWE433A-SGA	SGA Downcomer C Wall	270	670	K	2.63	0.66
756	TW 17	TWE434A-SGA	SGA Downcomer D Wall	270	670	K	2.63	0.66
757	TW 18	TWE471A-SGB	SGB Downcomer A Wall	270	670	K	2.63	0.66
758	TW 19	TWE472A-SGB	SGB Downcomer B Wall	270	670	K	2.63	0.66
759	TW 20	TWE473A-SGB	SGB Downcomer C Wall	270	670	K	2.63	0.66
760	TW 21	TWE474A-SGB	SGB Downcomer D Wall	270	670	K	2.63	0.66
761	TW 22	TWE-E-015B-PV	PV Inner Surf. EL.-1.5m,E	270	720	K	2.75	0.61
762	TW 23	TWE-W-015B-PV	PV Inner Surf. EL.-1.5m,W	270	720	K	2.75	0.61
763	TW 24	TWE-N000B-PV	PV Inner Surf. EL.0.0m,N	270	720	K	2.75	0.61
764	TW 25	TWE-S000B-PV	PV Inner Surf. EL.0.0m,S	270	720	K	2.75	0.61
765	TW 26	TWE-E000B-PV	PV Inner Surf. EL.0.0m,E	270	720	K	2.75	0.61
766	TW 27	TWE-W000B-PV	PV Inner Surf. EL.0.0m,W	270	720	K	2.75	0.61
767	TW 28	TWE-N018B-PV	PV Inner Surf. EL.1.8m,N	270	720	K	2.75	0.61
768	TW 29	TWE-S018B-PV	PV Inner Surf. EL.1.8m,S	270	720	K	2.75	0.61
769	TW 30	TWE-E018B-PV	PV Inner Surf. EL.1.8m,E	270	720	K	2.75	0.61
770	TW 31	TWE-W018B-PV	PV Inner Surf. EL.1.8m,W	270	720	K	2.75	0.61
771	TW 32	TWE-N036B-PV	PV Inner Surf. EL.3.6m,N	270	720	K	2.75	0.61
772	TW 33	TWE-S036B-PV	PV Inner Surf. EL.3.6m,S	270	720	K	2.75	0.61
773	TW 34	TWE-E036B-PV	PV Inner Surf. EL.3.6m,E	270	720	K	2.75	0.61
774	TW 35	TWE-W036B-PV	PV Inner Surf. EL.3.6m,W	270	720	K	2.75	0.61
775	TW 36	TWE-N060B-PV	PV Inner Surf. EL.6.0m,N	270	720	K	2.75	0.61
776	TW 37	TWE-S060B-PV	PV Inner Surf. EL.6.0m,S	270	720	K	2.75	0.61
777	TW 38	TWE-E060B-PV	PV Inner Surf. EL.6.0m,E	270	720	K	2.75	0.61
778	TW 39	TWE-W060B-PV	PV Inner Surf. EL.6.0m,W	270	720	K	2.75	0.61
779	TW 40	TWE-E080B-PV	PV Inner Surf. EL.8.0m,E	270	720	K	2.75	0.61
780	TW 41	TWE-W080B-PV	PV Inner Surf. EL.8.0m,W	270	720	K	2.75	0.61
781	TW 43	TWE-S000D-CB	CB Outer Surf. EL.0.0m,S	270	970	K	3.49	0.50
782	TW 44	TWE-E000D-CB	CB Outer Surf. EL.0.0m,E	270	970	K	3.49	0.50
783	TW 45	TWE-W000D-CB	CB Outer Surf. EL.0.0m,W	270	970	K	3.49	0.50
784	TW 50	TWE-N018D-CB	CB Outer Surf. EL.1.8m,N	270	970	K	3.49	0.50
785	TW 51	TWE-S018D-CB	CB Outer Surf. EL.1.8m,S	270	970	K	3.49	0.50
786	TW 52	TWE-E018D-CB	CB Outer Surf. EL.1.8m,E	270	970	K	3.49	0.50
787	TW 53	TWE-W018D-CB	CB Outer Surf. EL.1.8m,W	270	970	K	3.49	0.50
788	TW 57	TWE-W026D-CB	CB Outer Surf. EL.2.6m,W	270	970	K	3.49	0.50
789	TW 58	TWE-N036D-CB	CB Outer Surf. EL.3.6m,N	270	970	K	3.49	0.50
790	TW 59	TWE-S036D-CB	CB Outer Surf. EL.3.6m,S	270	970	K	3.49	0.50
791	TW 60	TWE-E036D-CB	CB Outer Surf. EL.3.6m,E	270	970	K	3.49	0.50
792	TW 61	TWE-W036D-CB	CB Outer Surf. EL.3.6m,W	270	970	K	3.49	0.50
793	TW 62	TWE-N049D-CB	CB Outer Surf. EL.4.9m,N	270	970	K	3.49	0.50
794	TW 63	TWE-S049D-CB	CB Outer Surf. EL.4.9m,S	270	970	K	3.49	0.50
795	TW 64	TWE-E049D-CB	CB Outer Surf. EL.4.9m,E	270	970	K	3.49	0.50
796	TW 65	TWE-W049D-CB	CB Outer Surf. EL.4.9m,W	270	970	K	3.49	0.50
797	TW 66	TWE-N060D-CB	CB Outer Surf. EL.6.0m,N	270	970	K	3.49	0.50
798	TW 67	TWE-S060D-CB	CB Outer Surf. EL.6.0m,S	270	970	K	3.49	0.50
799	TW 68	TWE-E060D-CB	CB Outer Surf. EL.6.0m,E	270	970	K	3.49	0.50
800	TW 69	TWE-W060D-CB	CB Outer Surf. EL.6.0m,W	270	970	K	3.49	0.50
801	TW 70	TWE-N000E-CB	CB Inner Surf. EL.0.0m,N	270	970	K	3.49	0.50
802	TW 71	TWE-S000E-CB	CB Inner Surf. EL.0.0m,S	270	970	K	3.49	0.50
803	TW 72	TWE-E000E-CB	CB Inner Surf. EL.0.0m,E	270	970	K	3.49	0.50
804	TW 73	TWE-W000E-CB	CB Inner Surf. EL.0.0m,W	270	970	K	3.49	0.50
805	TW 78	TWE-N018E-CB	CB Inner Surf. EL.1.8m,N	270	970	K	3.49	0.50
806	TW 79	TWE-S018E-CB	CB Inner Surf. EL.1.8m,S	270	970	K	3.49	0.50
807	TW 80	TWE-E018E-CB	CB Inner Surf. EL.1.8m,E	270	970	K	3.49	0.50
808	TW 81	TWE-W018E-CB	CB Inner Surf. EL.1.8m,W	270	970	K	3.49	0.50
809	TW 86	TWE-N036E-CB	CB Inner Surf. EL.3.6m,N	270	970	K	3.49	0.50
810	TW 87	TWE-S036E-CB	CB Inner Surf. EL.3.6m,S	270	970	K	3.49	0.50
811	TW 88	TWE-E036E-CB	CB Inner Surf. EL.3.6m,E	270	970	K	3.49	0.50
812	TW 92	TWE-E049E-CB	CB Inner Surf. EL.4.9m,E	270	970	K	3.49	0.50
813	TW 94	TWE-N060E-CB	CB Inner Surf. EL.6.0m,N	270	970	K	3.49	0.50
814	TW 95	TWE-S060E-CB	CB Inner Surf. EL.6.0m,S	270	970	K	3.49	0.50
815	TW 96	TWE-E060E-CB	CB Inner Surf. EL.6.0m,E	270	970	K	3.49	0.50
816	TW 97	TWE-W060E-CB	CB Inner Surf. EL.6.0m,W	270	970	K	3.49	0.50
817	TW 108	TWE-063-B09-UCSP	UCSP L.Surf. EL.6.3m,B09	270	970	K	3.49	0.50

Table A-1 (Cont'd)

SEQ No.	Function ID.	Tagname	Location	Range		Unit	Uncertainty	
				LO	HI		±ABS.	±%FR
818	TW 109	TWE-065-B09-UCSP	UCSP U.Surf. EL.6.5m,B09	270	970	K	3.49	0.50
819	TW 110	TWE-E047G-UP	UP Str. Surf. EL.4.7m,East	270	970	K	3.49	0.50
820	TW 111	TWE-W047G-UP	UP Str. Surf. EL.4.7m,West	270	970	K	3.49	0.50
821	TW 112	TWE-E056G-UP	UP Str. Surf. EL.5.6m,East	270	970	K	3.49	0.50
822	TW 113	TWE-W056G-UP	UP Str. Surf. EL.5.6m,West	270	970	K	3.49	0.50
823	TW 114	TWE-080G-UH	UH Str. Surf. EL.8.0m,CTR	270	970	K	3.49	0.50
824	TW 154	TWE-B03436	B03 Rod(4,3) Pos.6	270	1470	K	5.31	0.44
825	TW 155	TWE-B03438	B03 Rod(4,3) Pos.8	270	1470	K	5.31	0.44
826	TW 217	TWE-B08222	B08 Rod(2,2) Pos.2	270	970	K	5.31	0.44
827	TW 218	TWE-B08224	B08 Rod(2,2) Pos.4	270	970	K	5.31	0.44
828	TW 219	TWE-B08225	B08 Rod(2,2) Pos.5	270	970	K	5.31	0.44
829	TW 220	TWE-B08226	B08 Rod(2,2) Pos.6	270	970	K	5.31	0.44
830	TW 222	TWE-B08228	B08 Rod(2,2) Pos.8	270	970	K	5.31	0.44
831	TW 225	TWE-B08435	B08 Rod(4,3) Pos.5	270	1470	K	5.31	0.44
832	TW 227	TWE-B08437	B08 Rod(4,3) Pos.7	270	1470	K	5.31	0.44
833	TW 236	TWE-B10442	B10 Rod(4,4) Pos.2	270	1470	K	5.31	0.44
834	TW 237	TWE-B10444	B10 Rod(4,4) Pos.4	270	1470	K	5.31	0.44
835	TW 239	TWE-B10447	B10 Rod(4,4) Pos.7	270	1470	K	5.31	0.44
836	TW 259	TWE-B12262	B12 Rod(2,6) Pos.2	270	970	K	5.31	0.44
837	TW 260	TWE-B12264	B12 Rod(2,6) Pos.4	270	970	K	5.31	0.44
838	TW 261	TWE-B12265	B12 Rod(2,6) Pos.5	270	970	K	5.31	0.44
839	TW 262	TWE-B12266	B12 Rod(2,6) Pos.6	270	970	K	5.31	0.44
840	TW 264	TWE-B12268	B12 Rod(2,6) Pos.8	270	970	K	5.31	0.44
841	TW 283	TWE-B13442	B13 Rod(4,4) Pos.2	270	1470	K	5.31	0.44
842	TW 284	TWE-B13444	B13 Rod(4,4) Pos.4	270	1470	K	5.31	0.44
843	TW 286	TWE-B13446	B13 Rod(4,4) Pos.6	270	1470	K	5.31	0.44
844	TW 287	TWE-B13447	B13 Rod(4,4) Pos.7	270	1470	K	5.31	0.44
845	TW 288	TWE-B13448	B13 Rod(4,4) Pos.8	270	1470	K	5.31	0.44
846	TW 339	TWE-B17445	B17 Rod(4,4) Pos.5	270	1470	K	5.31	0.44
847	TW 341	TWE-B17447	B17 Rod(4,4) Pos.7	270	1470	K	5.31	0.44
848	TW 391	TWE-B21662	B21 Rod(6,6) Pos.2	270	1470	K	5.31	0.44
849	TW 392	TWE-B21664	B21 Rod(6,6) Pos.4	270	1470	K	5.31	0.44
850	TW 394	TWE-B21666	B21 Rod(6,6) Pos.6	270	1470	K	5.31	0.44
851	TW 395	TWE-B21667	B21 Rod(6,6) Pos.7	270	1470	K	5.31	0.44
852	TW 409	TWE-B22441	B22 Rod(4,4) Pos.1	270	1470	K	5.31	0.44
853	TW 410	TWE-B22443	B22 Rod(4,4) Pos.3	270	1470	K	5.31	0.44
854	TW 411	TWE-B22445	B22 Rod(4,4) Pos.5	270	1470	K	5.31	0.44
855	TW 414	TWE-B22449	B22 Rod(4,4) Pos.9	270	1470	K	5.31	0.44
856	TW 457	TWE-IN0641-SGA	SGA Inlet Plenum	270	720	K	2.75	0.61
857	TW 459	TWE-IN0643-SGA	SGA Inlet Plenum	270	720	K	2.75	0.61
858	TW 463	TWE-086B-SGA	SGA Inner Surf. Pos.1	270	670	K	2.63	0.66
859	TW 464	TWE-137B-SGA	SGA Inner Surf. Pos.7	270	670	K	2.63	0.66
860	TW 465	TWE-178B-SGA	SGA Inner Surf. Pos.10	270	670	K	2.63	0.66
861	TW 466	TWE-223B-SGA	SGA Inner Surf.	270	670	K	2.63	0.66
862	TW 467	TWE-IN0861-SGA	SGA U-Tube(1,IN) Pos.1	270	720	K	2.75	0.61
863	TW 468	TWE-EX0861-SGA	SGA U-Tube(1,EX) Pos.1	270	720	K	2.75	0.61
864	TW 469	TWE-IN0862-SGA	SGA U-Tube(2,IN) Pos.1	270	720	K	2.75	0.61
865	TW 470	TWE-EX0862-SGA	SGA U-Tube(2,EX) Pos.1	270	720	K	2.75	0.61
866	TW 471	TWE-IN0863-SGA	SGA U-Tube(3,IN) Pos.1	270	720	K	2.75	0.61
867	TW 472	TWE-EX0863-SGA	SGA U-Tube(3,EX) Pos.1	270	720	K	2.75	0.61
868	TW 473	TWE-IN0991-SGA	SGA U-Tube(1,IN) Pos.3	270	720	K	2.75	0.61
869	TW 474	TWE-EX0991-SGA	SGA U-Tube(1,EX) Pos.3	270	720	K	2.75	0.61
870	TW 475	TWE-IN0992-SGA	SGA U-Tube(2,IN) Pos.3	270	720	K	2.75	0.61
871	TW 476	TWE-EX0992-SGA	SGA U-Tube(2,EX) Pos.3	270	720	K	2.75	0.61
872	TW 477	TWE-IN0993-SGA	SGA U-Tube(3,IN) Pos.3	270	720	K	2.75	0.61
873	TW 478	TWE-EX0993-SGA	SGA U-Tube(3,EX) Pos.3	270	720	K	2.75	0.61
874	TW 479	TWE-IN1121-SGA	SGA U-Tube(1,IN) Pos.5	270	720	K	2.75	0.61
875	TW 480	TWE-EX1121-SGA	SGA U-Tube(1,EX) Pos.5	270	720	K	2.75	0.61
876	TW 481	TWE-IN1122-SGA	SGA U-Tube(2,IN) Pos.5	270	720	K	2.75	0.61
877	TW 482	TWE-EX1122-SGA	SGA U-Tube(2,EX) Pos.5	270	720	K	2.75	0.61
878	TW 483	TWE-IN1123-SGA	SGA U-Tube(3,IN) Pos.5	270	720	K	2.75	0.61
879	TW 484	TWE-EX1123-SGA	SGA U-Tube(3,EX) Pos.5	270	720	K	2.75	0.61
880	TW 485	TWE-IN1371-SGA	SGA U-Tube(1,IN) Pos.7	270	720	K	2.75	0.61
881	TW 486	TWE-EX1371-SGA	SGA U-Tube(1,EX) Pos.7	270	720	K	2.75	0.61
882	TW 487	TWE-IN1372-SGA	SGA U-Tube(2,IN) Pos.7	270	720	K	2.75	0.61
883	TW 488	TWE-EX1372-SGA	SGA U-Tube(2,EX) Pos.7	270	720	K	2.75	0.61
884	TW 489	TWE-IN1373-SGA	SGA U-Tube(3,IN) Pos.7	270	720	K	2.75	0.61
885	TW 490	TWE-EX1373-SGA	SGA U-Tube(3,EX) Pos.7	270	720	K	2.75	0.61
886	TW 491	TWE-IN1632-SGA	SGA U-Tube(2,IN) Pos.9	270	720	K	2.75	0.61
887	TW 492	TWE-EX1632-SGA	SGA U-Tube(2,EX) Pos.9	270	720	K	2.75	0.61
888	TW 493	TWE-IN1633-SGA	SGA U-Tube(3,IN) Pos.9	270	720	K	2.75	0.61
889	TW 494	TWE-EX1633-SGA	SGA U-Tube(3,EX) Pos.9	270	720	K	2.75	0.61
890	TW 495	TWE-IN1701-SGA	SGA U-Tube(1,IN) Pos.10	270	720	K	2.75	0.61
891	TW 496	TWE-IN1782-SGA	SGA U-Tube(2,IN) Pos.10	270	720	K	2.75	0.61
892	TW 497	TWE-IN1863-SGA	SGA U-Tube(3,IN) Pos.11	270	720	K	2.75	0.61
893	TW 499	TWE-IN0642-SGB	SGB Inlet Plenum	270	720	K	2.75	0.61
894	TW 500	TWE-IN0643-SGB	SGB Inlet Plenum	270	720	K	2.75	0.61
895	TW 504	TWE-086B-SGB	SGB Inner Surf. Pos.1	270	670	K	2.63	0.66
896	TW 505	TWE-137B-SGB	SGB Inner Surf. Pos.7	270	670	K	2.63	0.66
897	TW 506	TWE-178B-SGB	SGB Inner Surf. Pos.10	270	670	K	2.63	0.66
898	TW 507	TWE-223B-SGB	SGB Inner Surf.	270	670	K	2.63	0.66
899	TW 508	TWE-IN0861-SGB	SGB U-Tube(1,IN) Pos.1	270	720	K	2.75	0.61

Table A-1 (Cont'd)

SEQ No.	Function ID.	Tagname	Location	Range		Unit	Uncertainty	
				LO	HI		±ABS.	±%FR
900	TW 509	TWE-EX0861-SGB	SGB U-Tube(1,EX) Pos.1	270	720	K	2.75	0.61
901	TW 510	TWE-IN0862-SGB	SGB U-Tube(2,IN) Pos.1	270	720	K	2.75	0.61
902	TW 511	TWE-EX0862-SGB	SGB U-Tube(2,EX) Pos.1	270	720	K	2.75	0.61
903	TW 512	TWE-IN0863-SGB	SGB U-Tube(3,IN) Pos.1	270	720	K	2.75	0.61
904	TW 513	TWE-EX0863-SGB	SGB U-Tube(3,EX) Pos.1	270	720	K	2.75	0.61
905	TW 514	TWE-IN0991-SGB	SGB U-Tube(1,IN) Pos.3	270	720	K	2.75	0.61
906	TW 515	TWE-EX0991-SGB	SGB U-Tube(1,EX) Pos.3	270	720	K	2.75	0.61
907	TW 516	TWE-IN0992-SGB	SGB U-Tube(2,IN) Pos.3	270	720	K	2.75	0.61
908	TW 517	TWE-EX0992-SGB	SGB U-Tube(2,EX) Pos.3	270	720	K	2.75	0.61
909	TW 518	TWE-IN0993-SGB	SGB U-Tube(3,IN) Pos.3	270	720	K	2.75	0.61
910	TW 519	TWE-EX0993-SGB	SGB U-Tube(3,EX) Pos.3	270	720	K	2.75	0.61
911	TW 520	TWE-IN1121-SGB	SGB U-Tube(1,IN) Pos.5	270	720	K	2.75	0.61
912	TW 521	TWE-EX1121-SGB	SGB U-Tube(1,EX) Pos.5	270	720	K	2.75	0.61
913	TW 522	TWE-IN1122-SGB	SGB U-Tube(2,IN) Pos.5	270	720	K	2.75	0.61
914	TW 523	TWE-EX1122-SGB	SGB U-Tube(2,EX) Pos.5	270	720	K	2.75	0.61
915	TW 524	TWE-IN1123-SGB	SGB U-Tube(3,IN) Pos.5	270	720	K	2.75	0.61
916	TW 525	TWE-EX1123-SGB	SGB U-Tube(3,EX) Pos.5	270	720	K	2.75	0.61
917	TW 526	TWE-IN1371-SGB	SGB U-Tube(1,IN) Pos.7	270	720	K	2.75	0.61
918	TW 527	TWE-EX1371-SGB	SGB U-Tube(1,EX) Pos.7	270	720	K	2.75	0.61
919	TW 528	TWE-IN1372-SGB	SGB U-Tube(2,IN) Pos.7	270	720	K	2.75	0.61
920	TW 529	TWE-EX1372-SGB	SGB U-Tube(2,EX) Pos.7	270	720	K	2.75	0.61
921	TW 530	TWE-IN1373-SGB	SGB U-Tube(3,IN) Pos.7	270	720	K	2.75	0.61
922	TW 531	TWE-EX1373-SGB	SGB U-Tube(3,EX) Pos.7	270	720	K	2.75	0.61
923	TW 532	TWE-IN1632-SGB	SGB U-Tube(2,IN) Pos.9	270	720	K	2.75	0.61
924	TW 533	TWE-EX1632-SGB	SGB U-Tube(2,EX) Pos.9	270	720	K	2.75	0.61
925	TW 534	TWE-IN1633-SGB	SGB U-Tube(3,IN) Pos.9	270	720	K	2.75	0.61
926	TW 535	TWE-EX1633-SGB	SGB U-Tube(3,EX) Pos.9	270	720	K	2.75	0.61
927	TW 536	TWE-IN1701-SGB	SGB U-Tube(1,IN) Pos.10	270	720	K	2.75	0.61
928	TW 537	TWE-IN1782-SGB	SGB U-Tube(2,IN) Pos.10	270	720	K	2.75	0.61
929	TW 538	TWE-IN1863-SGB	SGB U-Tube(3,IN) Pos.11	270	720	K	2.75	0.61
930	TW 545	TWE270A-PR	PZR Spray Line Outer Surf.	270	720	K	2.75	0.61
931	TW 598	TWE-121D-UHDP	PLR-UH-9 Outer Surf.	270	970	K	3.49	0.50
932	TW 631	TWE-B01225	B01 Rod(2,2) Pos.5	270	1470	K	6.32	0.53
933	TW 635	TWE-B04221	B04 Rod(2,2) Pos.1	270	970	K	3.69	0.53
934	TW 638	TWE-B04226	B04 Rod(2,2) Pos.6	270	970	K	3.69	0.53
935	TW 640	TWE-B04229	B04 Rod(2,2) Pos.9	270	970	K	3.69	0.53
936	TW 649	TWE-B11225	B11 Rod(2,2) Pos.5	270	1470	K	6.32	0.53
937	TW 650	TWE-B11226	B11 Rod(2,2) Pos.6	270	1470	K	6.32	0.53
938	TW 653	TWE-B16221	B16 Rod(2,2) Pos.1	270	970	K	3.69	0.53
939	TW 654	TWE-B16223	B16 Rod(2,2) Pos.3	270	970	K	3.69	0.53
940	TW 656	TWE-B16226	B16 Rod(2,2) Pos.6	270	970	K	3.69	0.53
941	TW 658	TWE-B16229	B16 Rod(2,2) Pos.9	270	970	K	3.69	0.53
942	TW 673	TWE-EN037B-PV	PV East-North EL.3662	270	630	K	3.05	0.85
943	TW 674	TWE-E037B-PV	PV East EL.3662	270	630	K	3.05	0.85
944	TW 676	TWE-EN040B-PV	PV East-North EL.4037	270	630	K	3.05	0.85
945	TW 678	TWE-ES040B-PV	PV East-South EL.4037	270	630	K	3.05	0.85
946	TW 679	TWE-E042B-PV	PV East EL.4210	270	630	K	3.05	0.85
947	TW 680	TWE-WN037B-PV	PV West-North EL.3662	270	630	K	3.05	0.85
948	TW 681	TWE-W037B-PV	PV West EL.3662	270	630	K	3.05	0.85
949	TW 682	TWE-WS037B-PV	PV West-South EL.3662	270	630	K	3.05	0.85
950	TW 685	TWE-WS040B-PV	PV West-South EL.4037	270	630	K	3.05	0.85
951	TW 687	TWE-SW045B-PV	PV South-West EL.4497	270	630	K	3.05	0.85
952	TW 688	TWE-S045B-PV	PV South EL.4497	270	630	K	3.05	0.85
953	TW 689	TWE-SE045B-PV	PV South-East EL.4497	270	630	K	3.05	0.85
954	TW 690	TWE-SW051B-PV	PV South-West EL.5074	270	630	K	3.05	0.85
955	TW 691	TWE-S051B-PV	PV South EL.5074	270	630	K	3.05	0.85
956	TW 692	TWE-SE051B-PV	PV South-East EL.5074	270	630	K	3.05	0.85
957	TW 693	TWE-S054B-PV	PV South EL.5363	270	630	K	3.05	0.85
958	TW 694	TWE-NE045B-PV	PV North-East EL.4497	270	630	K	3.05	0.85
959	TW 696	TWE-NW045B-PV	PV North-West EL.4497	270	630	K	3.05	0.85
960	TW 697	TWE-NE051B-PV	PV North-East EL.5074	270	630	K	3.05	0.85
961	TW 698	TWE-N051B-PV	PV North EL.5074	270	630	K	3.05	0.85
962	TW 700	TWE-N054B-PV	PV North EL.5363	270	630	K	3.05	0.85
963	TW 709	TWE-IN038B02-UCP	UCP L.Surf. EL.3.8m,B02	270	970	K	3.49	0.50
964	TW 710	TWE-IN038B04-UCP	UCP L.Surf. EL.3.8m,B04	270	970	K	3.49	0.50
965	TW 711	TWE-IN038B06-UCP	UCP L.Surf. EL.3.8m,B06	270	970	K	3.49	0.50
966	TW 712	TWE-IN038B08-UCP	UCP L.Surf. EL.3.8m,B08	270	970	K	3.49	0.50
967	TW 713	TWE-IN038B21-UCP	UCP L.Surf. EL.3.8m,B21	270	970	K	3.49	0.50
968	TW 714	TWE-EX040B02-UCP	UCP U.Surf. EL.4.0m,B02	270	970	K	3.49	0.50
969	TW 715	TWE-EX040B04-UCP	UCP U.Surf. EL.4.0m,B04	270	970	K	3.49	0.50
970	TW 716	TWE-EX040B06-UCP	UCP U.Surf. EL.4.0m,B06	270	970	K	3.49	0.50
971	TW 717	TWE-EX040B08-UCP	UCP U.Surf. EL.4.0m,B08	270	970	K	3.49	0.50
972	TW 718	TWE-EX040B21-UCP	UCP U.Surf. EL.4.0m,B21	270	970	K	3.49	0.50
973	TW 727	TWE-B03437	B03 Rod(4,3) Pos.7	270	1470	K	5.31	0.44
974	TW 732	TWE-B08431	B08 Rod(4,3) Pos.1	270	1470	K	5.31	0.44
975	TW 733	TWE-B08433	B08 Rod(4,3) Pos.3	270	1470	K	5.31	0.44
976	TW 734	TWE-B08439	B08 Rod(4,3) Pos.9	270	1470	K	5.31	0.44
977	TW 739	TWE-B10446	B10 Rod(4,4) Pos.6	270	1470	K	5.31	0.44
978	TW 740	TWE-B10448	B10 Rod(4,4) Pos.8	270	1470	K	5.31	0.44
979	TW 757	TWE-B17441	B17 Rod(4,4) Pos.1	270	1470	K	5.31	0.44
980	TW 758	TWE-B17443	B17 Rod(4,4) Pos.3	270	1470	K	5.31	0.44
981	TW 759	TWE-B17449	B17 Rod(4,4) Pos.9	270	1470	K	5.31	0.44

Table A-1 (Cont'd)

SEQ No.	Function ID.	Tagname	Location	Range		Unit	Uncertainty	
				LO	HI		±ABS.	±%FR
982	TW 768	TWE-B22447	B22 Rod(4,4) Pos.7	270	1470	K	5.31	0.44
983	TW 773	TWE211A-PR	PZR Wall DL.2025	270	720	K	2.75	0.61
984	TW 774	TWE211B-PR	PZR Wall DL.4238	270	720	K	2.75	0.61
985	TW 775	TWE211C-PR	PZR Wall DL.5995	270	720	K	2.75	0.61
986	TW 776	TWE211D-PR	PZR Wall DL.7965	270	720	K	2.75	0.61
987	TW 777	TWE211E-PR	PZR Wall DL.9795	270	720	K	2.75	0.61
988	TW 778	TWE211F-PR	PZR Wall DL.11321	270	720	K	2.75	0.61
989	TW 779	TWE678-ACC	Acc-Cold Tank Wall	270	720	K	2.75	0.61
990	TW 780	TWE688-ACH	Acc-Hot Tank Wall	270	720	K	2.75	0.61
991	TW 783	TWE-A80-ADS	RSV(1-3) Line	270	720	K	2.75	0.61
992	TW 845	TWE111A-PR	PZR Outer Wall DL.-289	270	720	K	2.75	0.61
993	TW 846	TWE115A-PR	PZR Outer Wall DL.105	270	720	K	2.75	0.61
994	TW 847	TWE189A-PR	PZR Outer Wall DL.7219	270	720	K	2.75	0.61
995	TW 848	TWE198A-PR	PZR Outer Wall DL.8417	270	720	K	2.75	0.61
996	TW 849	TWE-022A-PV	PV Outer Wall EL.-2245	270	720	K	2.75	0.61
997	TW 850	TWE-027A-PV	PV Outer Wall EL.-2657	270	720	K	2.75	0.61
998	TW 851	TWE-028A-PV	PV Outer Wall EL.-2677	270	720	K	2.75	0.61
999	TW 852	TWE731A-HLA	HLA Outer Wall	270	720	K	2.75	0.61
1000	TW 853	TWE078A-SGA	SGA Outer Wall DL.-161	270	670	K	2.63	0.66
1001	TW 854	TWE245A-SGA	SGA Outer Wall DL.16572	270	670	K	2.63	0.66
1002	TW 859	TWE-A82-ADS	RSV123 Spool Piece	270	720	K	2.75	0.61
1003	TW 860	TWE-A83-ADS	RSV1 Orifice	270	720	K	2.75	0.61
1004	TW 862	TWE-A84-ADS	RSV AOV81 Body Wall	270	720	K	2.75	0.61
1005	TW 863	TWE-A85-ADS	RSV AOV81 Outer Frame	270	720	K	2.75	0.61
1006	TW 864	TWE292-PR	PZR VP-Line Pipe Wall	270	720	K	2.75	0.61
1007	TW 865	TWE442-SGA	SGA 8B MSL Pipe Wall	270	570	K	2.42	0.81
1008	TW 866	TWE441-SGA	SGA 8B MSL Support	270	570	K	2.42	0.81
1009	TW 867	TWE444-SGA	SGA 3B MSL Pipe Wall	270	570	K	2.42	0.81
1010	TW 868	TWE445-SGA	SGA 3B MSL Support	270	570	K	2.42	0.81
1011	TW 869	TWE446-SGA	SGA MSIV Body Wall	270	570	K	2.42	0.81
1012	TW 870	TWE447-SGA	SGA MSIV Outer Frame	270	570	K	2.42	0.81
1013	TW 871	TWE443-SGA	SGA BU-Line Pipe Wall	270	570	K	2.42	0.81
1014	TW 873	TWE-B03432	B03 Rod(4,3) Pos.2	270	1470	K	6.32	0.53
1015	TW 874	TWE-B03434	B03 Rod(4,3) Pos.4	270	1470	K	6.32	0.53
1016	FE 1	FE010-HLA	HLA Leakage (Normal)	0	0.4	kg/s	0.01	1.54
1017	FE 2	FE020A-LSA	Primary Loop LSA (High)	0	90	kg/s	1.25	1.39
1018	FE 3	FE020B-LSA	Primary Loop LSA (Low)	0	15.81	kg/s	0.22	1.37
1019	FE 4	FE150-HLB	HLB Leakage (Normal)	0	0.4	kg/s	0.01	1.54
1020	FE 5	FE160A-LSB	Primary Loop LSB (High)	0	90	kg/s	1.25	1.39
1021	FE 6	FE160B-LSB	Primary Loop LSB (Low)	0	15.81	kg/s	0.22	1.37
1022	FE 13	FE430-SGA	SGA Feedwater	0	4	kg/s	0.05	1.35
1023	FE 14	FE431-SGA	SGA Downcomer	0	7	kg/s	0.09	1.26
1024	FE 15	FE432-SGA	SGA Downcomer	0	7	kg/s	0.09	1.26
1025	FE 16	FE433-SGA	SGA Downcomer	0	7	kg/s	0.09	1.26
1026	FE 17	FE434-SGA	SGA Downcomer	0	7	kg/s	0.09	1.26
1027	FE 18	FE440-SGA	SGA Steam Line	0	5	kg/s	0.10	2.04
1028	FE 19	FE450-SGA	SGA Relief Valve Line	0	4	kg/s	0.07	1.82
1029	FE 21	FE470-SGB	SGB Feedwater	0	4	kg/s	0.05	1.35
1030	FE 22	FE471-SGB	SGB Downcomer	0	7	kg/s	0.09	1.26
1031	FE 23	FE472-SGB	SGB Downcomer	0	7	kg/s	0.09	1.26
1032	FE 24	FE473-SGB	SGB Downcomer	0	7	kg/s	0.09	1.26
1033	FE 25	FE474-SGB	SGB Downcomer	0	7	kg/s	0.09	1.26
1034	FE 26	FE480-SGB	SGB Steam Line	0	5	kg/s	0.10	2.04
1035	FE 27	FE490-SGB	SGB Relief Valve Line	0	4	kg/s	0.07	1.82
1036	FE 29	FE510-SH	Main-Steam Header	0	10	kg/s	0.22	2.16
1037	FE 33	FE570A-BU	Break Venturi (Hi)	0	10	kg/s	0.14	1.43
1038	FE 34	FE570B-BU	Break Venturi (Lo)	0	2.24	kg/s	0.08	3.50
1039	FE 35	FE580-ST	ST Vent Line	0	0.3	kg/s	-	-
1040	FE 36	FE590-ST	ST Bleed Line	0	20	kg/s	-	-
1041	FE 37	FE650-ACC	Acc-Cold Flow to CLA	0	15	kg/s	0.19	1.25
1042	FE 40	FE680-ACH	Acc-Hot Flow to CLB	0	10	kg/s	0.12	1.23
1043	FE 49	FE830-PL	LPI Flow to CLA (High)	0	15	kg/s	0.24	1.62
1044	FE 50	FE840-PL	LPI Flow to CLB (High)	0	15	kg/s	0.24	1.62
1045	FE 61	FE841-PL	LPI Flow to CLB	0	12	kg/s	0.16	1.35
1046	FE 62	FE010B-HLA	HLA Leakage (Reverse)	0	0.4	kg/s	0.01	1.53
1047	FE 63	FE150B-HLB	HLB Leakage (Reverse)	0	0.4	kg/s	0.01	1.53
1048	FE 65	FE440B-SGA	SGA Main Steam Line (Low)	0	1	kg/s	0.02	2.04
1049	FE 67	FE480B-SGB	SGB Main Steam Line (Low)	0	1	kg/s	0.02	2.04
1050	FE 70	FE520-PAA	Aux. Feedwater A (High)	0	1.5	kg/s	0.02	1.23
1051	FE 71	FE520B-PAA	Aux. Feedwater A (Low)	0	1	kg/s	0.01	1.23
1052	FE 72	FE530B-PAB	Aux. Feedwater B (Low)	0	1	kg/s	0.01	1.23
1053	FE 79	FE830B-PL	LPI Flow to CLA (Low)	0	5	kg/s	0.08	1.60
1054	FE 80	FE840B-PL	LPI Flow to CLB (Low)	0	3	kg/s	0.05	1.60
1055	PE 1	PE561-BU	BU-1 Venturi	0	20	MPa	0.1077	0.54
1056	PE 2	PE581-BU	Break Venturi	0	20	MPa	0.1077	0.54
1057	PE 3	PE010-SGA	SGA Inlet Plenum	0	20	MPa	0.1077	0.54
1058	PE 4	PE020-LSA	PCA Suction	0	20	MPa	0.1077	0.54
1059	PE 5	PE030-CLA	PCA Delivery	0	20	MPa	0.1077	0.54
1060	PE 6	PE150-SGB	SGB Inlet Plenum	0	20	MPa	0.1077	0.54
1061	PE 7	PE160-LSB	PCB Suction	0	20	MPa	0.1077	0.54

Table A-1 (Cont'd)

SEQ No.	Function ID.	Tagname	Location	Range		Unit	Uncertainty	
				LO	HI		±ABS.	±%FR
1062	PE 8	PE170-CLB	PCB Delivery	0	20	MPa	0.1077	0.54
1063	PE 9	PE290-PV	PV Upper Head	0	20	MPa	0.1077	0.54
1064	PE 10	PE280A-PV	PV Upper Plenum (High)	0	20	MPa	0.1077	0.54
1065	PE 11	PE280B-PV	PV Upper Plenum (Low)	0	5	MPa	0.0269	0.54
1066	PE 12	PE270-PV	PV Lower Plenum	0	20	MPa	0.1077	0.54
1067	PE 13	PE300A-PR	Pressurizer (High)	0	20	MPa	0.1077	0.54
1068	PE 14	PE300B-PR	Pressurizer (Low)	0	5	MPa	0.0269	0.54
1069	PE 19	PE430-SGA	SGA Steam Dome	0	10	MPa	0.0539	0.54
1070	PE 20	PE440-SGA	SGA Steam Line	0	10	MPa	0.0539	0.54
1071	PE 21	PE450-SGB	SGB Steam Dome	0	10	MPa	0.0539	0.54
1072	PE 22	PE460-SGB	SGB Steam Line	0	10	MPa	0.0539	0.54
1073	PE 23	PE470-SH	Main-Steam Header	0	10	MPa	0.0539	0.54
1074	PE 24	PE480-JC	Jet Condenser	0	10	MPa	0.0539	0.54
1075	PE 25	PE610-ST	Break Flow Supp. Tank	0	1	MPa	0.0032	0.32
1076	PE 26	PE560-BU	BU-1 Orifice Upstream	0	20	MPa	0.1077	0.54
1077	PE 27	PE570-BU	BU-1 Orifice Downstream	0	20	MPa	0.1077	0.54
1078	PE 28	PE580-BU	Break Orifice Upstream	0	20	MPa	0.1077	0.54
1079	PE 29	PE590-BU	Break Orifice Downstream	0	20	MPa	0.1077	0.54
1080	PE 30	PE600-ST	Break-Flow Blowdown Line	0	2	MPa	0.0064	0.32
1081	PE 31	PE650-ACC	Acc-Cold Tank	0	10	MPa	0.0539	0.54
1082	PE 32	PE660-ACH	Acc-Hot Tank	0	10	MPa	0.0539	0.54
1083	PE 35	PE011-HLA	HLA Spool Piece	0	20	MPa	0.1077	0.54
1084	PE 36	PE071-CLA	CLA Spool Piece	0	20	MPa	0.1077	0.54
1085	PE 37	PE151-HLB	HLB Spool Piece	0	20	MPa	0.1077	0.54
1086	PE 38	PE211-CLB	CLB Spool Piece	0	20	MPa	0.1077	0.54
1087	PE 43	PE571-BU	RSV123 Inlet	0	20	MPa	0.1118	0.56
1088	PE 44	PE591-BU	Break Spool Piece	0	20	MPa	0.1118	0.56
1089	PE 46	PE820-RHR	PL Delivery	0	20	MPa	0.1077	0.54
1090	PE 53	PE430B-SGA	SGA Steam Dome (Low)	0	1	MPa	0.0032	0.32
1091	PE 54	PE450B-SGB	SGB Steam Dome (Low)	0	1	MPa	0.0032	0.32
1092	PE 62	PE-A50-DVIA	PV-DCA ECCS Line	0	20	MPa	0.0641	0.32
1093	PE 63	PE-A51-DVIA	PV-DCA ECCS Line	0	20	MPa	0.0641	0.32
1094	PE 64	PE-A55-DVIB	PV-DCB ECCS Line	0	20	MPa	0.0641	0.32
1095	PE 65	PE-A56-DVIB	PV-DCB ECCS Line	0	20	MPa	0.0641	0.32
1096	PE 73	PE-A83-ADS	RSV3 R.O Downstream	0	20	MPa	0.1077	0.54
1097	PE 78	PE435-SGA	SGA Steam Dome	0	10	MPa	0.0224	0.22
1098	PE 79	PE455-SGB	SGB Steam Dome	0	10	MPa	0.0224	0.22
1099	MI 1	RE010-PCA	PCA (Rotational Speed)	0	70	rps	0.39	0.55
1100	MI 2	RE150-PCB	PCB (Rotational Speed)	0	70	rps	0.39	0.55
1101	MI 5	OPE430-SGA	SGA Feedwater (FCV430)	0	100	%	0.54	0.54
1102	MI 6	OPE470-SGB	SGB Feedwater (FCV470)	0	100	%	0.54	0.54
1103	MI 8	OPE510-SH	Steam Flow (FCV510)	0	100	%	0.54	0.54
1104	MI 11	VBE010-PCA	PCA (Vibration)	0	200	um	0.10	5.01
1105	MI 12	VBE150-PCB	PCB (Vibration)	0	200	um	0.10	5.01
1106	MI 13	TQE010-PCA	PCA (Torque)	0	100	Nm	1.60	1.60
1107	MI 14	TQE150-PCB	PCB (Torque)	0	100	Nm	1.60	1.60
1108	MI 15	AE010-PCA	PCA (Electric Current)	0	150	A	1.56	1.04
1109	MI 16	AE150-PCB	PCB (Electric Current)	0	150	A	1.56	1.04
1110	MI 17	WE270A-T	Total Core Power	0	16	MW	0.07	0.44
1111	MI 18	WE270B-M	Core Power (Mid. Flux)	0	2	MW	0.01	0.44
1112	MI 19	WE270C-H1	Core Power (High Flux 1)	0	4	MW	0.02	0.44
1113	MI 20	WE270D-H2	Core Power (High Flux 2)	0	4	MW	0.02	0.44
1114	MI 21	WE270E-L1	Core Power (Low Flux 1)	0	2	MW	0.01	0.44
1115	MI 22	WE270F-L2	Core Power (Low Flux 2)	0	2	MW	0.01	0.44
1116	MI 23	WE270G-L3	Core Power (Low Flux 3)	0	2	MW	0.01	0.44
1117	MI 24	WE280A-PR	PZR Proportional Heater	0	10	kW	0.04	0.39
1118	MI 25	WE280B-PR	PZR Base Heater	0	150	kW	0.59	0.39
1119	MI 26	WE010-PCA	PCA Power	0	30	kW	–	–
1120	MI 27	WE150-PCB	PCB Power	0	30	kW	–	–
1121	MI 29	WE020-HLA	HLA Heater Power	0	5	kW	0.01	1.50
1122	MI 30	WE030-LSA	LSA Heater Power	0	7.5	kW	0.01	1.50
1123	MI 31	WE040-CLA	CLA Heater Power	0	2	kW	0.003	1.50
1124	MI 32	WE160-HLB	HLB Heater Power	0	5	kW	0.01	1.50
1125	MI 33	WE170-LSB	LSB Heater Power	0	7.5	kW	0.01	1.50
1126	MI 34	WE180-CLB	CLB Heater Power	0	2	kW	0.003	1.50
1127	MI 35	WE271A-PV	PV Heater Power	0	15	kW	0.02	1.50
1128	MI 36	WE271B-PV	PV Heater Power	0	15	kW	0.02	1.50
1129	MI 37	WE271C-PV	PV Heater Power	0	15	kW	0.02	1.50
1130	MI 38	WE271D-PV	PV Heater Power	0	15	kW	0.02	1.50
1131	MI 39	WE430A-SGA	SGA Heater Power	0	4	kW	0.01	1.50
1132	MI 40	WE430B-SGA	SGA Heater Power	0	4	kW	0.01	1.50
1133	MI 41	WE430C-SGA	SGA Heater Power	0	4	kW	0.01	1.50
1134	MI 42	WE430D-SGA	SGA Heater Power	0	4	kW	0.01	1.50
1135	MI 43	WE440A-SGA	SGA Downcomer Heater Power	0	2	kW	0.003	1.50
1136	MI 44	WE440B-SGA	SGA Downcomer Heater Power	0	2	kW	0.003	1.50
1137	MI 45	WE440C-SGA	SGA Downcomer Heater Power	0	2	kW	0.003	1.50
1138	MI 46	WE440D-SGA	SGA Downcomer Heater Power	0	2	kW	0.003	1.50
1139	MI 47	WE290-PR	PZR Surge Line Heater Power	0	4	kW	0.01	1.50
1140	MI 48	WE300-PR	PZR Spray Line Heater Power	0	7.5	kW	0.01	1.50
1141	MI 49	WE450A-SGB	SGB Heater Power	0	4	kW	0.01	1.50
1142	MI 50	WE450B-SGB	SGB Heater Power	0	4	kW	0.01	1.50

Table A-1 (Cont'd)

SEQ No.	Function ID.	Tagname	Location	Range		Unit	Uncertainty	
				LO	HI		±ABS.	±%FR
1143	MI 51	WE450C-SGB	SGB Heater Power	0	4	kW	0.01	1.50
1144	MI 52	WE450D-SGB	SGB Heater Power	0	4	kW	0.01	1.50
1145	MI 53	WE460A-SGB	SGB Downcomer Heater Power	0	2	kW	0.003	1.50
1146	MI 54	WE460B-SGB	SGB Downcomer Heater Power	0	2	kW	0.003	1.50
1147	MI 55	WE460C-SGB	SGB Downcomer Heater Power	0	2	kW	0.003	1.50
1148	MI 56	WE460D-SGB	SGB Downcomer Heater Power	0	2	kW	0.003	1.50
1149	LE 1	LE270-PV	PV	0	11	m	0.29	2.68
1150	LE 2	LE280-PR	PZR Overall Level	0	11.24	m	0.25	2.22
1151	LE 3	LE430-SGA	SGA Wide Range	0	17	m	0.38	2.26
1152	LE 4	LE440-SGA	SGA Narrow Range	0	6	m	0.14	2.32
1153	LE 5	LE441-SGA	SGA Boiling Section	0	11	m	0.25	2.27
1154	LE 6	LE450-SGB	SGB Wide Range	0	17	m	0.38	2.26
1155	LE 7	LE460-SGB	SGB Narrow Range	0	6	m	0.14	2.32
1156	LE 8	LE461-SGB	SGB Boiling Section	0	11	m	0.25	2.27
1157	LE 9	LE470-JC	Jet Condenser	0	5.5	m	0.13	2.33
1158	LE 10	LE560-ST	ST Wide Range	0	12	m	0.27	2.26
1159	LE 11	LE570-ST	ST Low Level	0	4	m	0.09	2.25
1160	LE 12	LE580-ST	ST Middle Level	0	4	m	0.11	2.65
1161	LE 13	LE590-ST	ST High Level	0	4	m	0.11	2.65
1162	LE 14	LE650-ACC	Acc-Cold Tank	0	5.5	m	0.12	2.25
1163	LE 15	LE660-ACH	Acc-Hot Tank	0	5.5	m	0.15	2.65
1164	LE 17	LE830-RWST	RWST Overall	0	10	m	-	-
1165	LE 18	LE442-SGA	SGA Downcomer	0	12	m	0.27	2.25
1166	LE 19	LE462-SGB	SGB Downcomer	0	12	m	0.27	2.25
1167	LE 20	DLE270-PV	PV Overall	0	111.06	kPa	1.07	0.96
1168	LE 21	DLE280-PR	PZR Overall	0	113.63	kPa	0.48	0.42
1169	LE 22	DLE430-SGA	SGA Wide Range	0	171.64	kPa	0.69	0.40
1170	LE 23	DLE440-SGA	SGA Narrow-Range	0	60.58	kPa	0.57	0.93
1171	LE 24	DLE441-SGA	SGA Boiling Section	0	111.06	kPa	0.61	0.55
1172	LE 25	DLE442-SGA	SGA Downcomer	0	114.27	kPa	0.62	0.54
1173	LE 26	DLE450-SGB	SGB Wide Range	0	171.64	kPa	0.69	0.40
1174	LE 27	DLE460-SGB	SGB Narrow-Range	0	60.58	kPa	0.57	0.93
1175	LE 28	DLE461-SGB	SGB Boiling Section	0	111.06	kPa	0.61	0.55
1176	LE 29	DLE462-SGB	SGB Downcomer	0	114.27	kPa	0.62	0.54
1177	LE 30	DLE470-JC	JC	0	55.53	kPa	0.56	1.01
1178	LE 31	DLE560-ST	ST Overall Level	0	121.16	kPa	0.59	0.49
1179	LE 32	DLE570-ST	ST Lower Region	0	40.39	kPa	0.16	0.40
1180	LE 33	DLE580-ST	ST Middle Region	0	40.39	kPa	0.27	0.68
1181	LE 34	DLE590-ST	ST Upper Region	0	40.39	kPa	0.27	0.68
1182	LE 35	DLE650-ACC	Acc-Cold Tank	0	55.53	kPa	0.53	0.95
1183	LE 36	DLE660-ACH	Acc-Hot Tank	0	55.53	kPa	1.02	1.84
1184	LE 38	DLE830-RWST	RWST	0	196.14	kPa	0.55	0.28
1185	DP 1	DPE010-HLA	Upper Plenum - HLA Nozzle	-40	40	kPa	1.02	1.28
1186	DP 2	DPE020-HLA	HLA Nozzle - HLA Break	-40	40	kPa	1.02	1.28
1187	DP 4	DPE040-HLA	HLA Break - SGA Inlet	-40	40	kPa	1.02	1.28
1188	DP 5	DPE050A-SGA	SGA Inlet - Tube 3 Top	-150	50	kPa	2.03	1.02
1189	DP 6	DPE050B-SGA	SGA Inlet - Tube 2 Top	-150	50	kPa	2.03	1.02
1190	DP 7	DPE050C-SGA	SGA Inlet - Tube 1 Top	-150	50	kPa	2.03	1.02
1191	DP 8	DPE050D-SGA	SGA Inlet - Tube 4 Top	-150	50	kPa	2.03	1.02
1192	DP 9	DPE050E-SGA	SGA Inlet - Tube 5 Top	-150	50	kPa	2.03	1.02
1193	DP 10	DPE050F-SGA	SGA Inlet - Tube 6 Top	-150	50	kPa	2.03	1.02
1194	DP 11	DPE060A-SGA	SGA Outlet - Tube 3 Top	-150	50	kPa	2.03	1.02
1195	DP 12	DPE060B-SGA	SGA Outlet - Tube 2 Top	-150	50	kPa	2.03	1.02
1196	DP 13	DPE060C-SGA	SGA Outlet - Tube 1 Top	-150	50	kPa	2.03	1.02
1197	DP 14	DPE060D-SGA	SGA Outlet - Tube 4 Top	-150	50	kPa	2.03	1.02
1198	DP 15	DPE060E-SGA	SGA Outlet - Tube 5 Top	-150	50	kPa	2.03	1.02
1199	DP 16	DPE060F-SGA	SGA Outlet - Tube 6 Top	-150	50	kPa	2.03	1.02
1200	DP 17	DPE070-LSA	SGA Outlet - LSA Bottom	-80	80	kPa	1.08	0.67
1201	DP 18	DPE080-LSA	LSA Bottom - PCA Suction	-50	50	kPa	1.03	1.03
1202	DP 19	DPE090-PCA	PCA Suction - Delivery	-50	50	kPa	1.03	1.03
1203	DP 20	DPE100-CLA	PZR Spray Line	-200	200	kPa	2.21	0.55
1204	DP 21	DPE110-CLA	PCA Delivery - CLA Break	-50	50	kPa	1.03	1.03
1205	DP 22	DPE120-CLA	CLA Break - CLA Nozzle	-50	50	kPa	1.03	1.03
1206	DP 23	DPE130-CLA	CLA Nozzle - Downcomer	-50	50	kPa	1.03	1.03
1207	DP 24	DPE140-HLA	Upper Plenum - Downcomer	-30	30	kPa	1.01	1.69
1208	DP 25	DPE150-HLB	Upper Plenum - HLB Nozzle	-30	30	kPa	1.01	1.69
1209	DP 26	DPE160-HLB	HLB Nozzle - HLB Break	-30	30	kPa	1.01	1.69
1210	DP 27	DPE170-HLB	HLB Break - SGB Break	-30	30	kPa	1.01	1.69
1211	DP 28	DPE180-HLB	SGB Break - SGB Inlet	-30	30	kPa	1.01	1.69
1212	DP 29	DPE190A-SGB	SGB Inlet - Tube 3 Top	-150	50	kPa	2.03	1.02
1213	DP 30	DPE190B-SGB	SGB Inlet - Tube 2 Top	-150	50	kPa	2.03	1.02
1214	DP 31	DPE190C-SGB	SGB Inlet - Tube 1 Top	-150	50	kPa	3.96	1.98
1215	DP 32	DPE190D-SGB	SGB Inlet - Tube 4 Top	-150	50	kPa	3.96	1.98
1216	DP 33	DPE190E-SGB	SGB Inlet - Tube 5 Top	-150	50	kPa	3.96	1.98
1217	DP 34	DPE190F-SGB	SGB Inlet - Tube 6 Top	-150	50	kPa	3.96	1.98
1218	DP 35	DPE200A-SGB	SGB Outlet - Tube 3 Top	-150	50	kPa	3.96	1.98
1219	DP 36	DPE200B-SGB	SGB Outlet - Tube 2 Top	-150	50	kPa	3.96	1.98
1220	DP 37	DPE200C-SGB	SGB Outlet - Tube 1 Top	-150	50	kPa	3.96	1.98
1221	DP 38	DPE200D-SGB	SGB Outlet - Tube 4 Top	-150	50	kPa	3.96	1.98
1222	DP 39	DPE200E-SGB	SGB Outlet - Tube 5 Top	-150	50	kPa	3.96	1.98

Table A-1 (Cont'd)

SEQ No.	Function ID.	Tagname	Location	Range		Unit	Uncertainty	
				LO	HI		±ABS.	±%FR
1223	DP 40	DPE200F-SGB	SGB Outlet - Tube 6 Top	-150	50	kPa	3.96	1.98
1224	DP 41	DPE210-LSB	SGB Outlet - LSB Bottom	-80	80	kPa	1.08	0.67
1225	DP 42	DPE220-LSB	LSB Bottom - PCB Suction	-50	50	kPa	1.03	1.03
1226	DP 43	DPE230-PCB	PCB Suction - Delivery	-50	50	kPa	1.03	1.03
1227	DP 44	DPE240-CLB	PCB Delivery - CLB Break	-20	20	kPa	1.01	2.51
1228	DP 45	DPE250-CLB	CLB Break - CLB Nozzle	-20	20	kPa	1.01	2.51
1229	DP 46	DPE260-CLB	CLB Nozzle - Downcomer	-20	20	kPa	1.01	2.51
1230	DP 47	DPE270-PV	PV Bottom - Top	-100	400	kPa	4.12	0.82
1231	DP 48	DPE280-PV	PV Lower Plenum	-50	100	kPa	1.07	0.71
1232	DP 49	DPE290-PV	Lower Core Support Plate	-50	100	kPa	1.07	0.71
1233	DP 50	DPE300-PV	Core (EL.-35 -3945)	-50	100	kPa	1.07	0.71
1234	DP 51	DPE320-PV	Upper Plenum	-50	100	kPa	1.07	0.71
1235	DP 52	DPE330-PV	Upper Head (EL.6135 - 9653)	-50	100	kPa	1.07	0.71
1236	DP 53	DPE310-PV	Upper Core Support Plate	-100	100	kPa	3.96	1.98
1237	DP 54	DPE350A-PV	CR Guide Tube Top Orifice	-100	100	kPa	3.96	1.98
1238	DP 55	DPE350B-PV	CR Guide Tube Top Orifice	-100	100	kPa	3.96	1.98
1239	DP 56	DPE360-PV	PV Downcomer Overall	-100	300	kPa	4.05	1.01
1240	DP 57	DPE370-PV	Lower Downcomer	-50	150	kPa	3.96	1.98
1241	DP 58	DPE380-PV	Upper Downcomer	-50	150	kPa	3.96	1.98
1242	DP 59	DPE390-PV	UP-DC Check Valve A	-50	100	kPa	1.12	0.56
1243	DP 62	DPE332-PV	Upper Head - Downcomer	-100	100	kPa	3.96	1.98
1244	DP 63	DPE331-PV	Upper Head	-100	100	kPa	3.96	1.98
1245	DP 67	DPE580A-BU	FE570A (Break Hi)	0	100	kPa	1.03	1.03
1246	DP 68	DPE580B-BU	FE570A (Break Lo)	0	5	kPa	0.32	6.33
1247	DP 70	DPE030B-HLA	PZR Surge Line (Low)	-300	300	kPa	2.48	0.41
1248	DP 71	DPE072-LSA	LSA (SG-Side)	0	45	kPa	0.34	0.75
1249	DP 72	DPE073-LSA	LSA (SG-Side)	-10	10	kPa	0.32	1.60
1250	DP 73	DPE074-LSA	LSA (SG-Side)	-10	10	kPa	0.32	1.60
1251	DP 74	DPE075-LSA	LSA (SG-Side)	-10	10	kPa	0.32	1.60
1252	DP 76	DPE212-LSB	LSB (SG-Side)	0	45	kPa	0.34	0.75
1253	DP 77	DPE213-LSB	LSB (SG-Side)	-10	10	kPa	0.32	1.60
1254	DP 78	DPE214-LSB	LSB (SG-Side)	-10	10	kPa	0.32	1.60
1255	DP 79	DPE215-LSB	LSB (SG-Side)	-10	10	kPa	0.32	1.60
1256	DP 80	DPE216-LSB	LSB (SG-Side)	0	30	kPa	0.33	1.08
1257	DP 81	DPE430-SGA	SGA Boiling Section	-30	0	kPa	0.33	1.08
1258	DP 82	DPE431-SGA	SGA Boiling Section	-30	0	kPa	0.33	1.08
1259	DP 83	DPE432-SGA	SGA Boiling Section	-30	0	kPa	0.33	1.08
1260	DP 84	DPE433-SGA	SGA Boiling Section	-30	0	kPa	0.33	1.08
1261	DP 85	DPE434-SGA	SGA Boiling Section	-30	0	kPa	0.33	1.08
1262	DP 86	DPE435-SGA	SGA Boiling Section	-30	0	kPa	0.33	1.08
1263	DP 87	DPE436-SGA	SGA Boiling Section	-30	0	kPa	0.33	1.08
1264	DP 88	DPE437-SGA	SGA Boiling Section	-30	0	kPa	0.33	1.08
1265	DP 89	DPE438-SGA	SGA Boiling Section	-30	0	kPa	0.33	1.08
1266	DP 90	DPE439-SGA	SGA Boiling Section	-30	0	kPa	0.33	1.08
1267	DP 91	DPE440-SGA	SGA Boiling Section	-40	0	kPa	0.33	0.83
1268	DP 92	DPE450-SGB	SGB Boiling Section	-30	0	kPa	0.33	1.08
1269	DP 93	DPE451-SGB	SGB Boiling Section	-30	0	kPa	0.33	1.08
1270	DP 94	DPE452-SGB	SGB Boiling Section	-30	0	kPa	0.33	1.08
1271	DP 95	DPE453-SGB	SGB Boiling Section	-30	0	kPa	0.33	1.08
1272	DP 96	DPE454-SGB	SGB Boiling Section	-30	0	kPa	0.33	1.08
1273	DP 97	DPE455-SGB	SGB Boiling Section	-30	0	kPa	0.33	1.08
1274	DP 98	DPE456-SGB	SGB Boiling Section	-30	0	kPa	0.33	1.08
1275	DP 99	DPE457-SGB	SGB Boiling Section	-30	0	kPa	0.33	1.08
1276	DP 100	DPE458-SGB	SGB Boiling Section	-30	0	kPa	0.33	1.08
1277	DP 101	DPE459-SGB	SGB Boiling Section	-30	0	kPa	0.33	1.08
1278	DP 102	DPE460-SGB	SGB Boiling Section	-40	0	kPa	0.33	0.83
1279	DP 103	DPE011-HLA	HLA Spool Piece	-10	10	kPa	0.32	1.60
1280	DP 104	DPE071-CLA	CLA Spool Piece	-10	10	kPa	0.32	1.60
1281	DP 105	DPE151-HLB	HLB Spool Piece	-10	10	kPa	0.32	1.60
1282	DP 106	DPE211-CLB	CLB Spool Piece	-10	10	kPa	0.32	1.60
1283	DP 107	DPE571-BU	RSV123 Inlet	0	200	kPa	1.12	0.56
1284	DP 109	DPE041-PR	PZR (DL.9795 - 11321)	-14.95	0	kPa	0.25	1.69
1285	DP 110	DPE042-PR	PZR (DL.7965 - 9795)	-17.93	0	kPa	0.23	1.27
1286	DP 111	DPE043-PR	PZR (DL.5995 - 7965)	-19.31	0	kPa	0.23	1.18
1287	DP 112	DPE044-PR	PZR (DL.4238 - 5995)	-17.22	0	kPa	0.23	1.32
1288	DP 113	DPE045-PR	PZR (DL.2025 - 4238)	-21.68	0	kPa	0.23	1.06
1289	DP 114	DPE046-PR	PZR (DL.80 - 2025)	-19.06	0	kPa	0.23	1.20
1290	DP 115	DPE101-PR	PZR-CLA	-200	200	kPa	1.30	0.32
1291	DP 116	DPE055A-SGA	SGA U-Tube I/O (High)	-30	30	kPa	0.29	0.49
1292	DP 117	DPE055B-SGA	SGA U-Tube I/O (Low)	-3	3	kPa	0.2	3.37
1293	DP 118	DPE195A-SGB	SGB U-Tube I/O (High)	-30	30	kPa	0.29	0.49
1294	DP 119	DPE195B-SGB	SGB U-Tube I/O (Low)	-3	3	kPa	0.2	3.37
1295	DP 120	DPE056-SGA	SGA Inlet Plenum	-40	40	kPa	1.02	1.28
1296	DP 122	DPE196-SGB	SGB Inlet Plenum	-40	40	kPa	0.48	0.60
1297	DP 123	DPE197-SGB	SGB Primary-Secondary	-1000	1000	kPa	9.44	0.47
1298	DP 133	DPE333-PV	Upper Head (EL.6634 - 8860)	-35	0	kPa	0.23	0.67
1299	DP 182	DPE491-SGB	SGB Feedwater Line	0	0	kPa	Not used	
1300	DP 183	DPE492-SGB	SGB Feedwater Line	-40	10	kPa	Not used	
1301	DE 1	DE011A-HLA	HLA Spool Piece, Beam A	0	10	V	-	-
1302	DE 2	DE011B-HLA	HLA Spool Piece, Beam B	0	10	V	-	-
1303	DE 3	DE011C-HLA	HLA Spool Piece, Beam C	0	10	V	-	-

Table A-1 (Cont'd)

SEQ No.	Function ID.	Tagname	Location	Range		Unit	Uncertainty	
				LO	HI		±ABS.	±%FR
1304	DE 4	DE051A-LSA	LSA Spool Piece, Beam A	0	10	V	–	–
1305	DE 5	DE051B-LSA	LSA Spool Piece, Beam B	0	10	V	–	–
1306	DE 6	DE051C-LSA	LSA Spool Piece, Beam C	0	10	V	–	–
1307	DE 7	DE071A-CLA	CLA Spool Piece, Beam A	0	10	V	–	–
1308	DE 8	DE071B-CLA	CLA Spool Piece, Beam B	0	10	V	–	–
1309	DE 9	DE071C-CLA	CLA Spool Piece, Beam C	0	10	V	–	–
1310	DE 10	DE151A-HLB	HLB Spool Piece, Beam A	0	10	V	–	–
1311	DE 11	DE151B-HLB	HLB Spool Piece, Beam B	0	10	V	–	–
1312	DE 12	DE151C-HLB	HLB Spool Piece, Beam C	0	10	V	–	–
1313	DE 13	DE191A-LSB	LSB Spool Piece, Beam A	0	10	V	–	–
1314	DE 14	DE191B-LSB	LSB Spool Piece, Beam B	0	10	V	–	–
1315	DE 15	DE191C-LSB	LSB Spool Piece, Beam C	0	10	V	–	–
1316	DE 16	DE211A-CLB	CLB Spool Piece, Beam A	0	10	V	–	–
1317	DE 17	DE211B-CLB	CLB Spool Piece, Beam B	0	10	V	–	–
1318	DE 18	DE211C-CLB	CLB Spool Piece, Beam C	0	10	V	–	–
1319	DE 19	DE052-LSA	PCA Suction	0	10	V	–	–
1320	DE 20	DE192-LSB	PCB Suction	0	10	V	–	–
1321	DE 21	DE281-PR	PZR Surge Line	0	10	V	–	–
1322	DE 33	DE591A-BU	Break Spool Piece, Beam A	0	10	V	–	–
1323	DE 34	DE591B-BU	Break Spool Piece, Beam B	0	10	V	–	–
1324	DE 35	DE591C-BU	Break Spool Piece, Beam C	0	10	V	–	–
1325	DE 40	DE291-SGB	SGB Feedwater Line	0	10	V	–	–
1326	RC 31	DE011A-HLA-EU	HLA Spool Piece, Beam A	–	–	kg/m^3	27	–
1327	RC 32	DE011B-HLA-EU	HLA Spool Piece, Beam B	–	–	kg/m^3	20	–
1328	RC 33	DE011C-HLA-EU	HLA Spool Piece, Beam C	–	–	kg/m^3	22	–
1329	RC 34	DE151A-HLB-EU	HLB Spool Piece, Beam A	–	–	kg/m^3	27	–
1330	RC 35	DE151B-HLB-EU	HLB Spool Piece, Beam B	–	–	kg/m^3	20	–
1331	RC 36	DE151C-HLB-EU	HLB Spool Piece, Beam C	–	–	kg/m^3	22	–
1332	RC 37	DE071A-CLA-EU	CLA Spool Piece, Beam A	–	–	kg/m^3	94.8	–
1333	RC 38	DE071B-CLA-EU	CLA Spool Piece, Beam B	–	–	kg/m^3	94.8	–
1334	RC 39	DE071C-CLA-EU	CLA Spool Piece, Beam C	–	–	kg/m^3	94.8	–
1335	RC 40	DE211A-CLB-EU	CLB Spool Piece, Beam A	–	–	kg/m^3	94.8	–
1336	RC 41	DE211B-CLB-EU	CLB Spool Piece, Beam B	–	–	kg/m^3	94.8	–
1337	RC 42	DE211C-CLB-EU	CLB Spool Piece, Beam C	–	–	kg/m^3	94.8	–
1338	RC 56	DE051A-LSA-EU	LSA Spool Piece, Beam A	–	–	kg/m^3	94.8	–
1339	RC 57	DE051B-LSA-EU	LSA Spool Piece, Beam B	–	–	kg/m^3	94.8	–
1340	RC 58	DE051C-LSA-EU	LSA Spool Piece, Beam C	–	–	kg/m^3	94.8	–
1341	RC 62	DE052-LSA-EU	PCA Suction	–	–	kg/m^3	94.8	–
1342	RC 63	DE192-LSB-EU	PCB Suction	–	–	kg/m^3	94.8	–
1343	RC 64	DE281-PR-EU	PZR Surge Line	–	–	kg/m^3	94.8	–
1344	RC 73	DE591A-BU-EU	Break Spool Piece, Beam A	–	–	kg/m^3	94.8	–
1345	RC 74	DE591B-BU-EU	Break Spool Piece, Beam B	–	–	kg/m^3	94.8	–
1346	RC 75	DE591C-BU-EU	Break Spool Piece, Beam C	–	–	kg/m^3	94.8	–
1347	RC 132	DE591-AVG	Break Spool Piece Average	–	–	kg/m^3	55.62	–
1348	RC 133	TWE-PCT	Peak Cladding Temp.	–	–	K	5.31	–
1349	RC 134	TWE-PCTLOC	Location of PCT	–	–	–	–	–
1350	RC 139	CL-CORE	Core (EL.-35 – 3945)	–	–	m	0.216	–
1351	RC 140	CL-UP	Upper Plenum (EL.4060 – 6135)	–	–	m	0.197	–
1352	RC 141	CL-UH	Upper Head (EL.7834 – 9653)	–	–	m	0.21	–
1353	RC 142	CL-DC	Downcomer	–	–	m	0.746	–
1354	RC 143	CL-HLA-SGA	HLA Riser Part	–	–	m	0.181	–
1355	RC 144	CL-TUA-U3	SGA Tube 3 Inlet – Top	–	–	m	0.43	–
1356	RC 145	CL-TUA-U2	SGA Tube 2 Inlet – Top	–	–	m	0.42	–
1357	RC 146	CL-TUA-U1	SGA Tube 1 Inlet – Top	–	–	m	0.413	–
1358	RC 147	CL-TUA-U4	SGA Tube 4 Inlet – Top	–	–	m	0.43	–
1359	RC 148	CL-TUA-U5	SGA Tube 5 Inlet – Top	–	–	m	0.42	–
1360	RC 149	CL-TUA-U6	SGA Tube 6 Inlet – Top	–	–	m	0.425	–
1361	RC 150	CL-TUA-D3	SGA Tube 3 Outlet – Top	–	–	m	0.442	–
1362	RC 151	CL-TUA-D2	SGA Tube 2 Outlet – Top	–	–	m	0.431	–
1363	RC 152	CL-TUA-D1	SGA Tube 1 Outlet – Top	–	–	m	0.422	–
1364	RC 153	CL-TUA-D4	SGA Tube 4 Outlet – Top	–	–	m	0.422	–
1365	RC 154	CL-TUA-D5	SGA Tube 5 Outlet – Top	–	–	m	0.431	–
1366	RC 155	CL-TUA-D6	SGA Tube 6 Outlet – Top	–	–	m	0.422	–
1367	RC 156	CL-LSA-D	SGA Out.Plenum – LSA Bottom	–	–	m	0.207	–
1368	RC 157	CL-LSA-U	LSA Bottom – PCA Suction	–	–	m	0.188	–
1369	RC 158	CL-SGA-IPL	SGA Inlet Plenum	–	–	m	0.185	–
1370	RC 159	CL-HLB-SGB	HLB Riser Part	–	–	m	0.179	–
1371	RC 160	CL-TUB-U3	SGB Tube 3 Inlet – Top	–	–	m	0.445	–
1372	RC 161	CL-TUB-U2	SGB Tube 2 Inlet – Top	–	–	m	0.433	–
1373	RC 162	CL-TUB-U1	SGB Tube 1 Inlet – Top	–	–	m	0.73	–
1374	RC 163	CL-TUB-U4	SGB Tube 4 Inlet – Top	–	–	m	0.74	–
1375	RC 164	CL-TUB-U5	SGB Tube 5 Inlet – Top	–	–	m	0.734	–
1376	RC 165	CL-TUB-U6	SGB Tube 6 Inlet – Top	–	–	m	0.73	–
1377	RC 166	CL-TUB-D3	SGB Tube 3 Outlet – Top	–	–	m	0.951	–
1378	RC 167	CL-TUB-D2	SGB Tube 2 Outlet – Top	–	–	m	0.74	–
1379	RC 168	CL-TUB-D1	SGB Tube 1 Outlet – Top	–	–	m	0.735	–
1380	RC 169	CL-TUB-D4	SGB Tube 4 Outlet – Top	–	–	m	0.747	–
1381	RC 170	CL-TUB-D5	SGB Tube 5 Outlet – Top	–	–	m	0.74	–
1382	RC 171	CL-TUB-D6	SGB Tube 6 Outlet – Top	–	–	m	0.735	–
1383	RC 172	CL-LSB-D	SGB Out.Plenum – LSB Bottom	–	–	m	0.207	–
1384	RC 173	CL-LSB-U	LSB Bottom – PCB Suction	–	–	m	0.188	–

Table A-1 (Cont'd)

SEQ No.	Function ID.	Tagname	Location	Range		Unit	Uncertainty	
				LO	HI		±ABS.	±%FR
1385	RC 174	CL-SGB-IPL	SGB Inlet Plenum	-	-	m	0.094	-
1386	RC 175	MC-UH	Upper Head (EL.6634 - 8860)	-	-	kg	79.08	-
1387	RC 176	MC-LSA-DW	SGA Out.Plenum+LSA Downflow	-	-	kg	42.68	-
1388	RC 177	MC-LSB-DW	SGB Out.Plenum+LSB Downflow	-	-	kg	41.33	-
1389	RC 178	MS-CORE	Core (EL.-35 - 3945)	-	-	kg	15.4	-
1390	RC 179	MS-UP	Upper Plenum (EL.4060 - 6135)	-	-	kg	24.37	-
1391	RC 180	MS-DC	Downcomer	-	-	kg	46.31	-
1392	RC 181	MS-TUA-UP-AV	SGA Tubes Upflow side	-	-	kg	8.3	-
1393	RC 182	MS-TUA-DW-AV	SGA Tubes Downflow side	-	-	kg	8.3	-
1394	RC 183	MS-SGA-IPL	SGA Inlet Plenum	-	-	kg	27.81	-
1395	RC 184	MS-LSA-UP	LSA Upflow side	-	-	kg	3.57	-
1396	RC 185	MS-TUB-UP-AV	SGB Tubes Upflow side	-	-	kg	9.65	-
1397	RC 186	MS-TUB-DW-AV	SGB Tubes Downflow side	-	-	kg	10.25	-
1398	RC 187	MS-SGB-IPL	SGB Inlet Plenum	-	-	kg	14.61	-
1399	RC 188	MS-LSB-UP	LSB Upflow side	-	-	kg	3.57	-
1400	RC 189	MS-ACC	Acc-Cold Tank	-	-	kg	39.26	-
1401	RC 190	MS-ACH	Acc-Hot Tank	-	-	kg	74.26	-
1402	RC 191	MS-ST	Break Flow Supp. Tank	-	-	kg	323.61	-
1403	RC 192	DM-ACC	Acc-Cold Tank	-	-	kg/s	13.55	-
1404	RC 193	DM-ACH	Acc-Hot Tank	-	-	kg/s	26.08	-
1405	RC 194	IM-ST	Break Flow Supp. Tank	-	-	kg/s	3.35	-
1406	RC 195	DM-RWST	RWST	-	-	kg/s	51.9	-
1407	RC 196	LG-HLA	HLA Water Level	-	-	m	0.012	-
1408	RC 197	LG-CLA	CLA Water Level	-	-	m	0.028	-
1409	RC 198	LG-HLB	HLB Water Level	-	-	m	0.012	-
1410	RC 199	LG-CLB	CLB Water Level	-	-	m	0.028	-
1411	RC 200	TS-UP	Upper Plenum	-	-	K	17.64	-
1412	RC 201	TS-PR	Pressurizer	-	-	K	17.64	-
1413	RC 202	TS-SGA	Steam Generator-A	-	-	K	7.82	-
1414	RC 203	TS-SGB	Steam Generator-B	-	-	K	7.82	-
1415	RC 279	DE291-SGB-EU	SGB Feedwater Line	-	-	kg/m^3	-	-